Quantum oscillations & topology

Xiangwei Huang, Carsten Putzke, Mark Guo, **Jonas Diaz**, PJWM

Ecole Polytechnique Federale de Lausanne, Institute of Materials, Switzerland

Kent Shirer, Maja Bachmann, Toni Helm, Markus König,
Yan Sun, Claudia Felser, Binghai Yan, Philip J.W. Moll

Max-Planck-Institute for Chemical Physics of Solids, Dresden, Germany

Tobias Meng

Technical University, Dresden, Germany

Laurel Winter, Jon Betts, Ross McDonald, Fedor Balakirev

National High Magnetic Field Laboratory, US

Eric D. Bauer, Filip Ronning

Los Alamos National Laboratory, US

Nityan Nair, James Analytis

University of California, Berkeley, US

Roni Ilan, Dima Pikulin, Takashi Oka, Roderich Moessner, Andy Mack

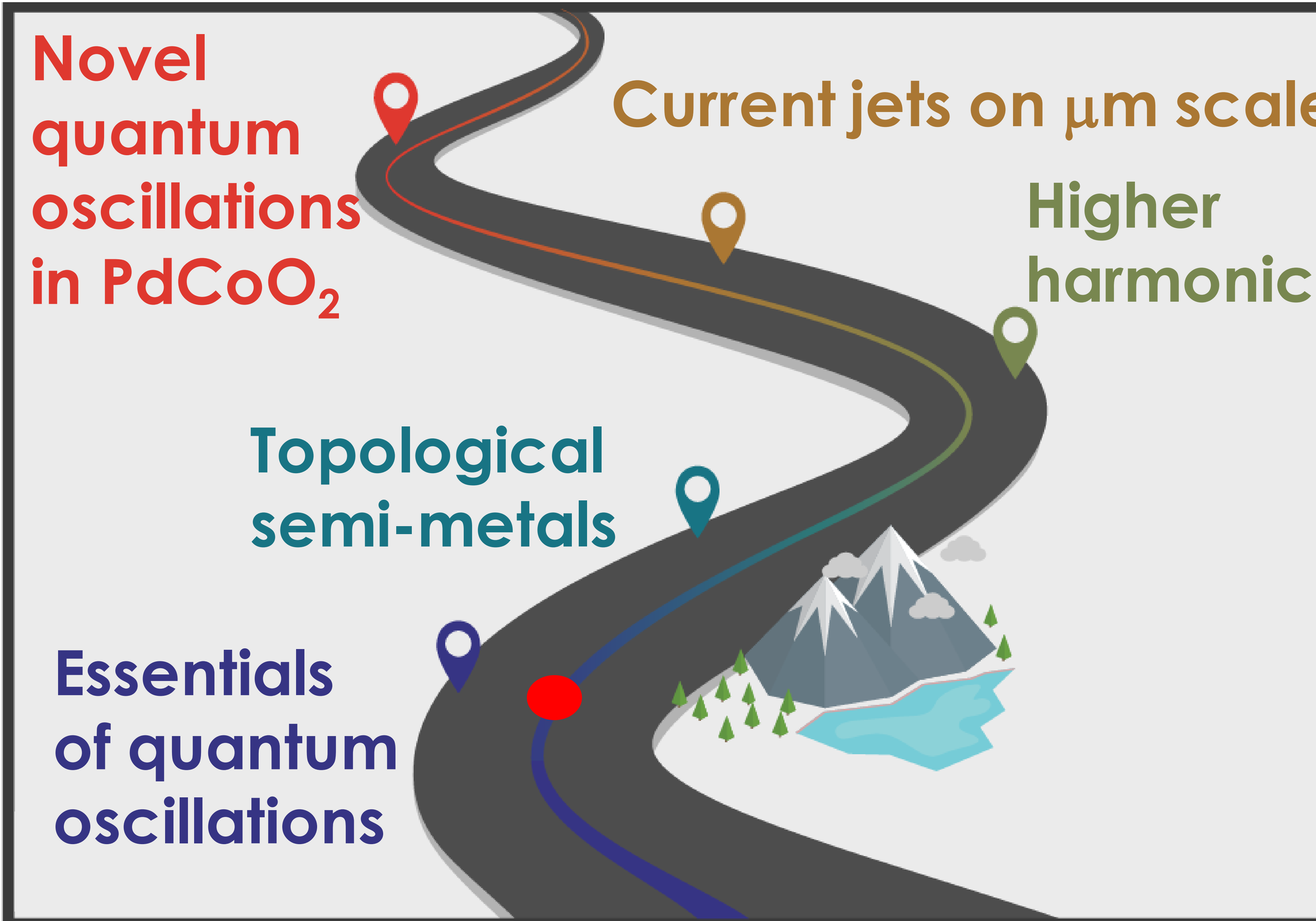
Novel quantum oscillations in $PdCoO_2$
Current jets on μm scale
Higher harmonics
Topological semi-metals
Essentials of quantum oscillations

Key points:

- Quantum treatment of electrons in a magnetic field
- Phases in magnetic fields
- Landau levels in 3D are one-dimensional modes along the field

Framework: Electrons in a magnetic field

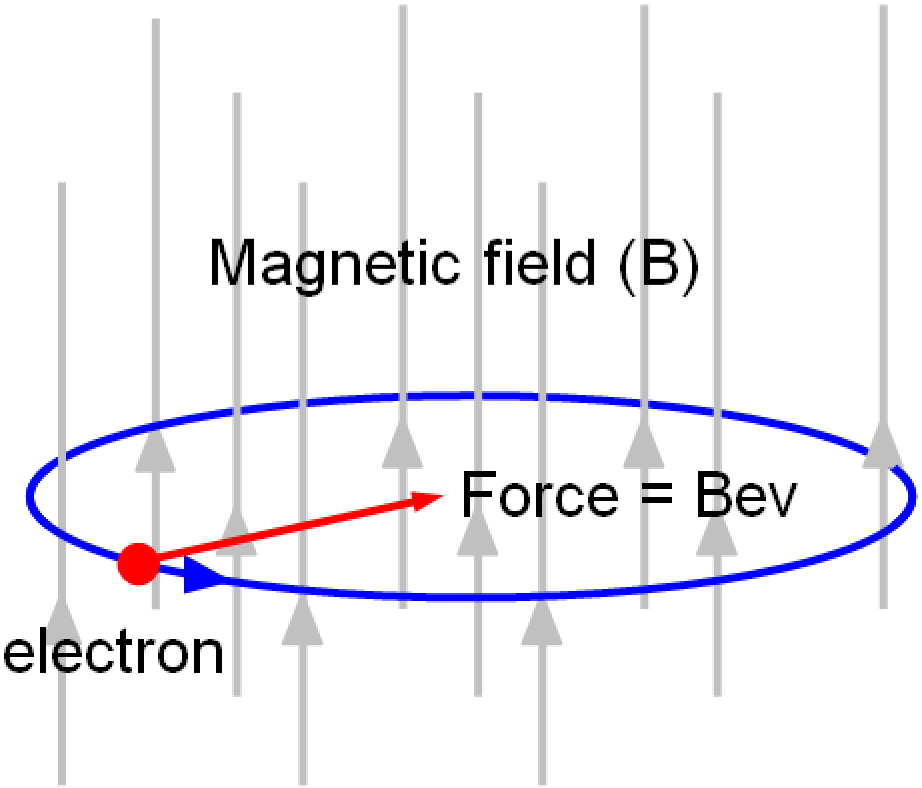

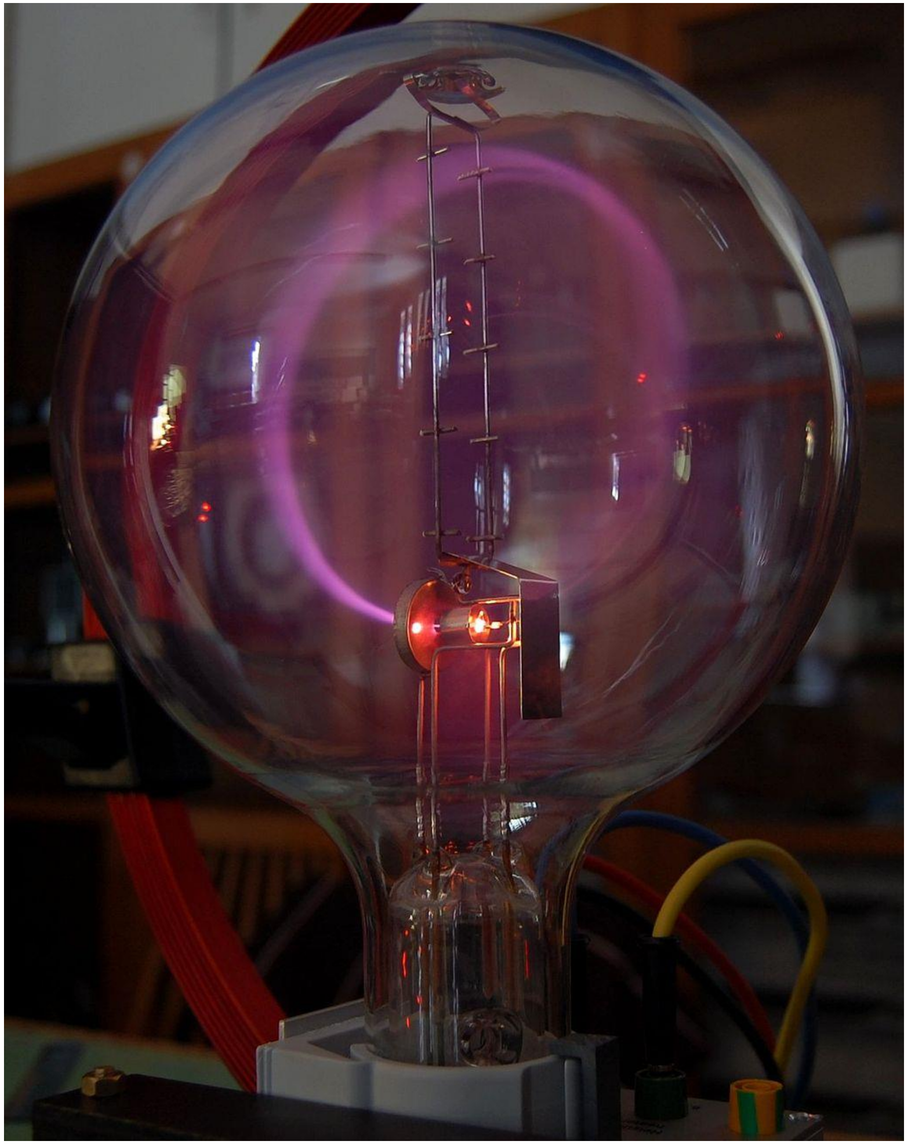

Classical Electrons in a magnetic field

Classical warmup:

$$\boldsymbol{F_L} = e\boldsymbol{v} \times \boldsymbol{B}$$

$$\boldsymbol{B} = \begin{pmatrix} 0 \\ 0 \\ B_z \end{pmatrix} \rightarrow F_L = eB_z \begin{pmatrix} v_y \\ -v_x \\ 0 \end{pmatrix}$$

$$m\ddot{x} = eB_z\dot{y} \qquad m\ddot{y} = -eB_z\dot{x}$$

$$\ddot{x} + \left(\frac{eB_z}{m}\right)^2 x = 0$$

- **Harmonic oscillators**
- **Cyclotron frequency** $\boldsymbol{\omega_c = \frac{eB}{m}}$

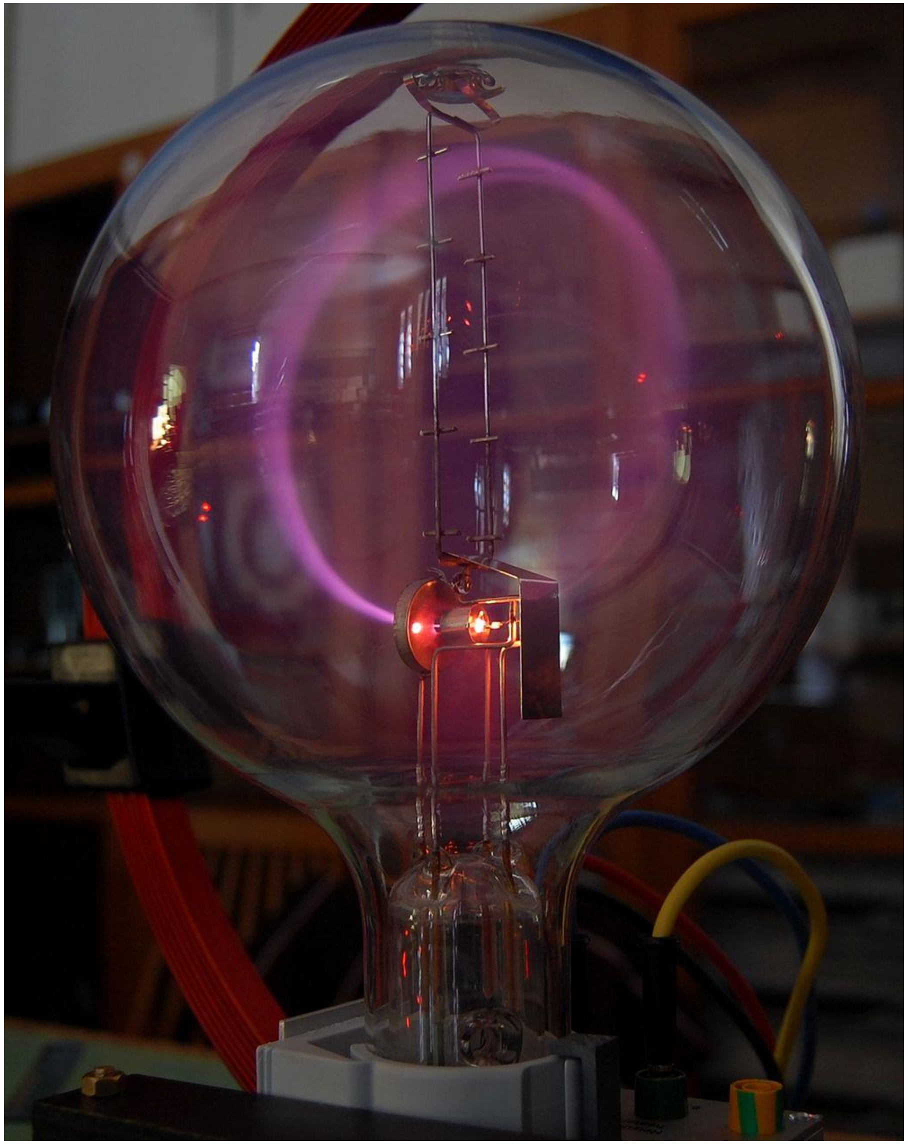

Classical Electrons in a magnetic field

Classical warmup:

$$\boldsymbol{F_L} = e\boldsymbol{v} \times \boldsymbol{B}$$

$$\boldsymbol{B} = \begin{pmatrix} 0 \\ 0 \\ B_z \end{pmatrix} \rightarrow F_L = eB_z \begin{pmatrix} v_y \\ -v_x \\ 0 \end{pmatrix}$$

$$m\ddot{x} = eB_z\dot{y} \qquad m\ddot{y} = -eB_z\dot{x}$$

$$\ddot{x} + \left(\frac{eB_z}{m}\right)^2 x = 0$$

- **Harmonic oscillators**
- **Cyclotron frequency** $\boldsymbol{\omega_c = \frac{eB}{m}}$

Cyclotron radius:

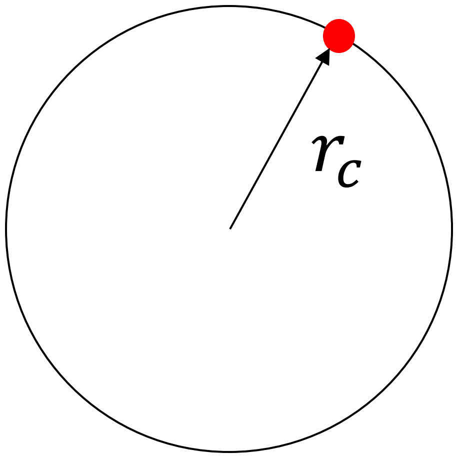

Distance / speed = time

$$\frac{2\pi r_c}{v} = T = \frac{2\pi}{\omega_c}$$

$$\boldsymbol{r_c = \frac{mv}{eB}}$$

Classically, any orbit size is allowed

Quantum description

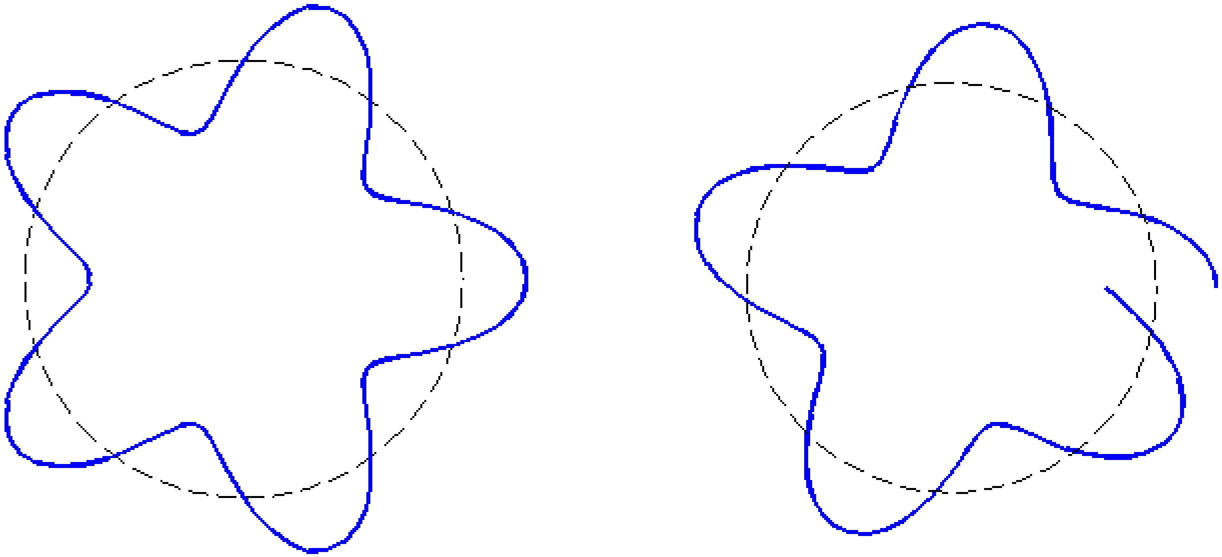

Classically, any cyclotron radius is allowed.

Single-valuedness of quantum wavefunction allows only discrete set of orbits

Quantum Electrons in a magnetic field

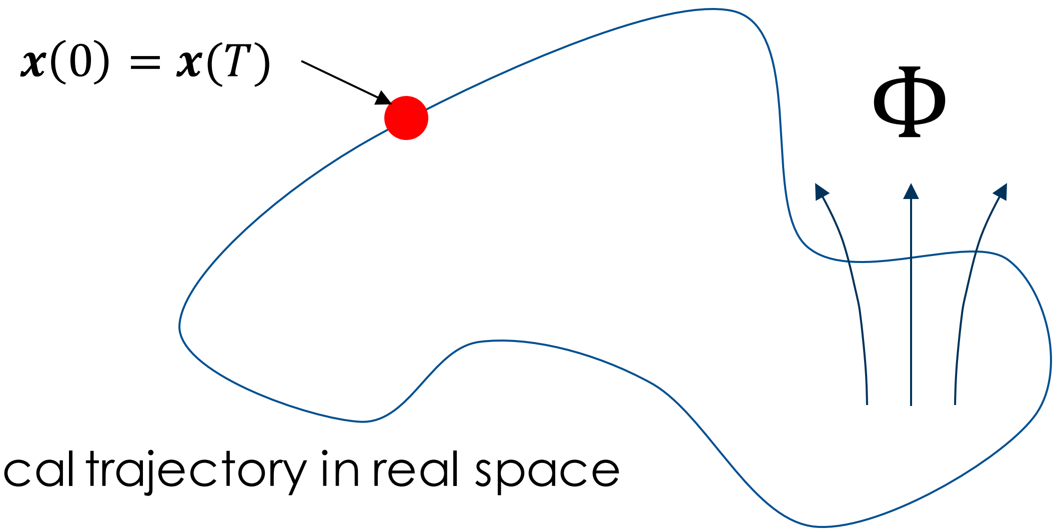

Closed classical trajectory in real space

Bohr-Sommerfeld quantization: $\hbar^{-1} \oint \boldsymbol{p}\, d\boldsymbol{r} = 2\pi(n + \gamma)$

$$\boldsymbol{B} = \nabla \times \boldsymbol{A} \quad \boldsymbol{p} \to \boldsymbol{p} - e\boldsymbol{A}$$

$$\hbar^{-1} \oint (\boldsymbol{p} - \boldsymbol{eA})\, d\boldsymbol{r} \;=\; \hbar^{-1} \oint \boldsymbol{p}\, d\boldsymbol{r} - \frac{e}{\hbar} \oint A\, d\boldsymbol{r}$$

Quantum Electrons in a magnetic field

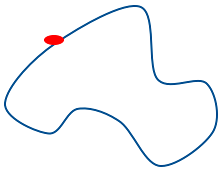

Bohr-Sommerfeld quantization: $\hbar^{-1}\oint \boldsymbol{p}\, d\boldsymbol{r} = 2\pi(n+\gamma)$

$$\boldsymbol{B} = \nabla \times \boldsymbol{A} \quad \boldsymbol{p} \to \boldsymbol{p} - e\boldsymbol{A}$$

$$\hbar^{-1}\oint(\boldsymbol{p} - \boldsymbol{eA})\, d\boldsymbol{r} \;=\; \hbar^{-1}\oint \boldsymbol{p}\, d\boldsymbol{r} - \frac{e}{h}\oint A\, d\boldsymbol{r}$$

$\frac{e}{h}\oint A\, d\boldsymbol{r} = \frac{e}{h} \int B\, d r^2 = \frac{e}{h}\Phi$ Magnetic flux through loop

$$\Phi_0 = \frac{h}{e} \sim 2 \cdot 10^{-15}\mathrm{Tm}^2$$

Stable real space orbits enclose an integer multiple of Φ_0

Types of quantum processes

The real space orbits enclose an integer multiple of Φ_0

Aharonov-Bohm

Orbit is **field-independent**

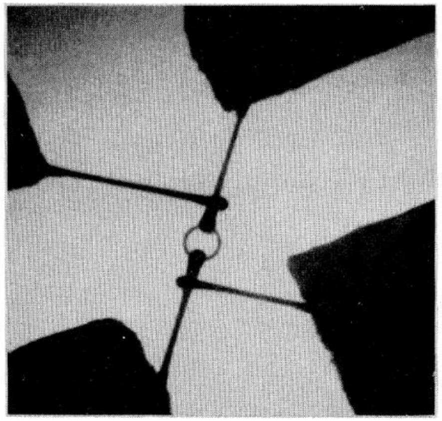

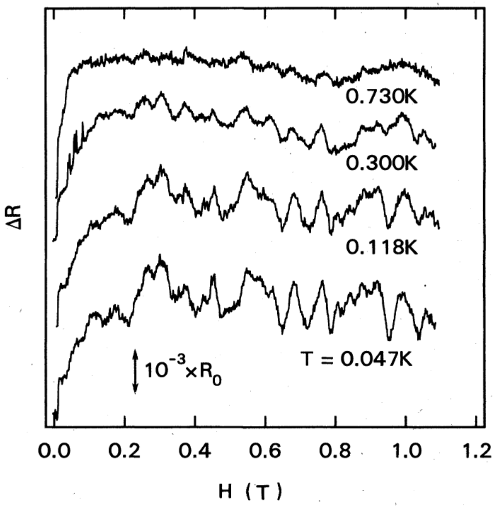

$$n\Phi_0 = B * r^2$$

$$B_n = \frac{\Phi_0}{r^2} \; n$$

Oscillations periodic in field

Y. Aharonov, D. Bohm. Phys. Rev. 115, 485-491 (1961
C.P. Umbach et al., PRB 30, 4048 (R) (1984)

Two facetts of the same physics

<u>The real space orbits enclose an integer multiple of Φ_0</u>

Aharonov-Bohm

Orbit is **field-independent**

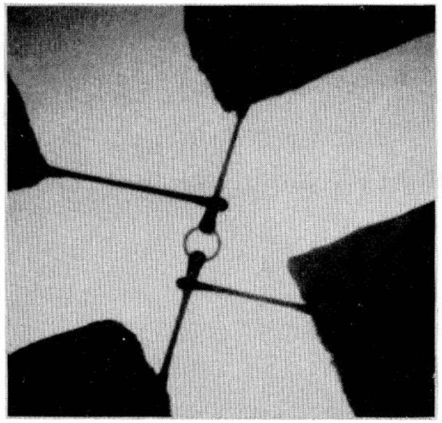

$$n\Phi_0 = B * r^2$$

$$B_n = \frac{\Phi_0}{r^2}\ n$$

Oscillations periodic in field

De Haas – van Alphen

Orbit is **field-dependent**

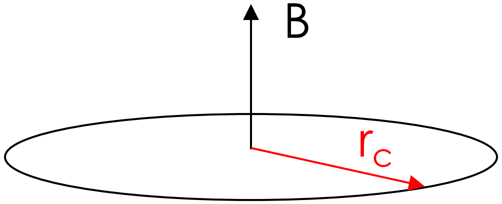

$$n\Phi_0 = B * r_c^2 \ \propto B^{-1}$$

$$B_n \propto \frac{\Phi_0}{n}$$

Oscillations periodic in inverse field

Types of quantum processes

The real space orbits enclose an integer multiple of Φ_0

De Haas – van Alphen

Orbit is **field-dependent**

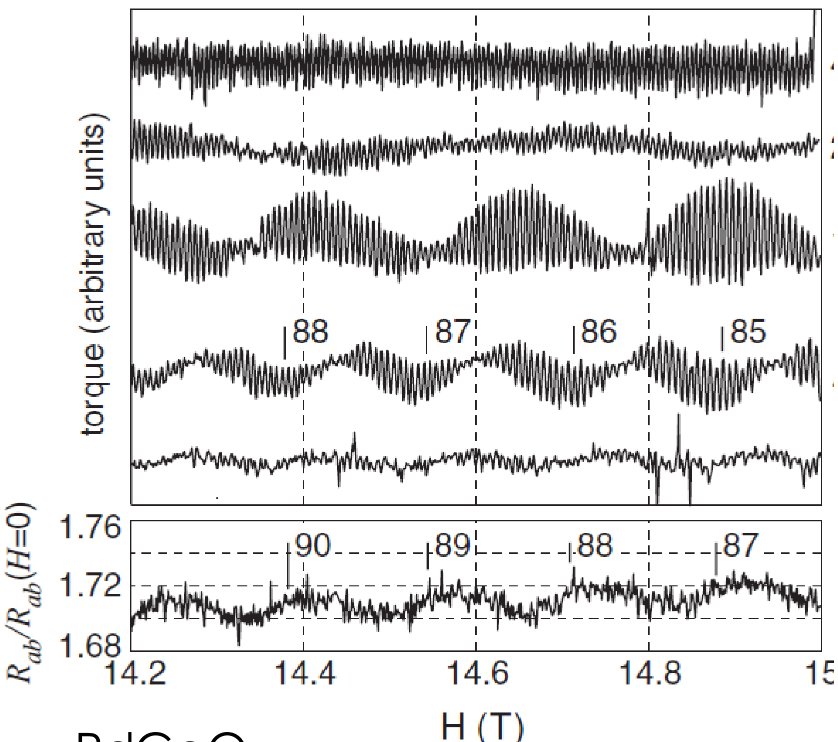

$PdCoO_2$

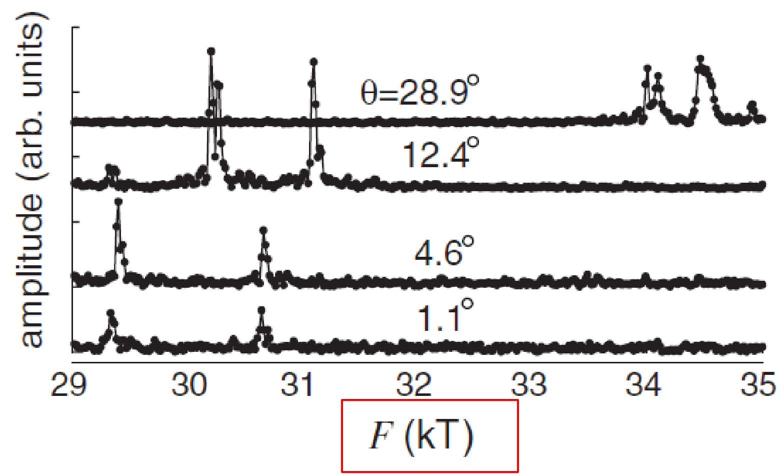

$$n\Phi_0 = B * r_c^2 \propto B^{-1}$$

$$B_n \propto \frac{\Phi_0}{n}$$

Oscillations periodic in inverse field

C. Hicks et al., PRL 109, 116401 (2012)

D. Shoenberg – Magnetic oscillations in met

Harmonic oscillator revisited

2D: $H = \frac{1}{2m}\left(p_x^2 + p_y^2\right) \rightarrow \frac{1}{2m}\left(p_x^2 + \left(p_y - eBx\right)^2\right)$ with $A = (0, Bx, 0)$ in Landau gauge

As $\left[p_y, p_x\right] = \left[p_y, x\right] = 0$, the solution can be written as $\psi(x, y) = \tilde{\psi}(x) e^{-ik_y y}$

$$H = \frac{1}{2m}\left(p_x^2 + \left(\hbar k_y - eBx\right)^2\right)$$

$$= \left(\frac{p_x^2}{2m} + \frac{1}{2} m \frac{e^2 B^2}{m^2}\left(\frac{\hbar k_y}{eB} - x\right)^2\right)$$

$$= \left(\frac{p_x^2}{2m} + \frac{1}{2} m \omega_c^2 (x_0 - x)^2\right)$$

Landau levels

Harmonic oscillators: localized states with discrete spectrum $E_n = \hbar\omega_c\left(n + \frac{1}{2}\right)$

2D density of states

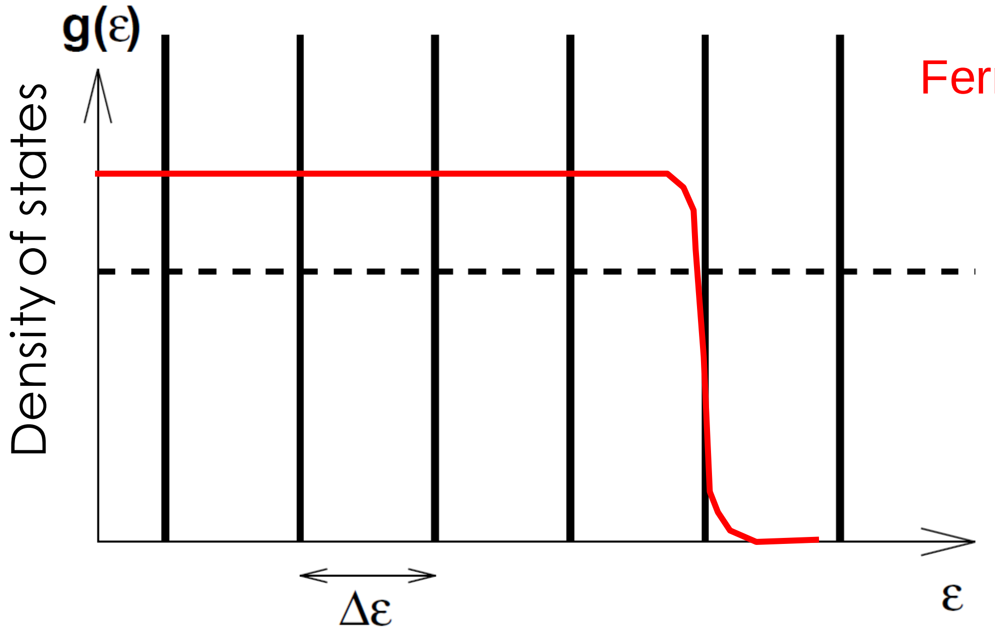

Fermi-Dirac distribution

$f(E,\mu,T)$

$$E_n = \hbar\omega_c\left(n + \frac{1}{2}\right)$$

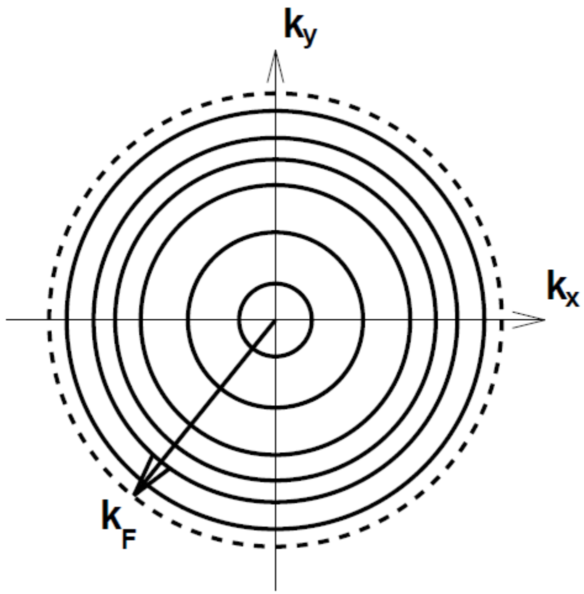

Harmonic oscillator revisited

3D: $H = \frac{1}{2m}\left(p_x^2 + p_y^2 + p_z^2\right) \rightarrow \frac{1}{2m}\left(p_x^2 + \left(p_y - eBx\right)^2 + p_z^2\right)$ with $A = (0, Bx, 0)$

As $\left[p_y, p_x\right] = \left[p_y, x\right] = \left[p_z, x\right] = 0$, the solutions are $\psi(x,y,z) = \tilde{\psi}(x)e^{-ik_y y}\, e^{-ik_z z}$

$$H = \frac{1}{2m}\left(p_x^2 + \left(\hbar k_y - eBx\right)^2 + \hbar^2 k_z^2\right)$$

$$= \left(\frac{p_x^2}{2m} + \frac{1}{2} m \frac{e^2 B^2}{m^2}\left(\frac{\hbar k_y}{eB} - x\right)^2 + \hbar^2 k_z^2\right)$$

$$= \left(\frac{p_x^2}{2m} + \frac{1}{2} m\omega_c^2 (x_0 - x)^2 + \hbar^2 k_z^2\right)$$

Landau levels in 3D

Harmonic oscillators, but unchanged plane waves along field $E_n = \hbar\omega_c\left(n + \frac{1}{2}\right) + \frac{\hbar^2 k_z^2}{2m}$

Harmonic oscillator revisited

3D: $H = \frac{1}{2m}\left(p_x^2 + p_y^2 + p_z^2\right) \rightarrow \frac{1}{2m}\left(p_x^2 + \left(p_y - eBx\right)^2 + p_z^2\right)$ with $A = (0, Bx, 0)$

- Magnetic fields break translational invariance perpendicular to them.
- Landau levels in 3D are one-dimensional modes dispersing along the field.

Landau levels in 3D

Harmonic oscillators, but unchanged plane waves along field $E_n = \hbar\omega_c\left(n + \frac{1}{2}\right) + \frac{\hbar^2 k_z^2}{2m}$

Harmonic oscillator revisited

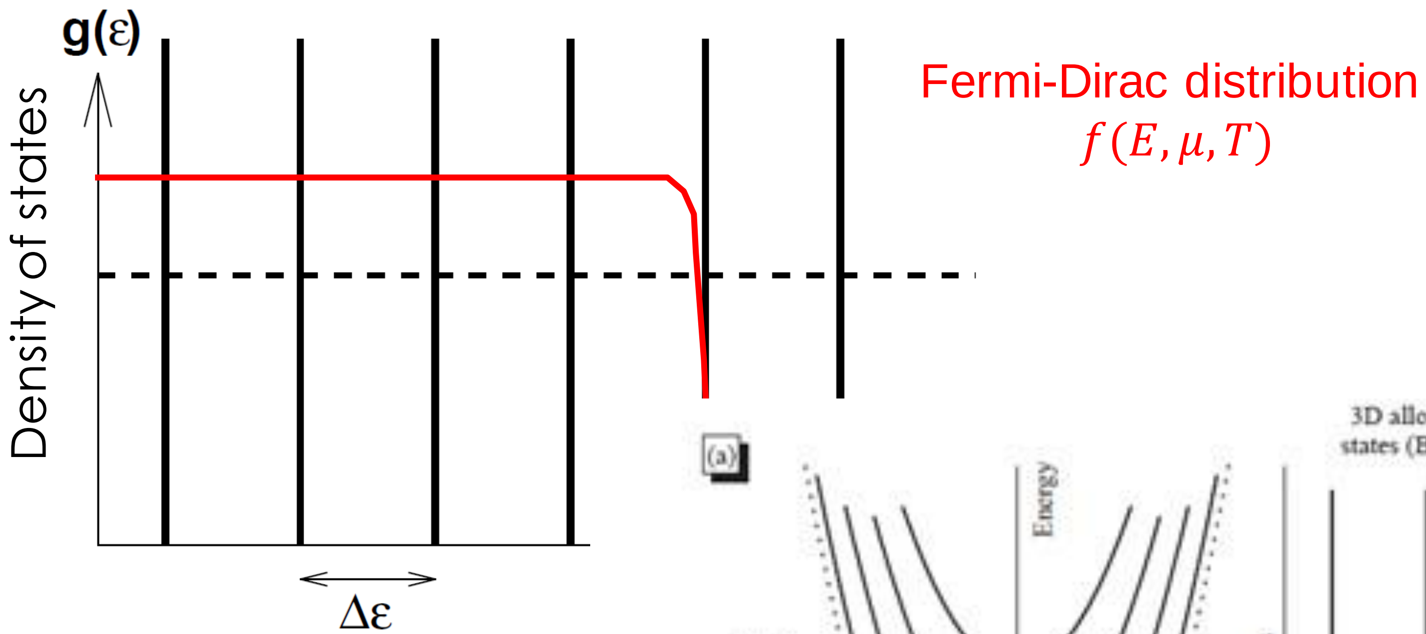

$$E_n = \hbar\omega_c\left(n + \frac{1}{2}\right) + \frac{\hbar^2 k_z^2}{2m}$$

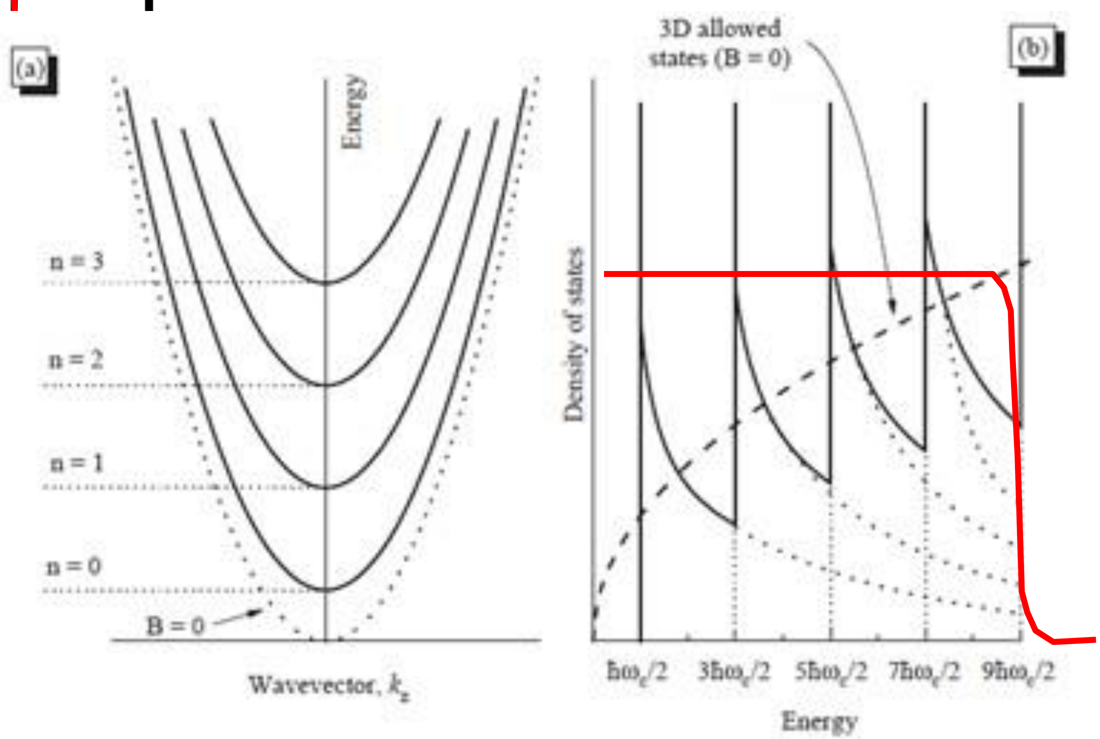

Fermiology

Lattice interactions can give complex dispersions

Example: TaP F. Arnold et al., Nat. Comm 7:11615 (2015)

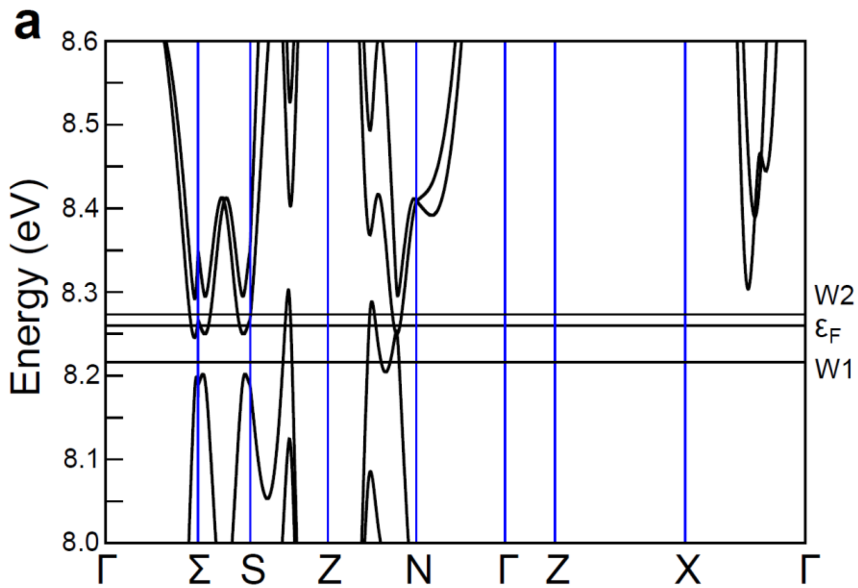

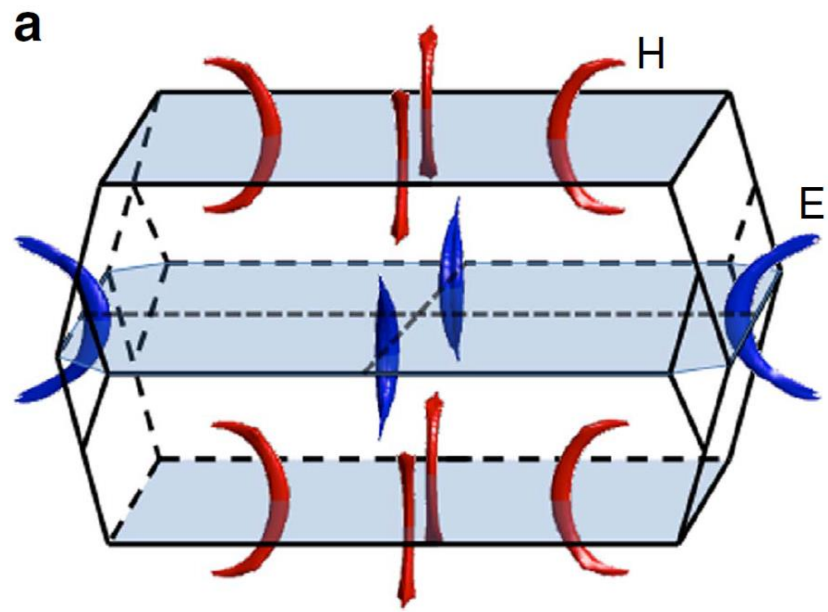

- Orbital arrangement leads to complex wave functions and dispersions
- Fermi surfaces are commonly non-spherical

Yet the concepts from free electrons can be directly translated, and quantum oscillations are a powerful tool to measure Fermi surface

Semiclassical equations of motion

Wavepacket centered at position **r** and momentum **k**

$$\hbar \frac{d\boldsymbol{k}}{dt} = \boldsymbol{F} = q(\boldsymbol{v}_{\boldsymbol{k}} \times \boldsymbol{B})$$

$$\frac{d\boldsymbol{r}(\boldsymbol{k})}{dt} = \boldsymbol{v}_{\boldsymbol{k}} = \hbar^{-1} \nabla E(\boldsymbol{k})$$

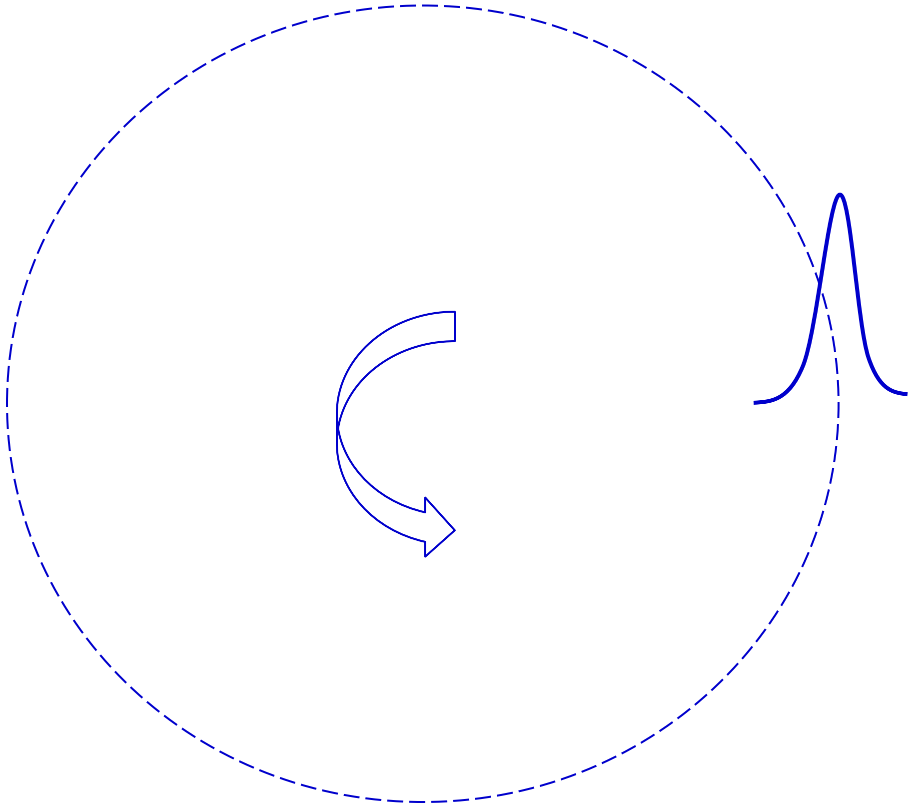

Consider arbitrary (and often crazy complex) E(k)

Semiclassical equations of motion

$$\hbar \frac{d\boldsymbol{k}}{dt} = \boldsymbol{F} = q(\boldsymbol{v_k} \times \boldsymbol{B})$$

$$\frac{d\boldsymbol{r}(\boldsymbol{k})}{dt} = \boldsymbol{v_k} = \hbar^{-1} \nabla E(\boldsymbol{k})$$

k-space orbit is always perpendicular to

$$\frac{\hbar}{q} \frac{d\boldsymbol{k}}{dt} \cdot \boldsymbol{B} = (\boldsymbol{v_k} \times \boldsymbol{B}) \cdot \boldsymbol{B} = 0$$

The energy does not change during the orbi

$$\frac{dE(\boldsymbol{k})}{dt} = \frac{dE}{d\boldsymbol{k}} \frac{d\boldsymbol{k}}{dt} = \boldsymbol{v_k} \frac{d\boldsymbol{k}}{dt} = \frac{q}{\hbar}\, v_k \cdot (v_k \times B) = 0$$

Cyclotron orbits in metals are paths on the Fermi surface perpendicular to B

Momentum space orbits

k-space orbit is always perpendicular to B

$$\frac{\hbar}{q}\frac{d\boldsymbol{k}}{dt}\cdot\boldsymbol{B} = (\boldsymbol{v_k}\times\boldsymbol{B})\cdot\boldsymbol{B} = 0$$

The energy does not change during the orbit

$$\frac{dE(\boldsymbol{k})}{dt} = \frac{dE}{d\boldsymbol{k}}\frac{d\boldsymbol{k}}{dt} = \boldsymbol{v_k}\frac{d\boldsymbol{k}}{dt} = \frac{q}{\hbar}\,v_k\cdot(v_k\times B) = 0$$

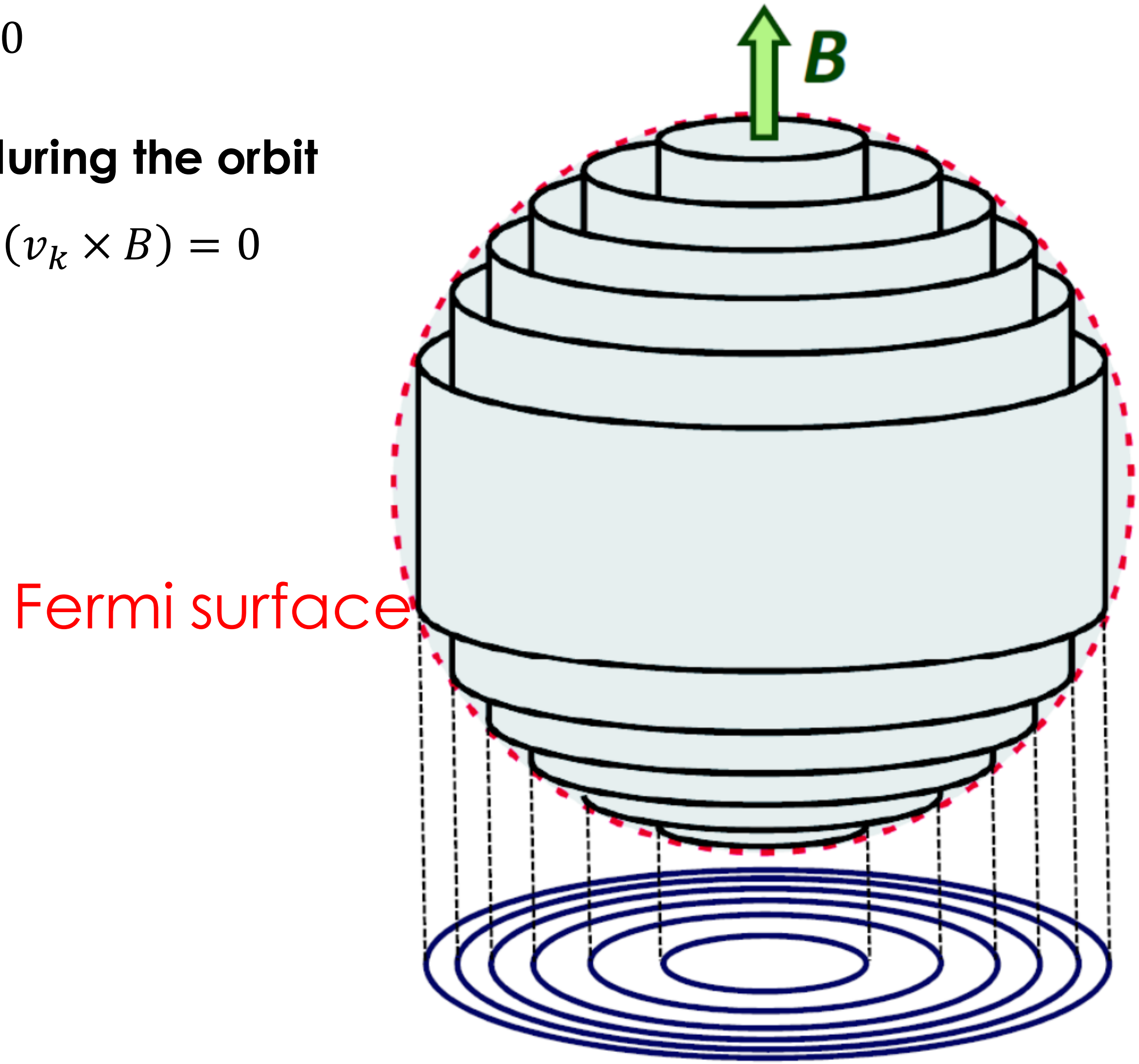

The magnetic length

At a given B, how large is the area through which one flux quantum thre

$$\Phi = l_B^2 B = \Phi_0 \;\rightarrow l_B^2 = \frac{\Phi_0}{B}$$: magnetic length

Length scale over which the magnetic field notably changes phase of wave

Length scales in metals:

$l_B \sim \mathit{sample\ size}$: semi-classics, Hall-effect, Boltzmann magnetotransport,...

$l_B \sim \mathit{phase\ coherence}$: quantum oscillations, Aharonov Bohm, interference

$l_B \sim \mathit{atomic\ scale}$: quantum limit, non-perturbative, Hofstadter physics,...

Real space orbits are trivially related to semi-classical k-space orbits

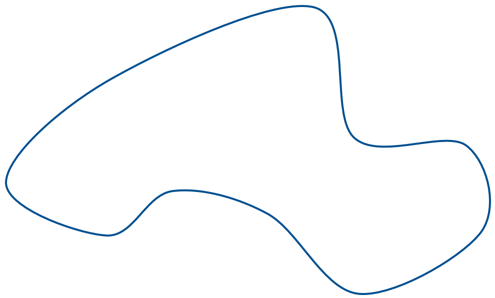

Momentum-space orbit

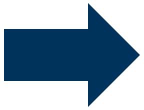

- Rotate by 90°
- Scale by l_B^2

Dimension!

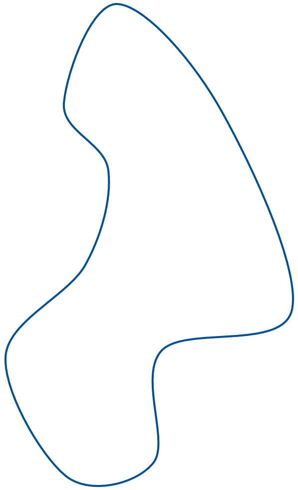

Real-space orbit

Real space orbits are trivially related to semi-classical k-space orbits

Bohr-Sommerfeld-quantization: $\Phi = B * A = 2\pi(n+\gamma)\Phi_0$

Real space orbit area A → k-space orbit area $S = A\, l_B^{-4}$

$$B * S * \left(\frac{\Phi_0}{B}\right)^2 = 2\pi(n+\gamma)\Phi_0$$

Onsager relation (Bohr-Sommerfeld for k-space orbit)

$$S(E, k_z)\ \ \Phi_0/B_n = 2\pi[n+\gamma]$$

Area of Orbit
in k-space

Quantum oscillation frequency = k-space orbit area

$$S(E,k_z)\ \Phi_0/B_n = 2\pi[n+\gamma]$$

Area of Orbit
in k-space

Solutions are periodic in $1/B_n$: $\frac{1}{B_n} = \frac{2\pi}{S\Phi_0}\ (n+\gamma)$

Frequency: $\mathrm{F} = \frac{1}{period} = \left(\frac{1}{B_{n+1}} - \frac{1}{B_n}\right)^{-1} = \frac{\hbar}{2\pi e}\ S$

Onsager relation: $F = \frac{\hbar}{2\pi e} S$

Experimentally measured quantum oscillation frequencies
= k-space orbit area of orbit, even in highly complex metals

Only extremal orbits are experimentally detectable

Geometric property of Fermi surface: $S(k_z)$
denote direction of field as z

Orbits with extremal cross-sections are observable

$$\frac{dS}{dk_z} = 0$$

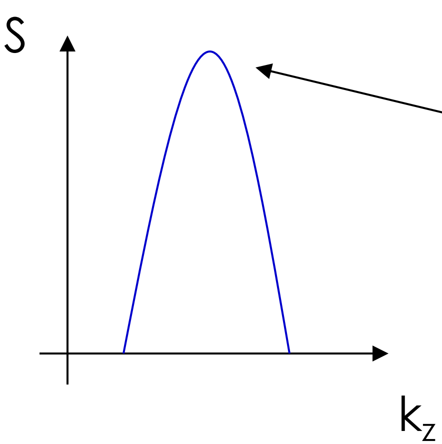

$$S_{ext} \propto F_{ext}$$

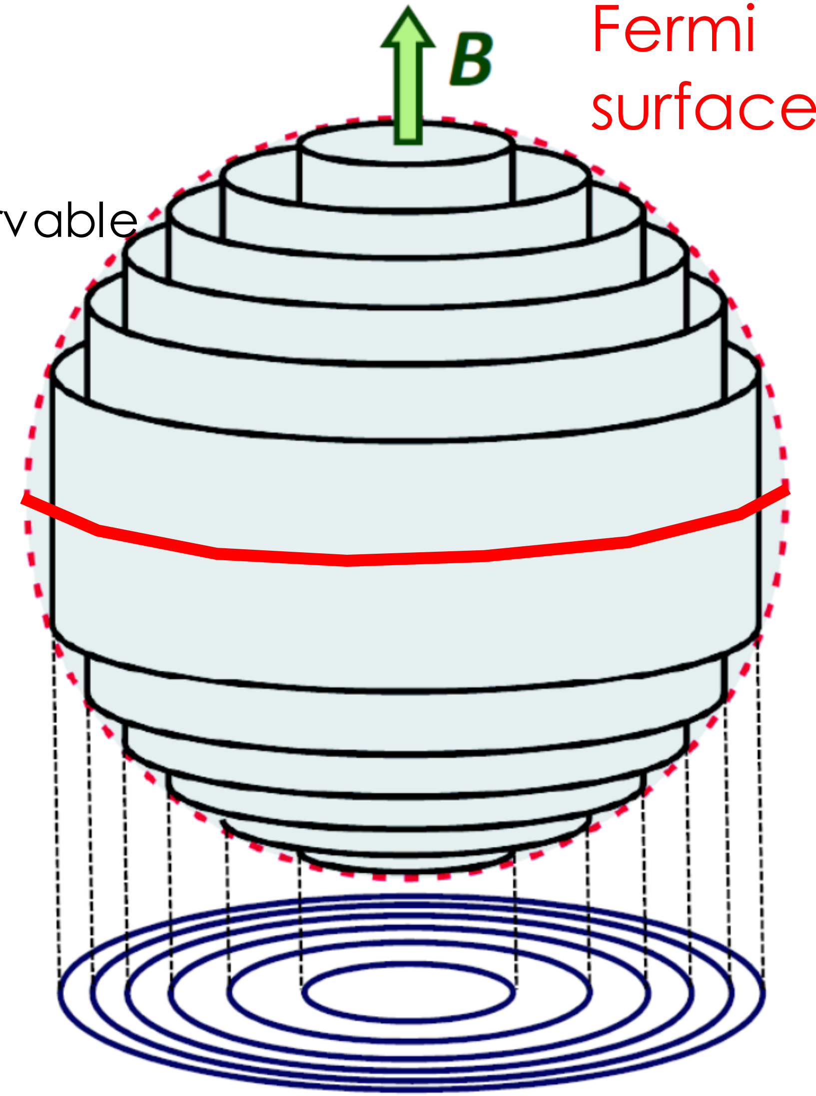

Quantum oscillations in pulsed fields in $PtSe_2$

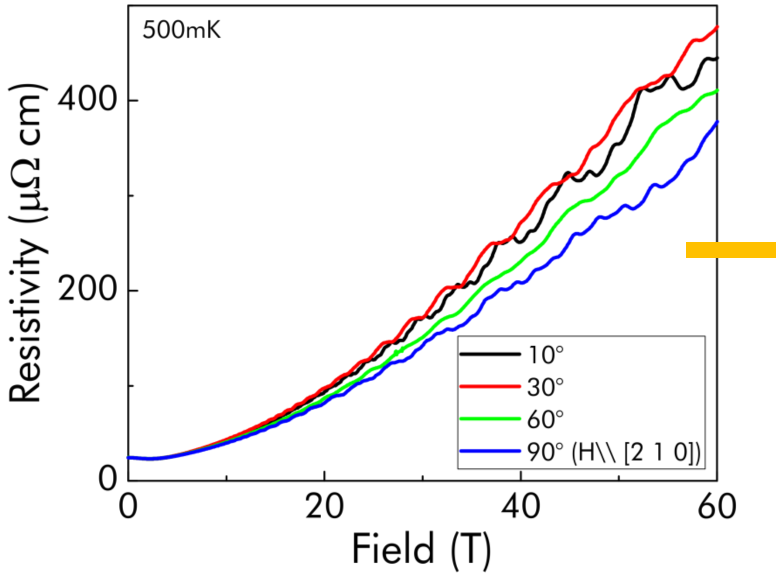

- High SNR in pulsed fields
  for high conductivity metal
- Multiple quantum orbits observed

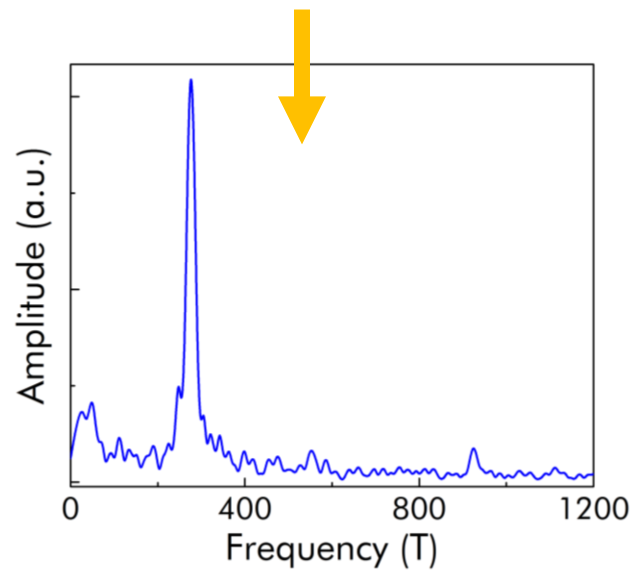

Quantum oscillation frequencies: *Fermiology*

Frequency = extremal Fermi surface area (Onsager)

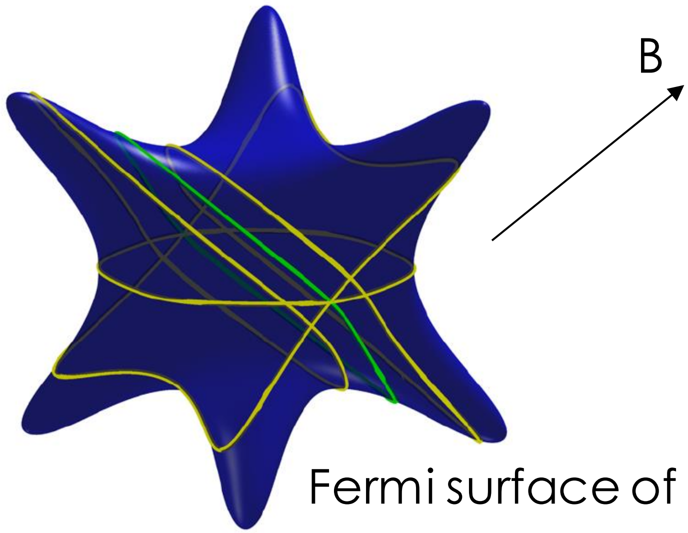

Fermi surface of $PtSe_2$

$$S(E,k_z)\ \Phi_0/B_n = 2\pi[n+\gamma]$$

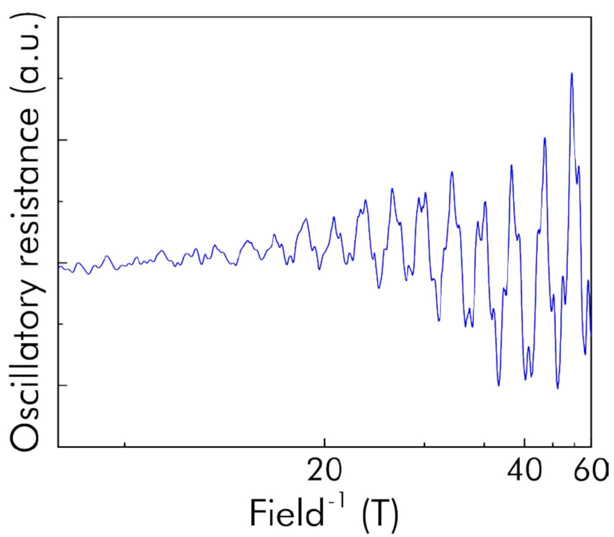

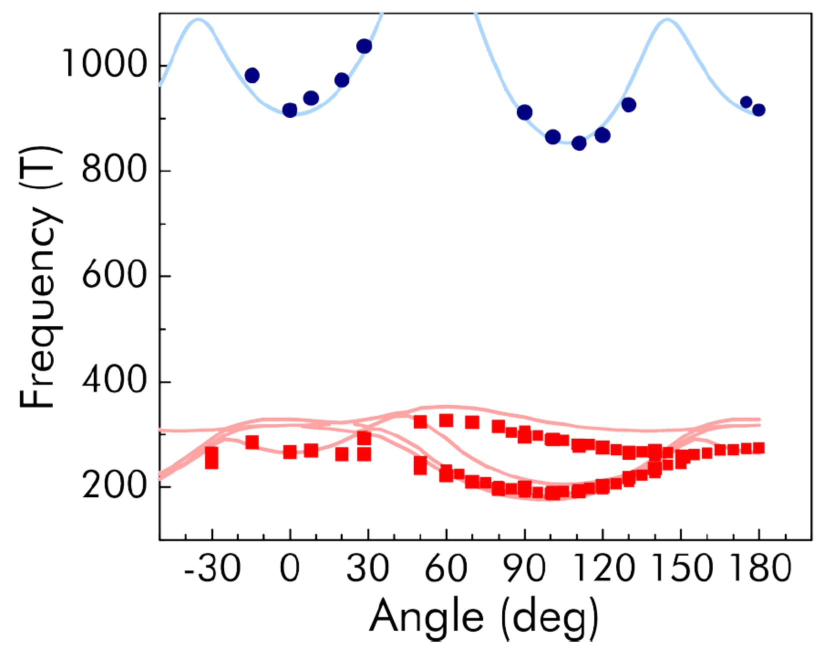

Tomographic reconstruction of Fermi surf
Rotate B w.r.t crystal.

Hao Yang et al **2018** New J. Phys.20 043008

Quantum oscillation frequencies: *effective mass*

The classical cyclotron frequency cannot be complete on quantum level $\omega_c =$

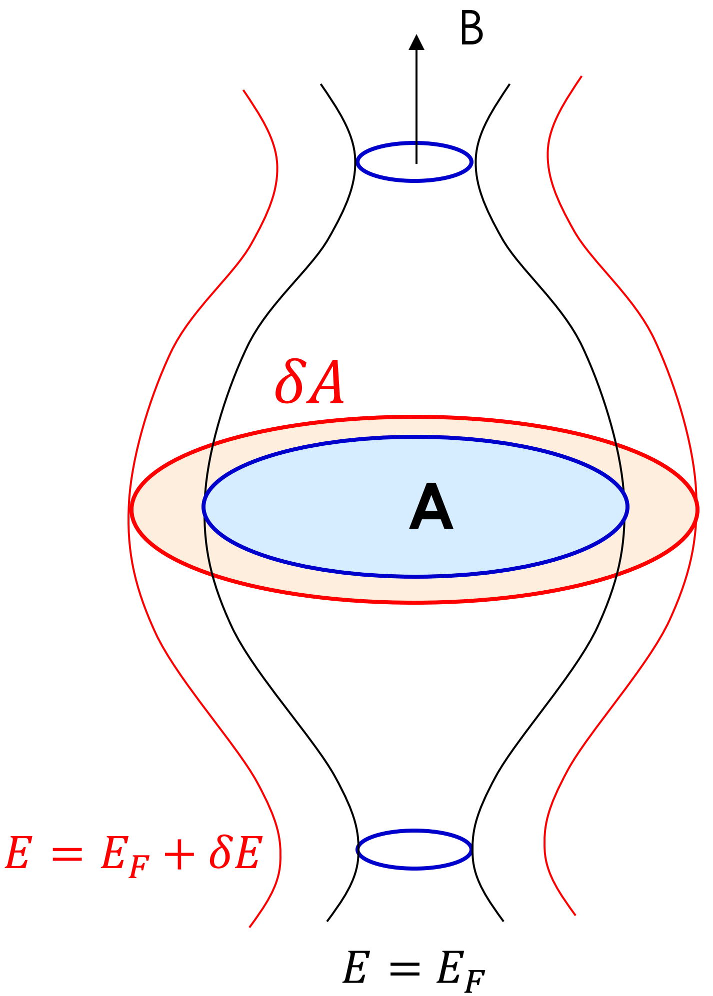

Cyclotron mass: $m_c = \frac{\hbar^2}{2\pi}\frac{\partial A}{\partial E}$

$$A = \pi k_F^2 \rightarrow k_F = \left(\frac{A}{\pi}\right)^{1/2}$$

Schrödinger Electrons

$$E = \frac{\hbar^2 k_F^2}{2m^*} = \frac{\hbar^2 A}{2m^* \pi} \rightarrow A = \frac{2m^* \pi}{\hbar^2} E \rightarrow m_c = m^*$$

Dirac Electrons

$$E = \hbar v_F k_F = \hbar v_F \left(\frac{A}{\pi}\right)^{1/2} \rightarrow$$

$$A = \pi \left(\frac{E}{\hbar v_F}\right)^2 \rightarrow m_c = \frac{\hbar}{v_F} E$$

Quantum oscillation frequencies: *effective mass*

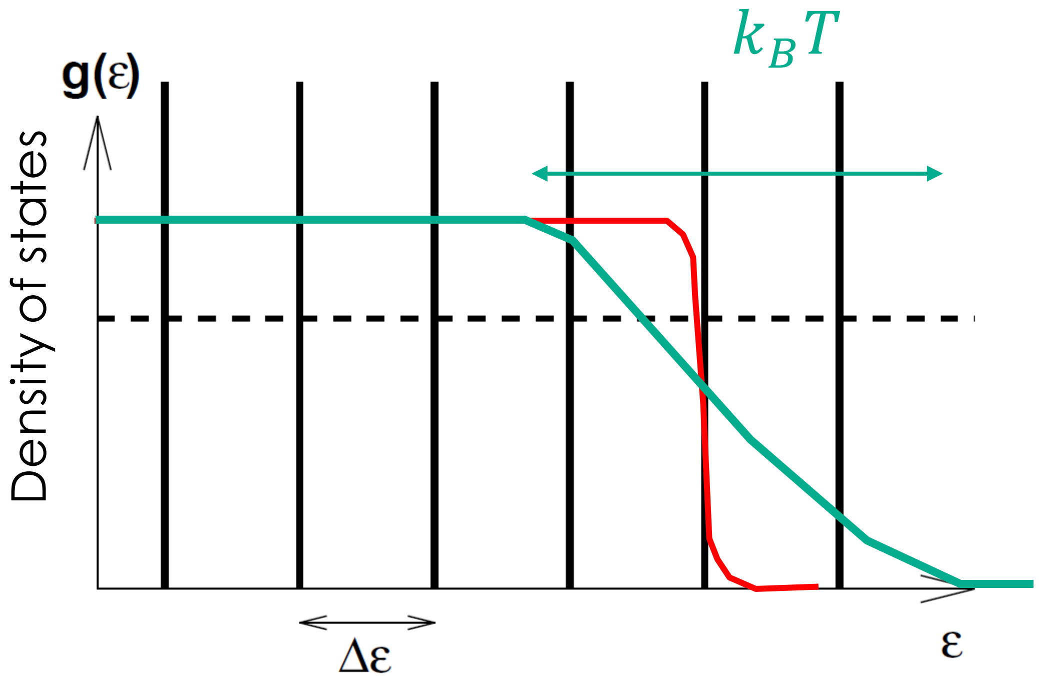

Fermi-Dirac distribution
$f(E, \mu, T)$

$$\hbar\omega_c = \frac{\hbar e B}{m_{cyc}}$$

- Quantum oscillations are suppressed by increasing temperature
- This suppression allows a direct determination of the cyclotron mass m_{cyc}

Effective Mass in $PtSe_2$

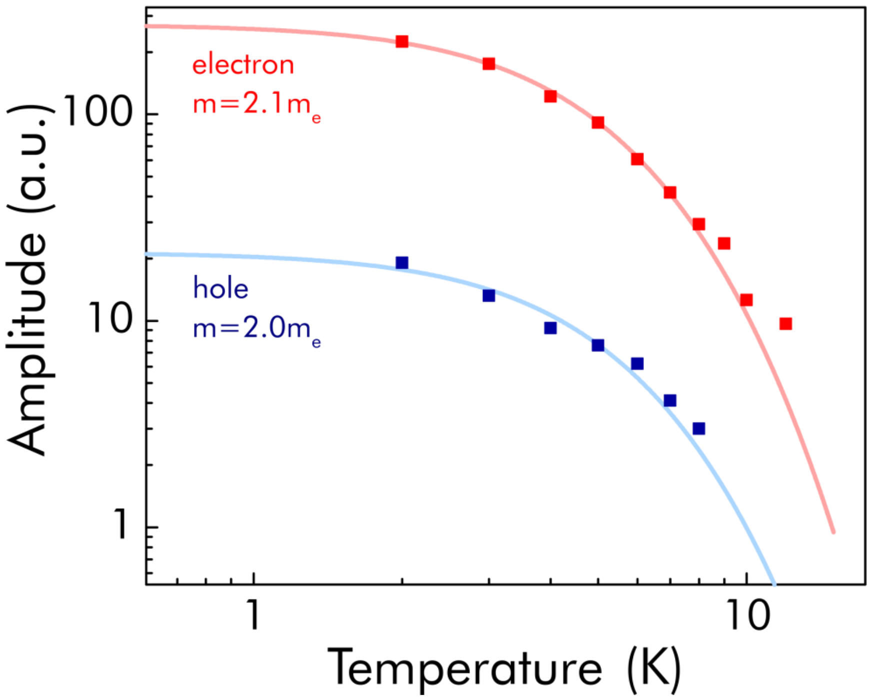

- Band structure: $m_{band} \sim 0.35 m_e$
- Quantum oscillations: $m_{eff} \sim 2 m_e$
- Sizeable mass enhancement

$$m_{eff} = (1 + \lambda)\, m_{band}$$

$$\lambda \sim 4.7$$

Hao Yang et al **2018** New J. Phys.20 043008

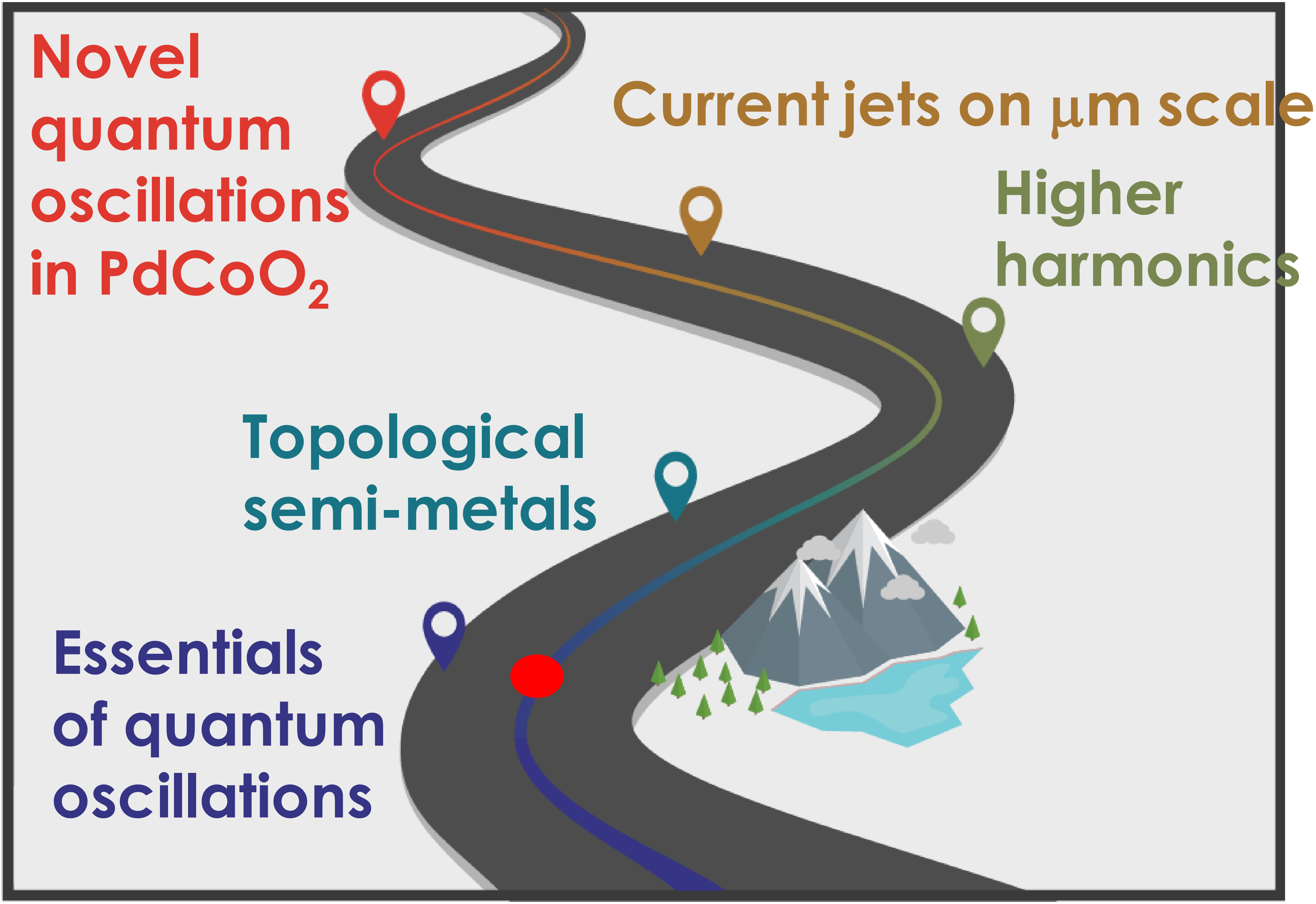
Novel quantum oscillations in $PdCoO_2$
Current jets on μm scale
Higher harmonics
Topological semi-metals
Essentials of quantum oscillations

Key points:

- Topological semi-metals offer a new playground for quantum oscillation
- Quantum oscillation phases encode critical information about the orbit
- Their analysis is challenging; a phase offset of π is NOT a sign of Berry.

New aspects of topology in semi-metals

Bulk

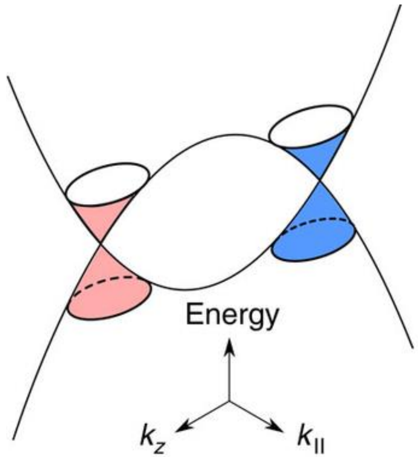

Surface

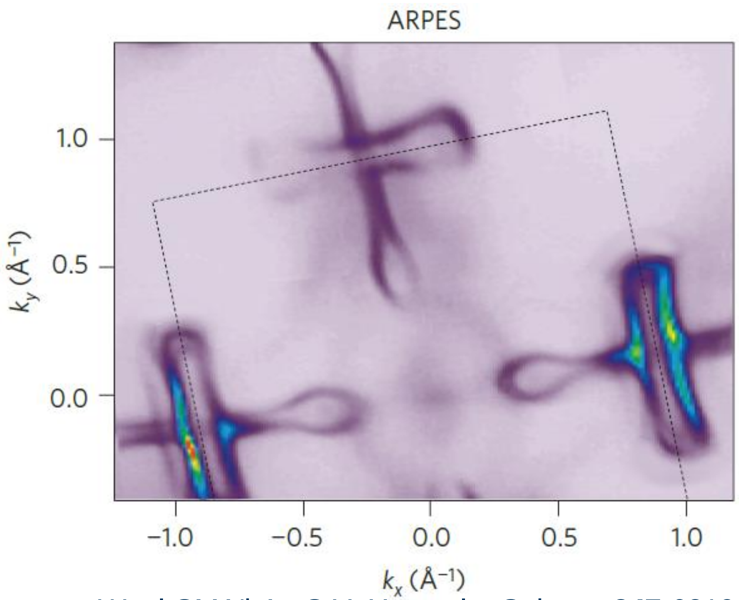

Weyl-SM NbAs S.Y. Xu et al., Science **347** 6219 (2015)

- Gapless linear crossings
- Additional internal degrees of freedom
- Chiral/Helical states
- Relativistic quantum mechanics toolbox
- Associated quantum transport

- Fermi arc surface states
- Bulk-boundary connection
- Topological protection

What physical observables are determined by topology?

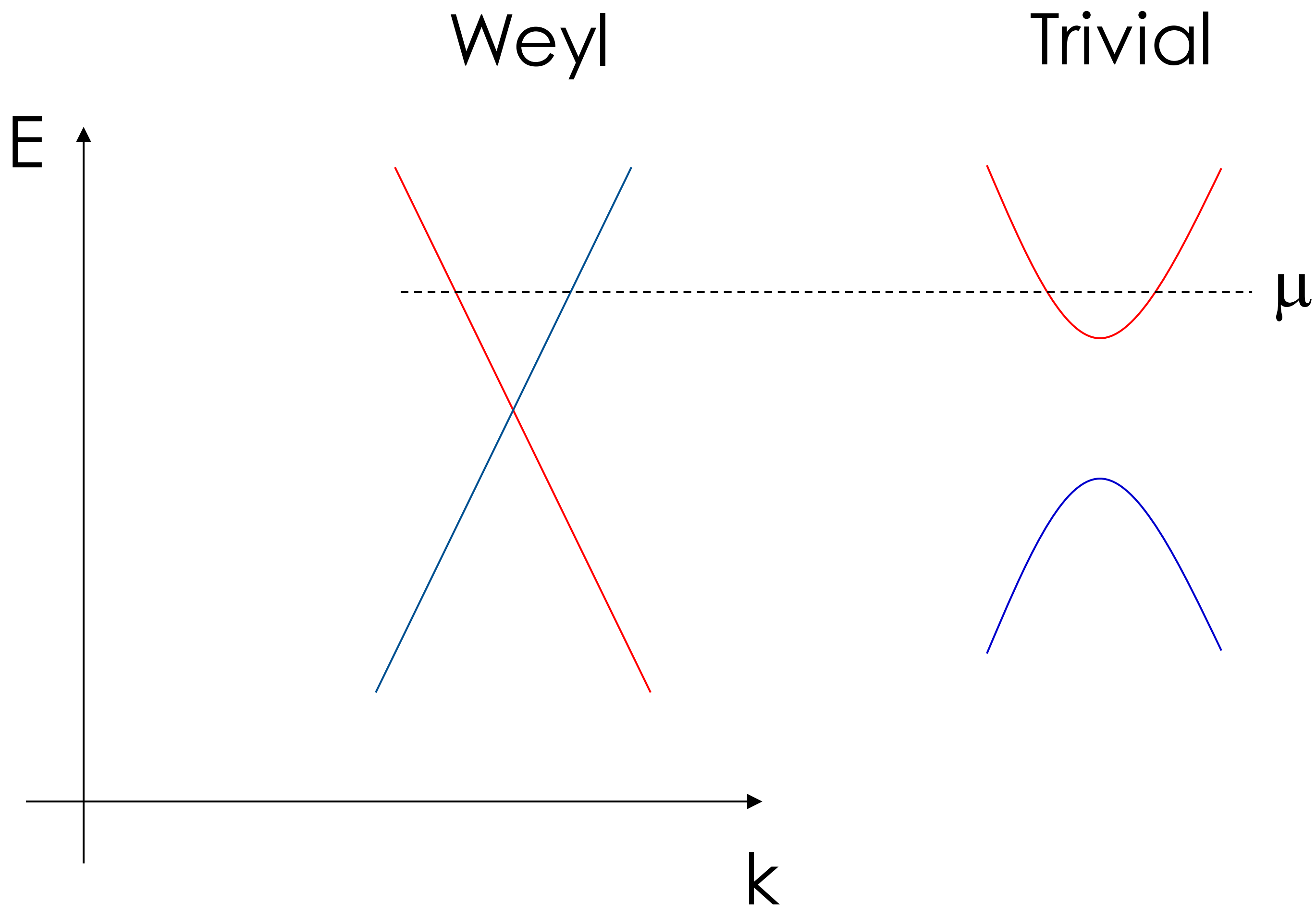

Significant difference in orbital content of waveform,
but how about macroscopic observables?

Quantum oscillations: frequency and phase

$$S(E,k_z)\ \Phi_0/B_n = 2\pi[n+\gamma]$$

Area of Orbit
in k-space

Phase factor

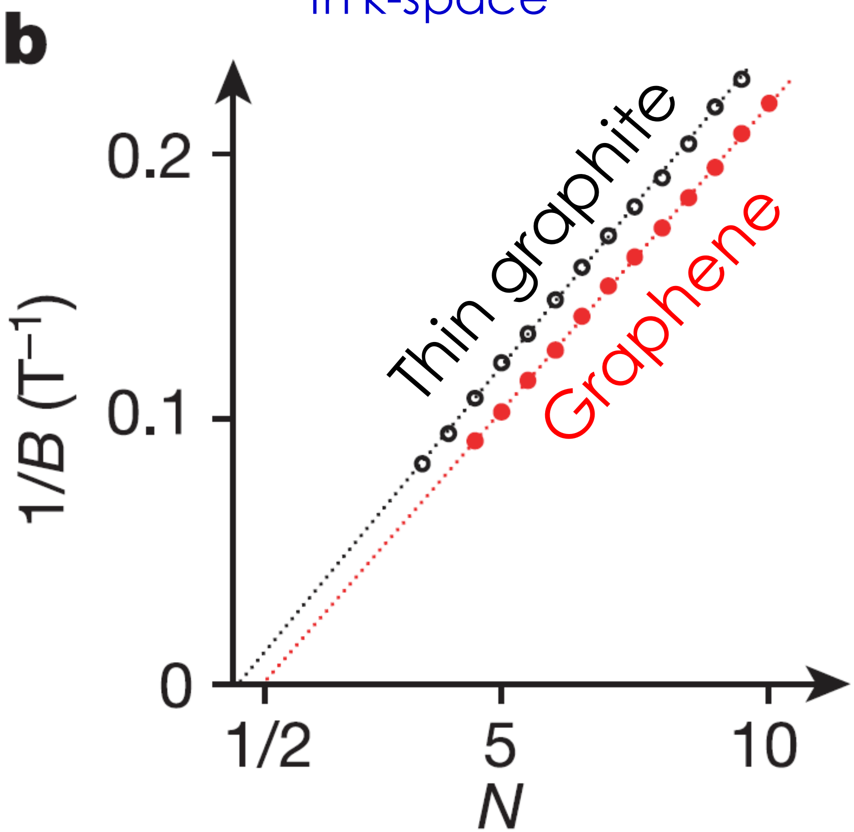

Simple logic:

1. Landau levels are harmonic oscillato
   ($\gamma = 1/2$, as in normal metals)

2. Wave package gains geometric pha
   ($\gamma = 1/2 - 1/2 = 0$)

π phase shift due to Berry phase

Its not that simple!

K.S. Novoselov et al., Nature 438, 197 (2005)
S.G. Sharapov et al., PRB 69, 075104 (2004)
V.P. Gusynin et al., PRB 71, 125124 (2005)

The phase is always a problem

THE DE HAAS–VAN ALPHEN EFFECT*

III. EXPERIMENTS AT FIELDS UP TO 32 kG

By J. S. DHILLON AND D. SHOENBERG, F.R.S.†
National Physical Laboratory of India, New Delhi

(*Received* 22 *October* 1954)

The periodic field dependence of magnetic anisotropy (de Haas–van Alphen effect) has been studied for bismuth and zinc crystals by the torque method between about 1·5 and 32 kG at 4·19° K and about 1·5° K; in each case the orientation was chosen so that only a single fundamental periodicity was present. Particular attention was paid to the phase and harmonic content of the oscillations and to the form of the field dependence of amplitude. For bismuth good agreement was found with the theoretical formula except that the signs of the fundamental and the odd harmonics had to be reversed. For zinc the field dependence of amplitude at high fields was quite at variance with

Bi is a topologically trivial semi-metal,
yet shows a quantum oscillation phase of π!

- Other corrections to phase beside Berry ($\sim\hbar$)
- Ill-defined problem due to degeneracies

Why is this hard? I can compute anything!

$$t_{ij} = t_{ij}\, e^{iA_{ij}\cdot d_{ij}}$$

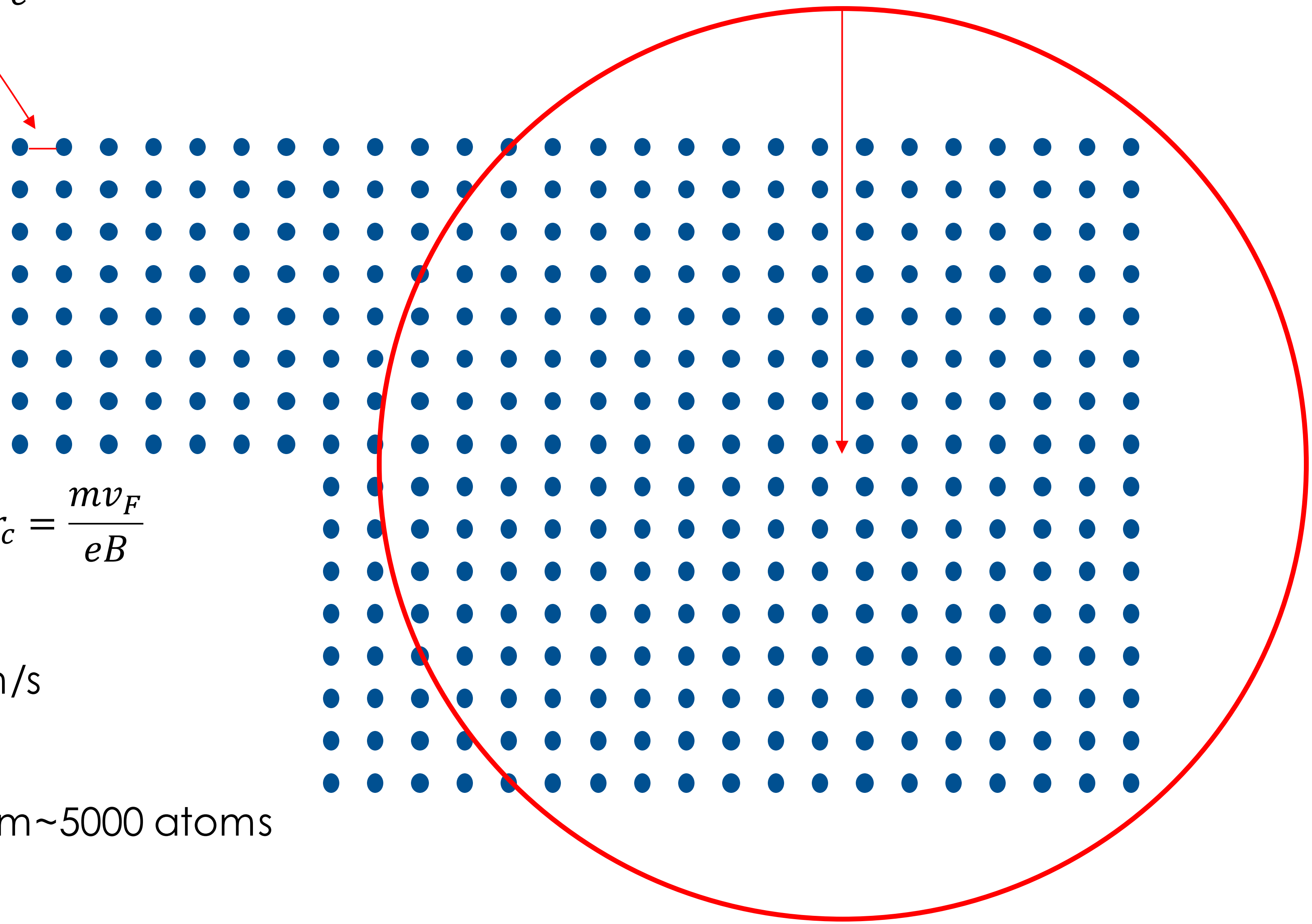

$$r_c = \frac{mv_F}{eB}$$

$m = 1m_e$
$v_F = 10^5$ m/s
$B = 1T$

r_C= 570nm~5000 atoms

IS

π

Maslov

J.B. Keller,
Ann. Phys. (N.Y.) 4, 180 (1958)

G.P. Mikitik, Yu.V. Sharlai,
PRL 82, 2147 (1999)

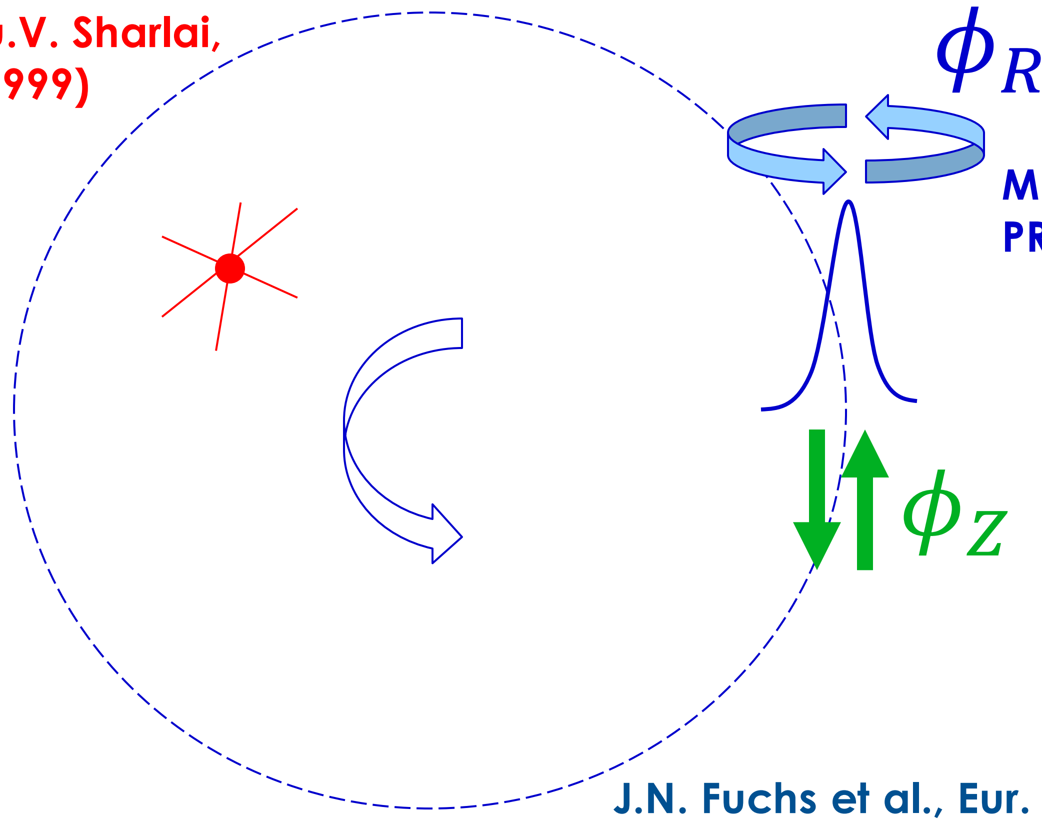

M.-C. Chang, Q. Niu,
PRB 53, 7010 (1996)

$\otimes$ B

J.N. Fuchs et al., Eur. Phys. J. B 77, 351 (2010)
A. Alexandridanata et al., PRX 8, 011027 (2018)

Key point: Degeneracies

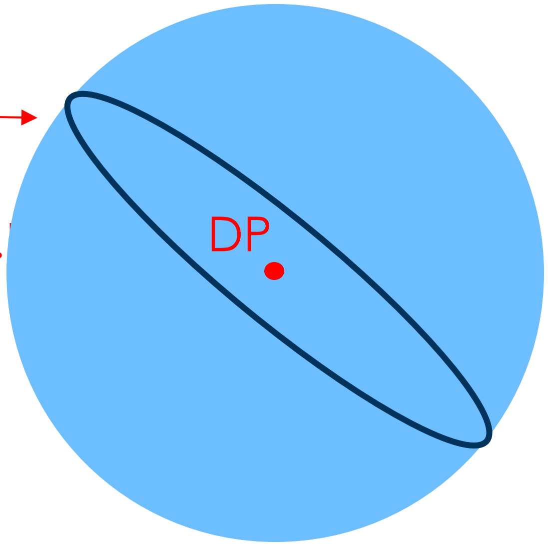

$\psi_1(k), \psi_2(k), \dots, \psi_D(k)$

Each state on orbit D-fold degenerate in k-space (*a*=1..

e.g. D=2: spin-degenerate orbit

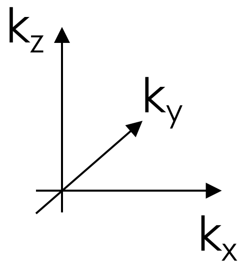

Crystal-symmetry related copies of Fermi surfaces

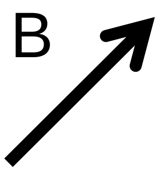

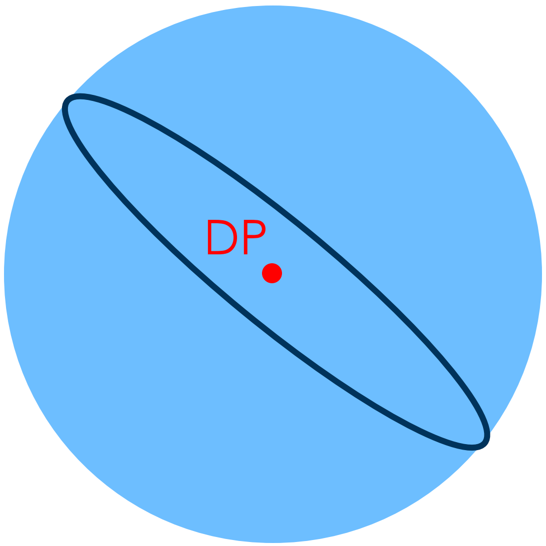

All have same area (=Frequency), but a priori not the same phase!

λ_a^i i^{th} orbit, a^{th} wavefunction

A. Alexandridanata et al., PRX 8, 011027 (2018)

Weyl semi-metal TaAs (I-broken!)

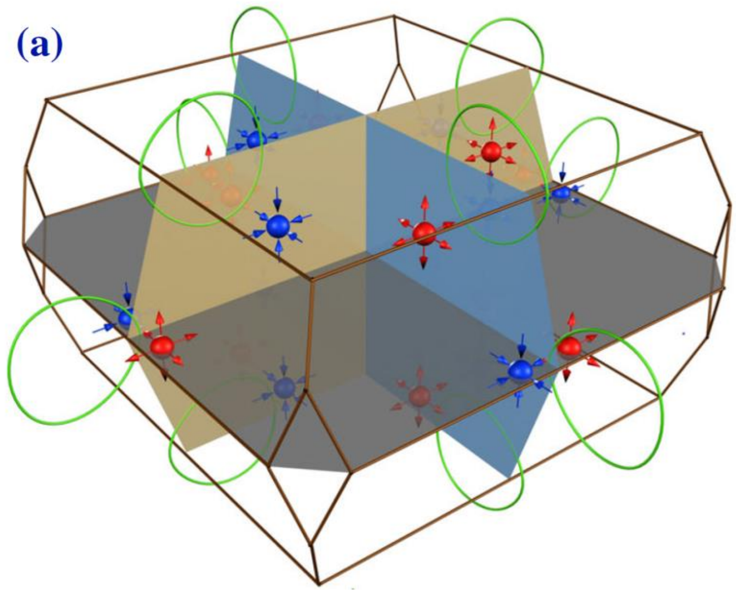

H. Weng et al., PRX 5, 011029 (2015)

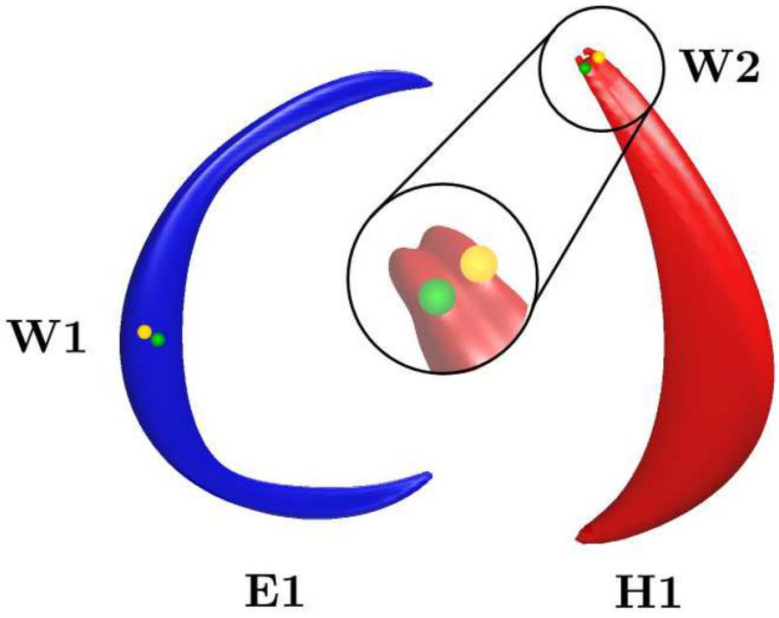

J. Klotz et al., PRB 93, 121105(R) (2016)

Topological semi-metals:

large number of orbit and wavefunction degeneracy usual!

Too many degrees of freedom!

Theory

$$\Delta\rho \sim \underbrace{\sin\left(\frac{F}{B}+\lambda_1\right)+\sin\left(\frac{F}{B}+\lambda_2\right)+\sin\left(\frac{F}{B}+\lambda_3\right)+\sin\left(\frac{F}{B}+\lambda_4\right)+\ldots}$$

Each orbit contributes an oscillatory component at same frequency...
... but a priory different phase!

Experiment

$$=\sin\left(\frac{F}{B}+\Theta\right)$$

Crystal symmetry reduces degrees of freedom

Crystal is T and I symmetric (hence D=2 spin degeneracy)
But orbit i is <u>*not*</u> T or I symmetric, only TI.

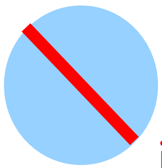

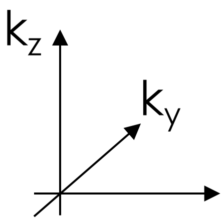

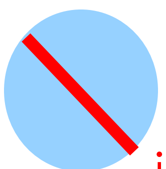

Preserves sign? Time reversal?

	u	s	Symmetry constraints		λ
(I) $\forall \boldsymbol{k}^{\perp}, \boldsymbol{k}^{\perp} = g \circ \boldsymbol{k}^{\perp}$	0	0	$\mathcal{A} = \bar{g}\mathcal{A}\bar{g}^{-1}$	$\bar{g}^2 = e^{i\pi F\mu\text{-}i\boldsymbol{k}\cdot\boldsymbol{R}}$	$\cdots$
	0	1	$\mathcal{A} = \bar{g}\mathcal{A}^{*}\bar{g}^{-1}$	$(\bar{g}K)^2 = e^{i\pi F\mu\text{-}i\boldsymbol{k}\cdot\boldsymbol{R}}$	$e^{i\sum_a \lambda_a} \in \mathbb{R}$
(II-A) $\boldsymbol{k}^{\perp} \in \mathfrak{o}, \lvert\mathfrak{o}\rvert = \lvert g \circ \mathfrak{o}\rvert$	0	0	$\mathcal{A} = \bar{g}\mathcal{A}\bar{g}^{-1}$	$\bar{g}^N = \mathcal{A}^{\pm N/L} e^{i\pi F\mu}$	$\cdots$
	0	1	$\mathcal{A} = \bar{g}\mathcal{A}^{*}\bar{g}^{-1}$	$(\bar{g}K)^N = \mathcal{A}^{\pm N/L} e^{i\pi F\mu}$	$e^{i\sum_a \lambda_a} \in \mathbb{R}$
	1	0	$\mathcal{A} = \bar{g}\mathcal{A}^{-1}\bar{g}^{-1}$	$\bar{g}^N = e^{i\pi F\mu\text{-}i\boldsymbol{k}\cdot\boldsymbol{R}}$	$e^{i\sum_a \lambda_a} \in \mathbb{R}$
	1	1	$\mathcal{A} = \bar{g}\mathcal{A}^{t}\bar{g}^{-1}$	$(\bar{g}K)^N = e^{i\pi F\mu\text{-}i\boldsymbol{k}\cdot\boldsymbol{R}}$	$\cdots$
(II-B) $\boldsymbol{k}^{\perp} \in \mathfrak{o}, \lvert\mathfrak{o}\rvert \neq \lvert g \circ \mathfrak{o}\rvert$	0	0	$\mathcal{A}_{i+1} = \bar{g}_i\mathcal{A}_i\bar{g}_i^{-1}$	$\bar{g}_N \ldots \bar{g}_1 = e^{i\pi F\mu - i\boldsymbol{k}\cdot\boldsymbol{R}}$	$\{\lambda_a^{i+1}\} = \{\lambda_a^{i}\}$
	0	1	$\mathcal{A}_{i+1} = \bar{g}_i\mathcal{A}_i^{*}\bar{g}_i^{-1}$	$\bar{g}_N K \ldots \bar{g}_1 K = e^{i\pi F\mu\text{-}i\boldsymbol{k}\cdot\boldsymbol{R}}$	$\{\lambda_a^{i+1}\} = \{\text{-}\lambda_a^{i}\}$
	1	0	$\mathcal{A}_{i+1} = \bar{g}_i\mathcal{A}_i^{-1}\bar{g}_i^{-1}$	$\bar{g}_N \ldots \bar{g}_1 = e^{i\pi F\mu\text{-}i\boldsymbol{k}\cdot\boldsymbol{R}}$	$\{\lambda_a^{i+1}\} = \{\text{-}\lambda_a^{i}\}$
	1	1	$\mathcal{A}_{i+1} = \bar{g}_i\mathcal{A}_i^{t}\bar{g}_i^{-1}$	$\bar{g}_N K \ldots \bar{g}_1 K = e^{i\pi F\mu\text{-}i\boldsymbol{k}\cdot\boldsymbol{R}}$	$\{\lambda_a^{i+1}\} = \{\lambda_a^{i}\}$

A. Alexandridanata et al., PRX 8, 011027 (2018)

3D DSM: zero-sum rule for each orbit: $\lambda_1^i + \lambda_2^i = 0$

4 unknowns but only 1 measured phase, 2 constraints

Crystal symmetry reduces degrees of freedom

Experimental phase

$$\Theta := \frac{\lambda_1 + \lambda_2}{2} + \pi\left(1 - \text{sign}\left[\cos\left(\frac{\lambda_1 - \lambda_2}{2}\right)\right]\right)/2$$

$$\Theta = \pi\big(1 - sign(\cos(\lambda_1))\big)/2$$

In the 3D DSM, both π and 0 are possible experimental phases.

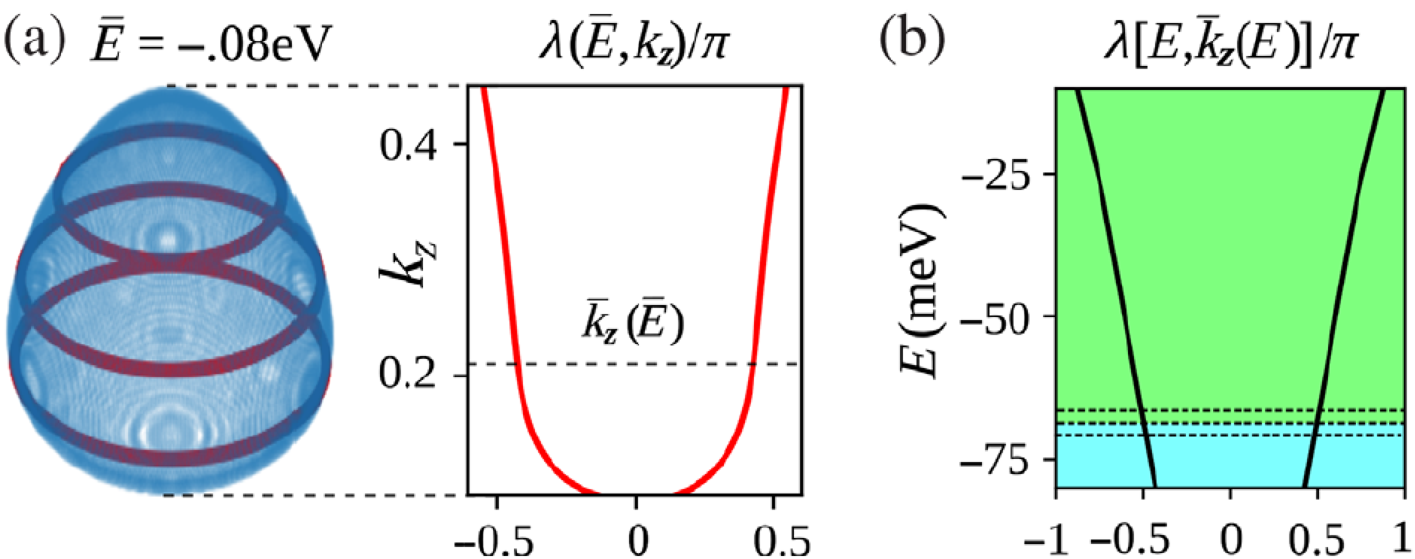

$\Theta = \pi$

$\Theta = 0$

Dirac semi-metal Cd_3As_2 : spherical bulk Fermi surface

Magnetoresistance

2 3D Dirac cones

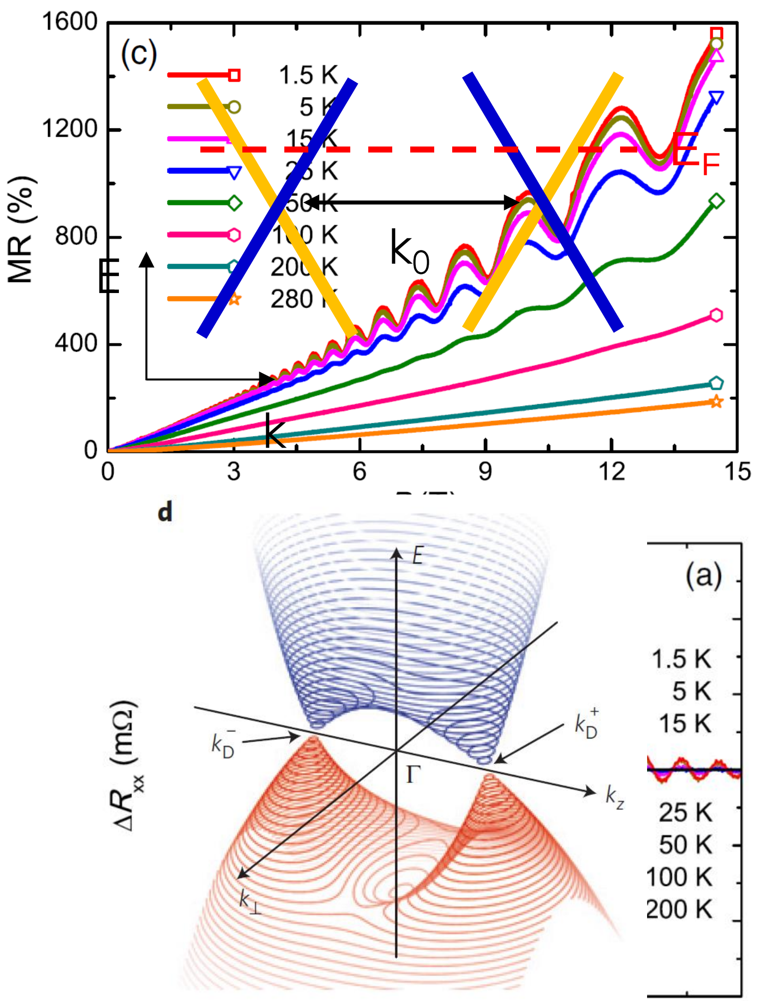

S. Jeon et al., Nature Materials 13 (2014)

(Almost) spherical Fermi surface around each Dirac point

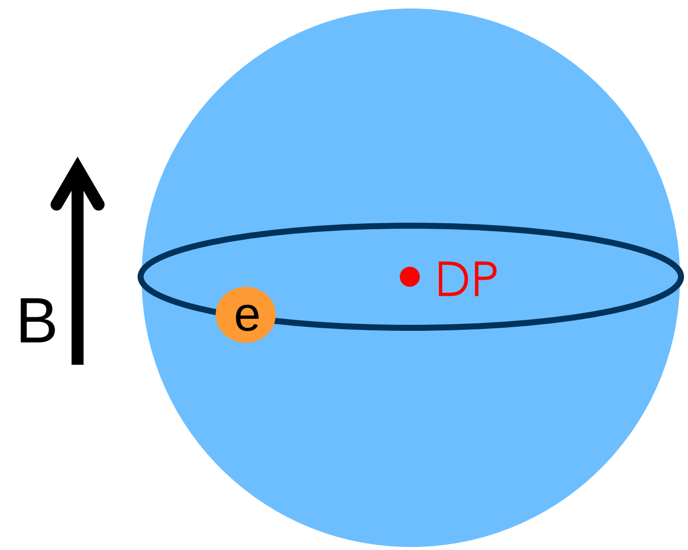

Cd_3As_2 bulk „spherical“ Fermi surfac
confirmed by single frequency

L.P. He et al., PRL **113** 246402 (2014)

Cd_3As_2 a shows a π offset: Berry?

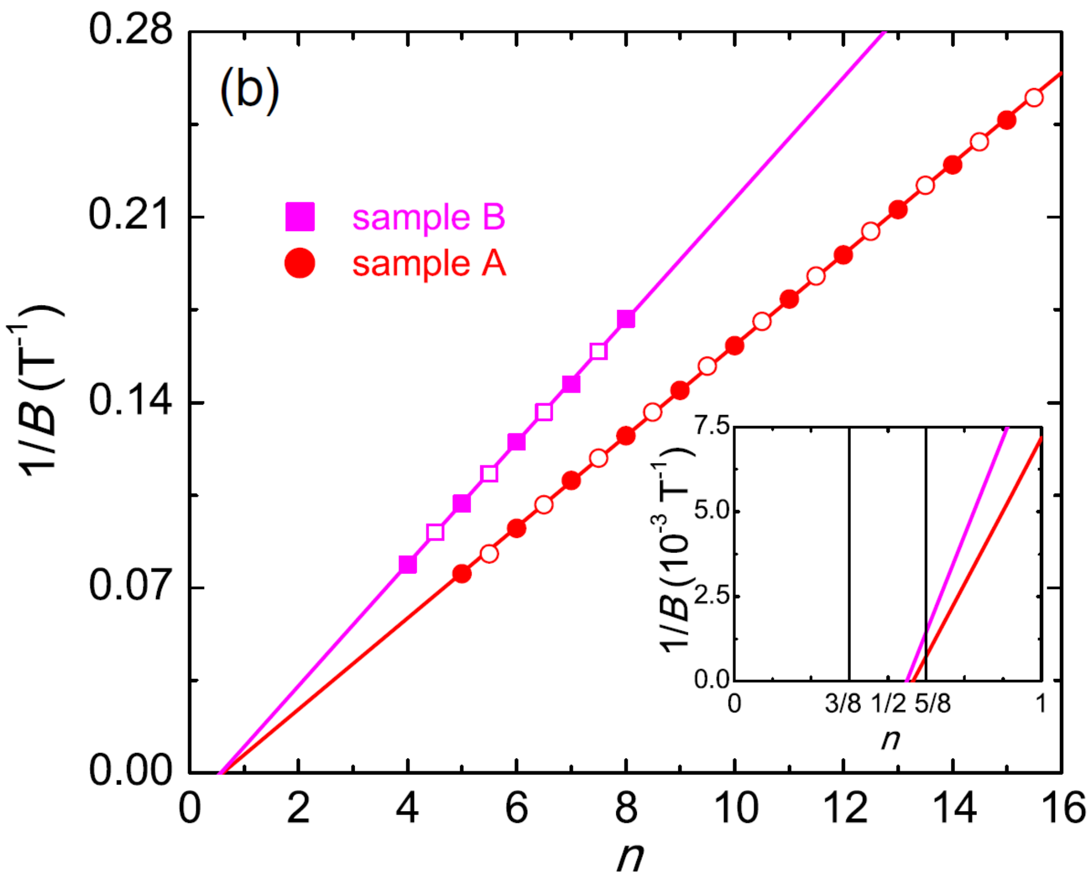

- Cd_3As_2 shows a QO phase of π.
- The Roth correction $\pm\pi/4$ is not a range.
  Minimum orbit: $+\frac{\pi}{4}$
  Maximum orbit: $-\frac{\pi}{4}$

Does this prove a Dirac dispersion

Unfortunately, not...

$$\Theta = \pi\big(1 - sign(\cos(\lambda_1))\big)/2$$

L. Roth, Phys. Rev. **145**, 434-448 (1966)
L.P. He et al., PRL **113** 246402 (2014)

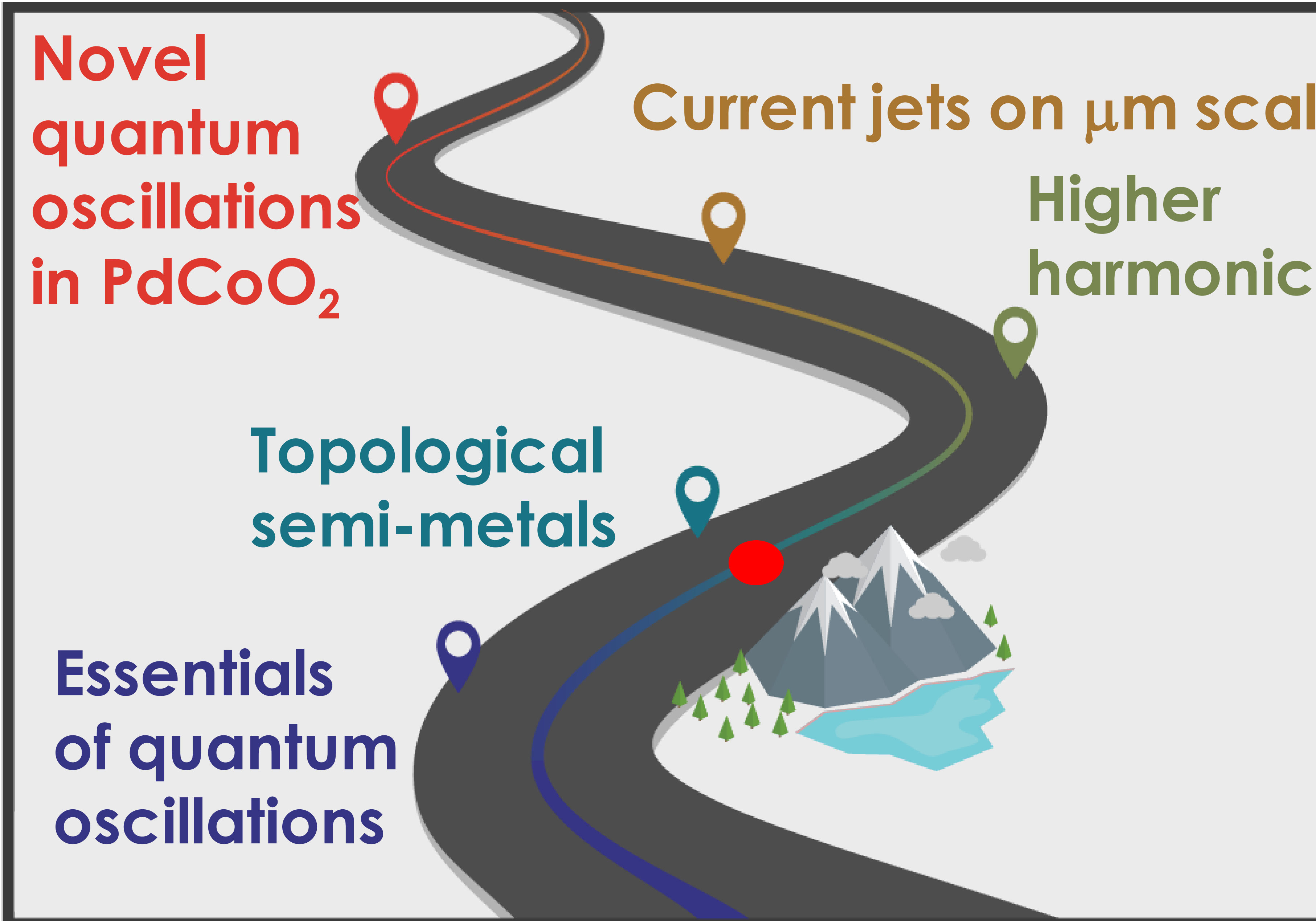
Novel quantum oscillations in $PdCoO_2$
Current jets on μm scale
Higher harmonics
Topological semi-metals
Essentials of quantum oscillations

Key points:

- Quantum oscillation phase is not quantized and can take any value.
- A phase-offset of π does not prove/disprove a Berry phase.
- A proper treatment of all corrections based on higher harmonics can, in some cases, allow a direct detection of topological phases.

Higher Harmonics save the day!

$$\delta\mathcal{M}_{\boldsymbol{i}} = -\frac{1}{(2\pi)^{3/2}}\frac{kT}{|\boldsymbol{B}|}\frac{S}{l|S_{zz}|^{1/2}}\sum_{a=1}^{D}\boxed{\sum_{r=1}^{\infty}}e^{-[(r\pi)/(\omega_c\tau)]}\frac{\sin[\boldsymbol{r}(l^2S+\lambda_a^{\boldsymbol{i}}-\phi_M)\pm\pi/4]}{r^{1/2}\sinh(2\pi^2 rkT/\hbar\omega_c)}$$

Harmonic
index *r*

Phases of higher harmonics provide further constraints allowing to solve for the actual λ!

A. Alexandridanata et al., PRX 8, 011027 (2018)

The tetragonal crystal structure of $LaRhIn_5$

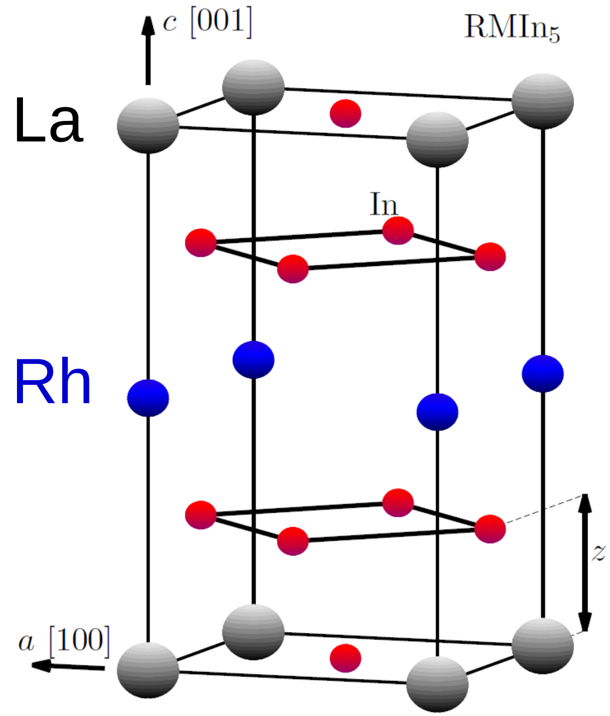

Band structure predicts a Dirac node and large metallic bands

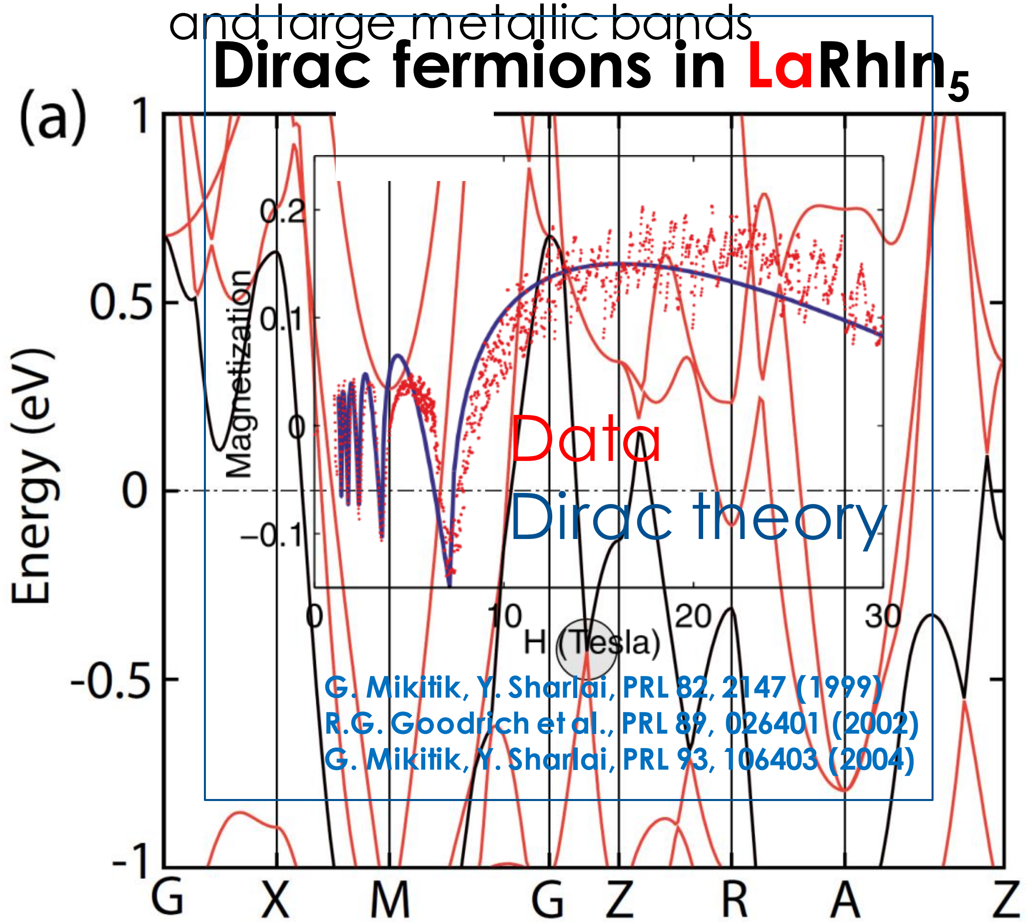

~0.1% of DOS due to Dirac Fermi surface

$LaRhIn_5$

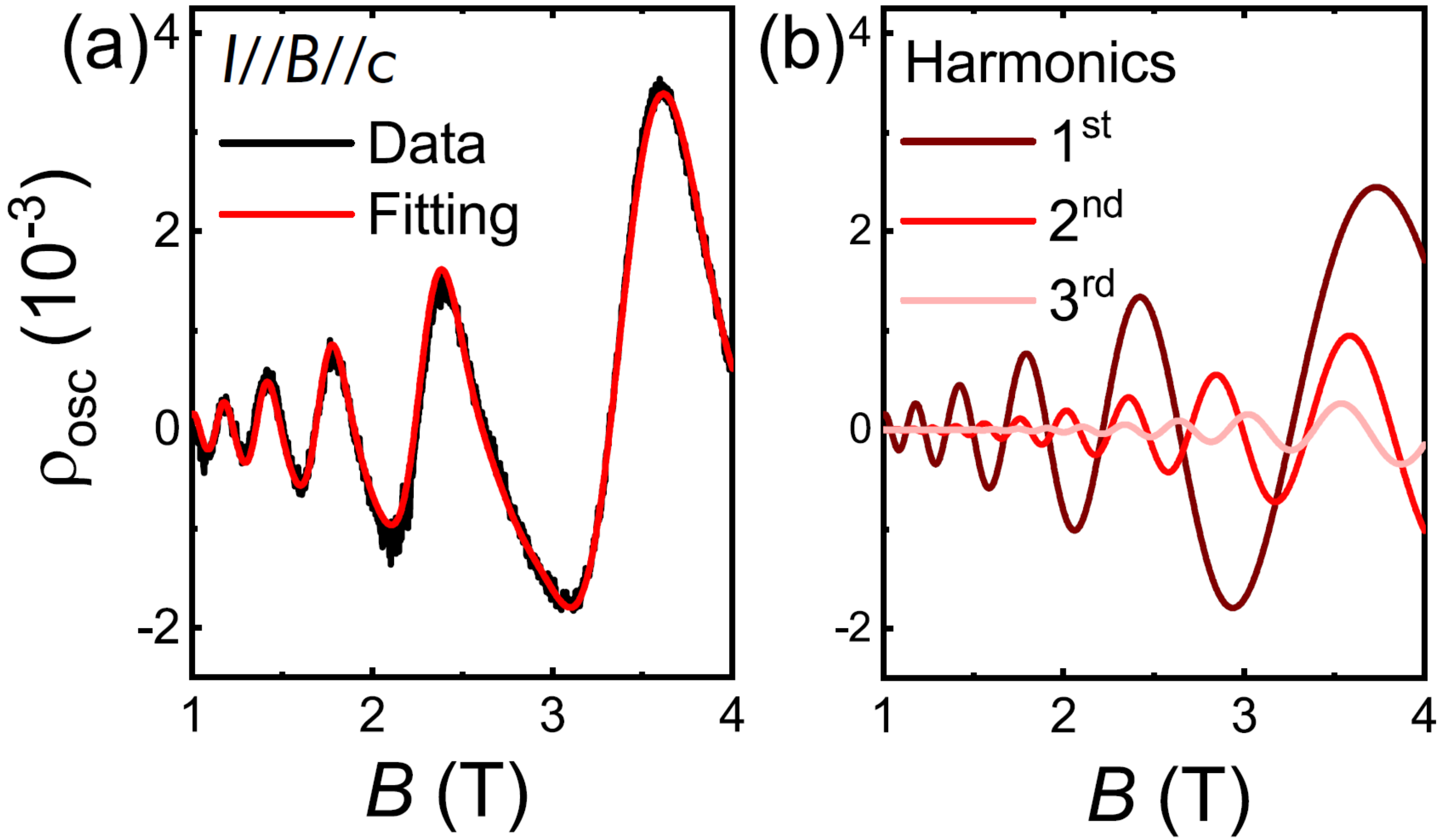

$$\frac{\Delta\rho}{\rho_{bg}} = \sum_{r=1}^{\infty} A' \sqrt{\frac{B}{r}} \boxed{cos(r\lambda_1^{\uparrow})} R_T^r R_D^r cos[r(2\pi\frac{F}{B} - \pi) + \phi_{LK}]$$

M. Guo et al., on arXiv soo

λ is in the amplitude ratio!

$$\frac{A_1}{A_r} = \frac{\cos(\lambda)}{\cos(r\lambda)}$$

Experimentally:

$$\lambda = 0.96 \pm 0.01\,\pi$$

Direct evidence for Berry phase of π

Despite multi-band, unknown LL positions,...

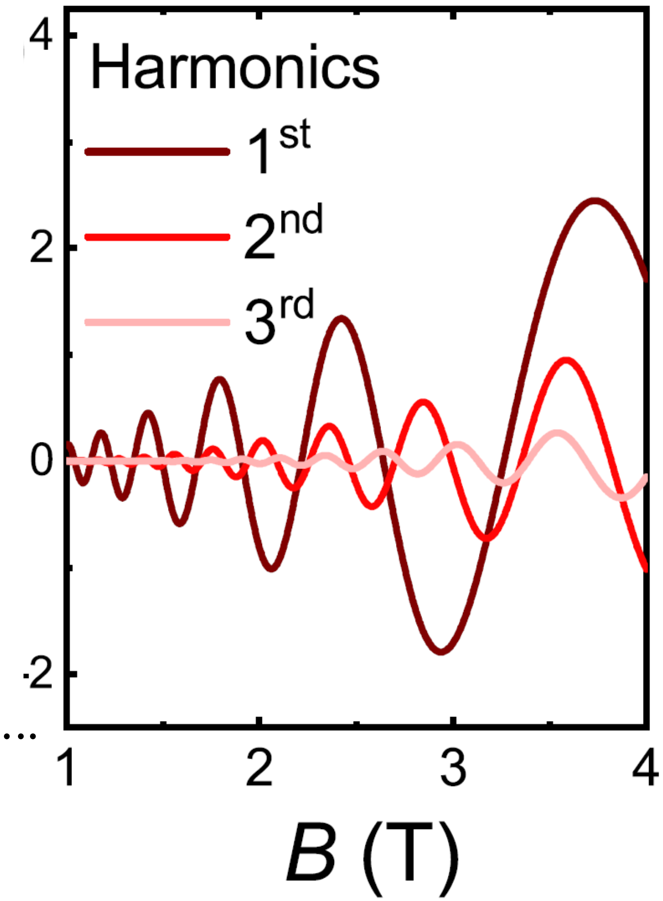

$$\frac{\Delta\rho}{\rho_{bg}} = \sum_{r=1}^{\infty} A' \sqrt{\frac{B}{r}}\, \boxed{cos(r\lambda_1^{\uparrow})} R_T^r R_D^r cos[r(2\pi\frac{F}{B} - \pi) + \phi_{LK}]$$

M. Guo et al., on arXiv soo

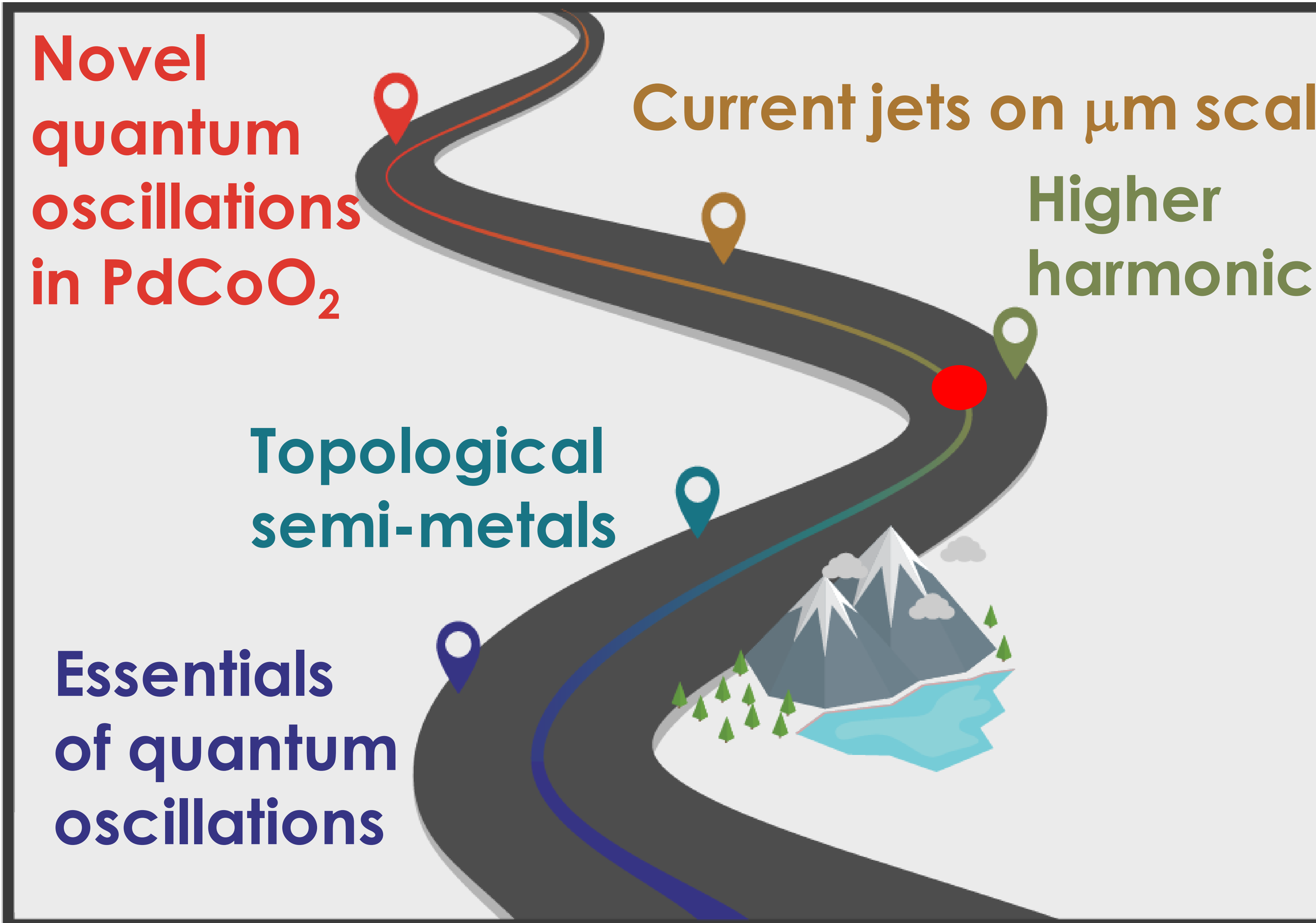
Novel quantum oscillations in $PdCoO_2$
Current jets on μm scale
Higher harmonics
Topological semi-metals
Essentials of quantum oscillations

Key points:

- Focused Ion Beam enables new quantum experiments in exotic materials
- New quantum process due to conserved chirality : Weyl orbit
- Beware of longitudinal magnetoresistance in semi-metals
- Controlled current beams over long distances in Cd_3As_2

Bulk-surface distinction vanishes in strong magnetic fields

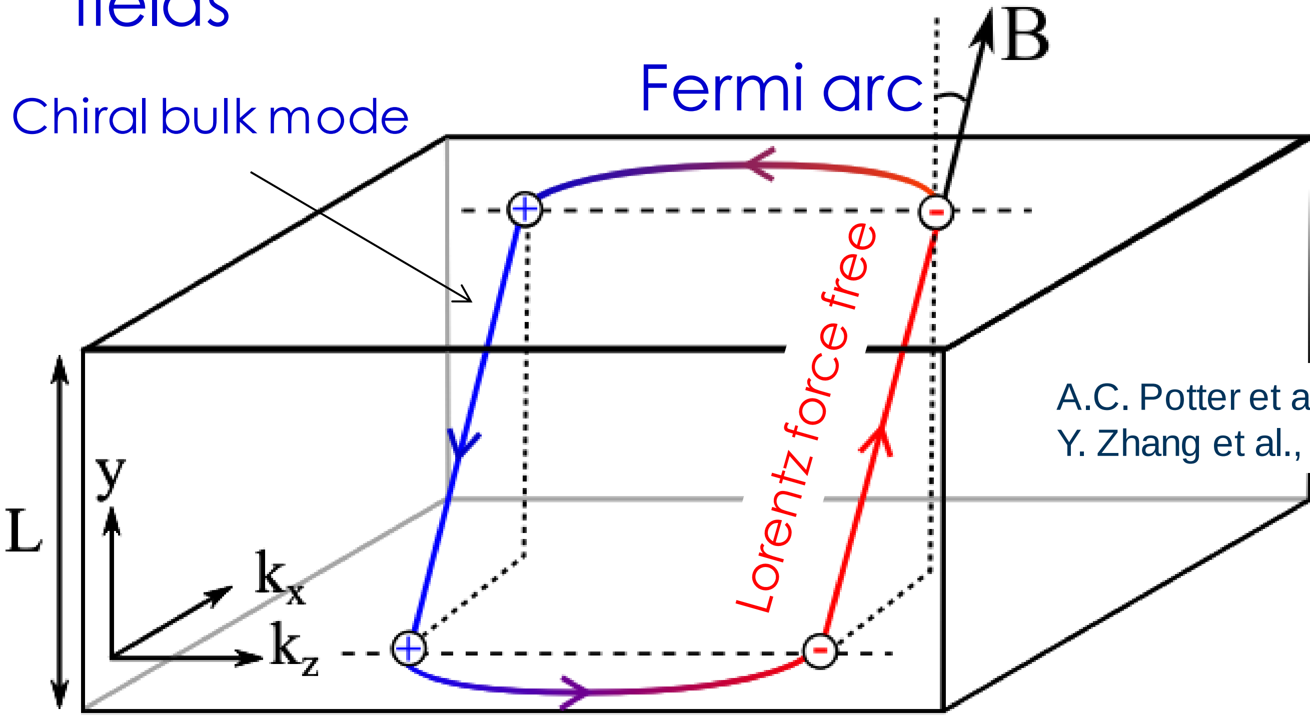

A.C. Potter et al., Nat. Comm. 5:5161 (2014);
Y. Zhang et al., Scientific Reports 6:23741 (2016)

New quantum process in Dirac-SM Cd_3As_2 nanodevices

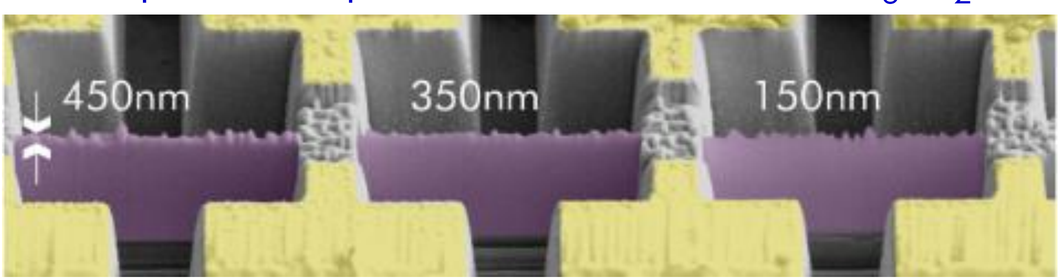

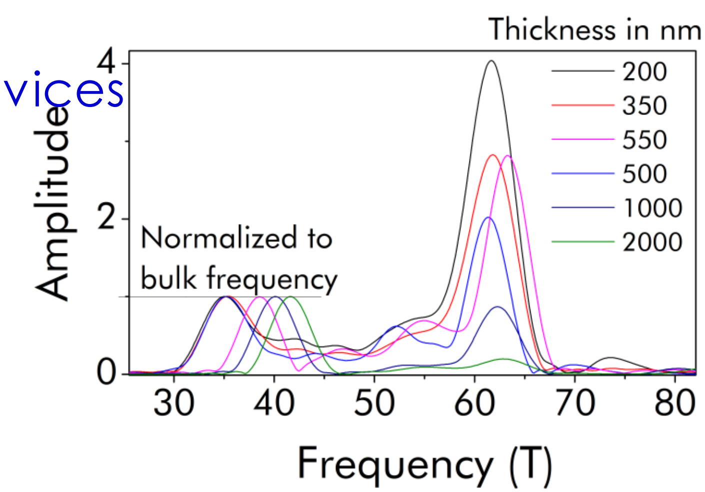

P.J.W.M et al., Nature **535**, 266–270 (2016)

Semi-classical effects: Currents at a distance

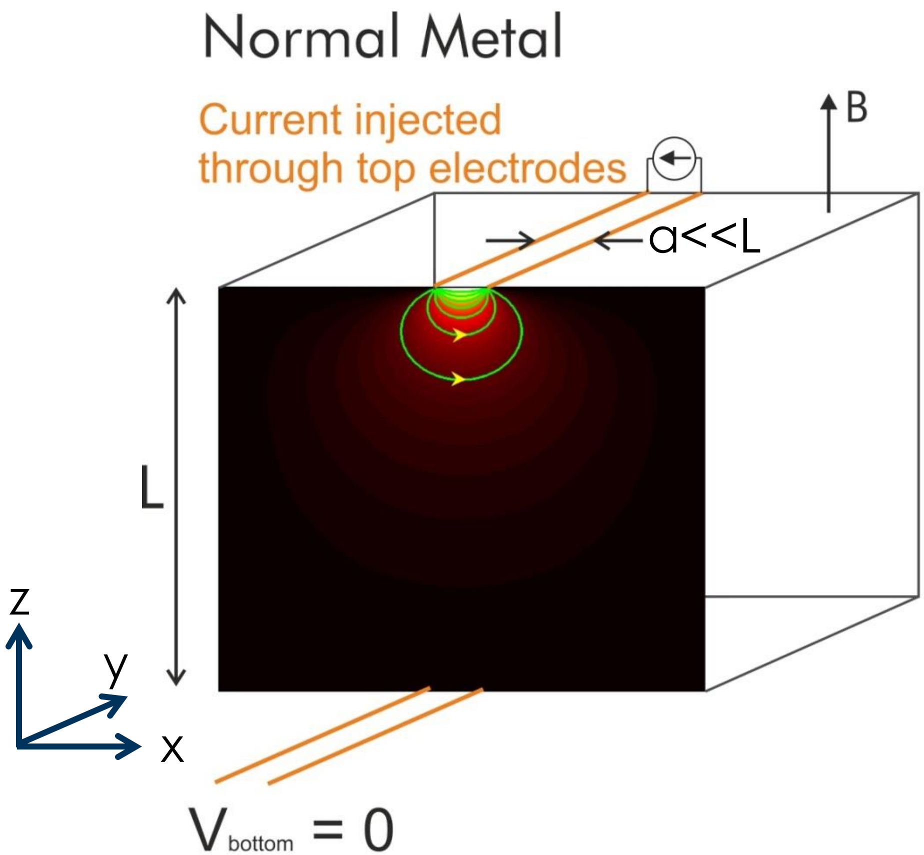

Baum, Berg, Parameswaran, Stern. Phys. Rev. X 5, 041046 (2015)

FIB Sample Preparation
Structure Milling

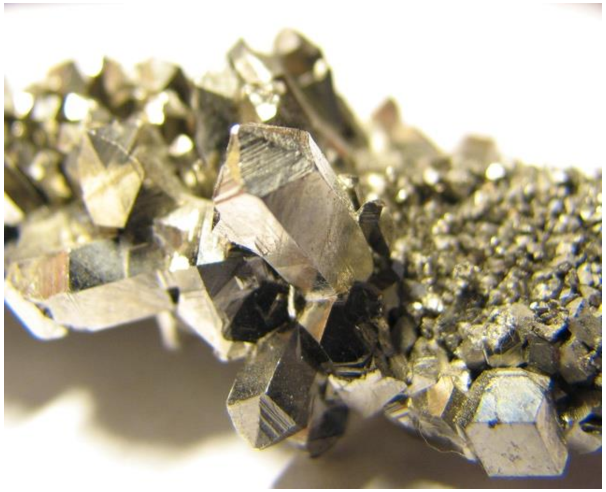

Start from bulk material…

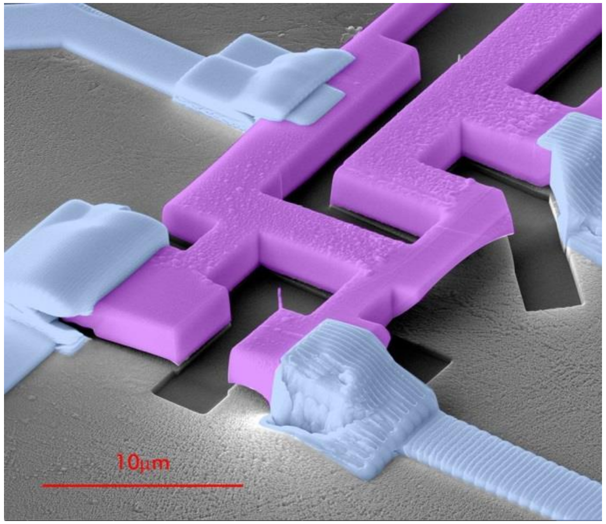

… and turn it into a microstructure

Focused Ion Beam microfabrication

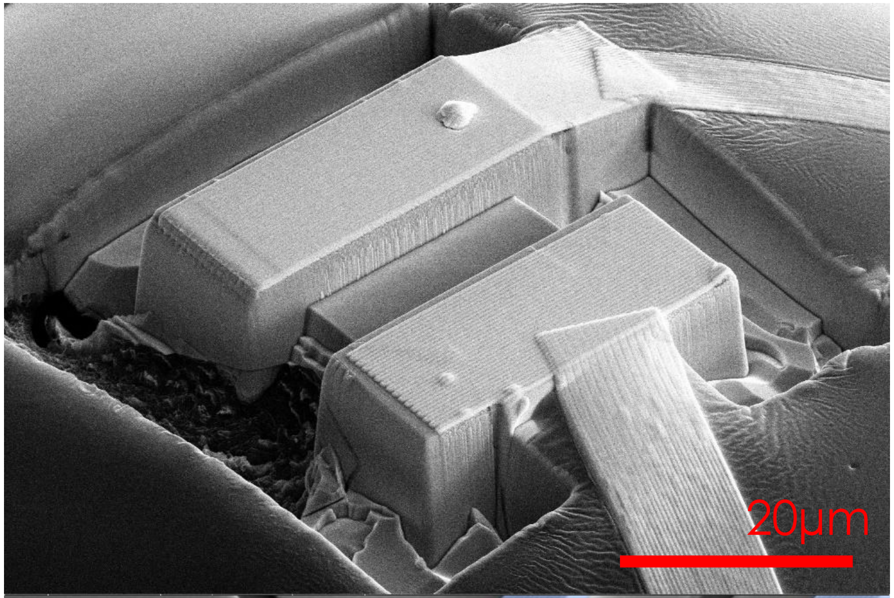

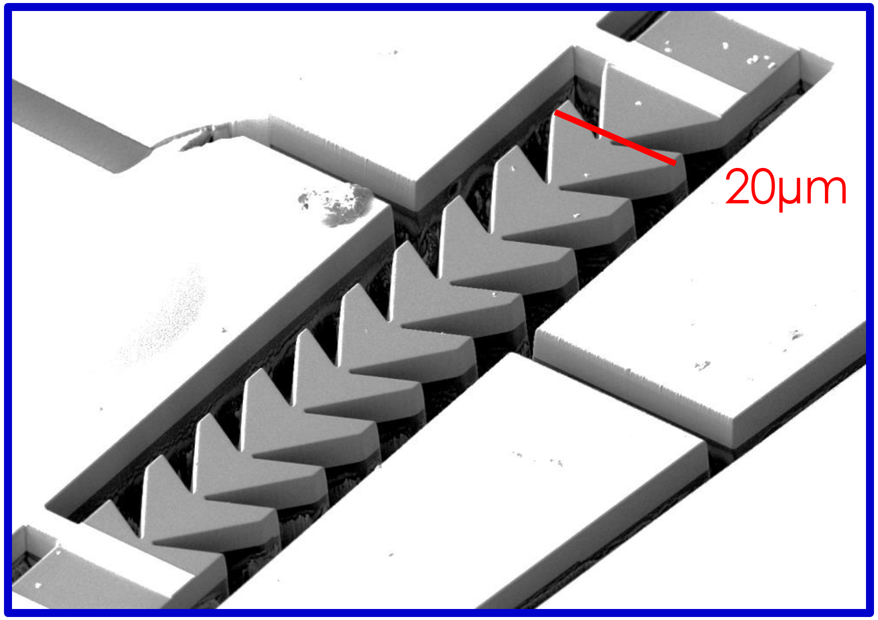

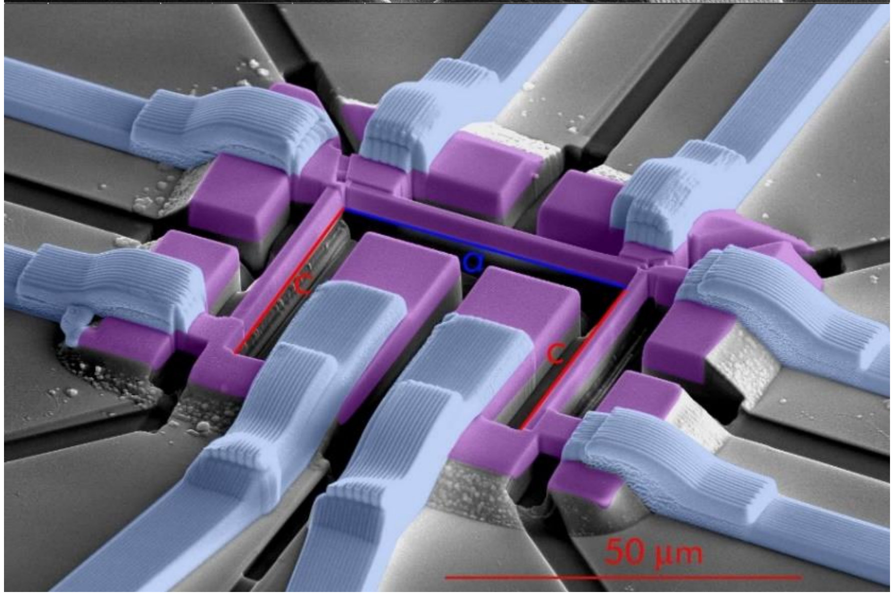

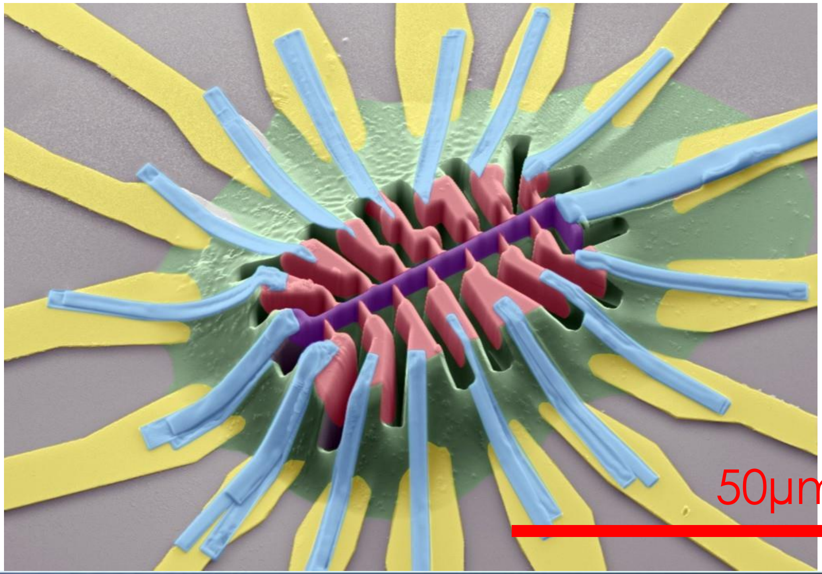

Non-local transport in Cd_3As_2

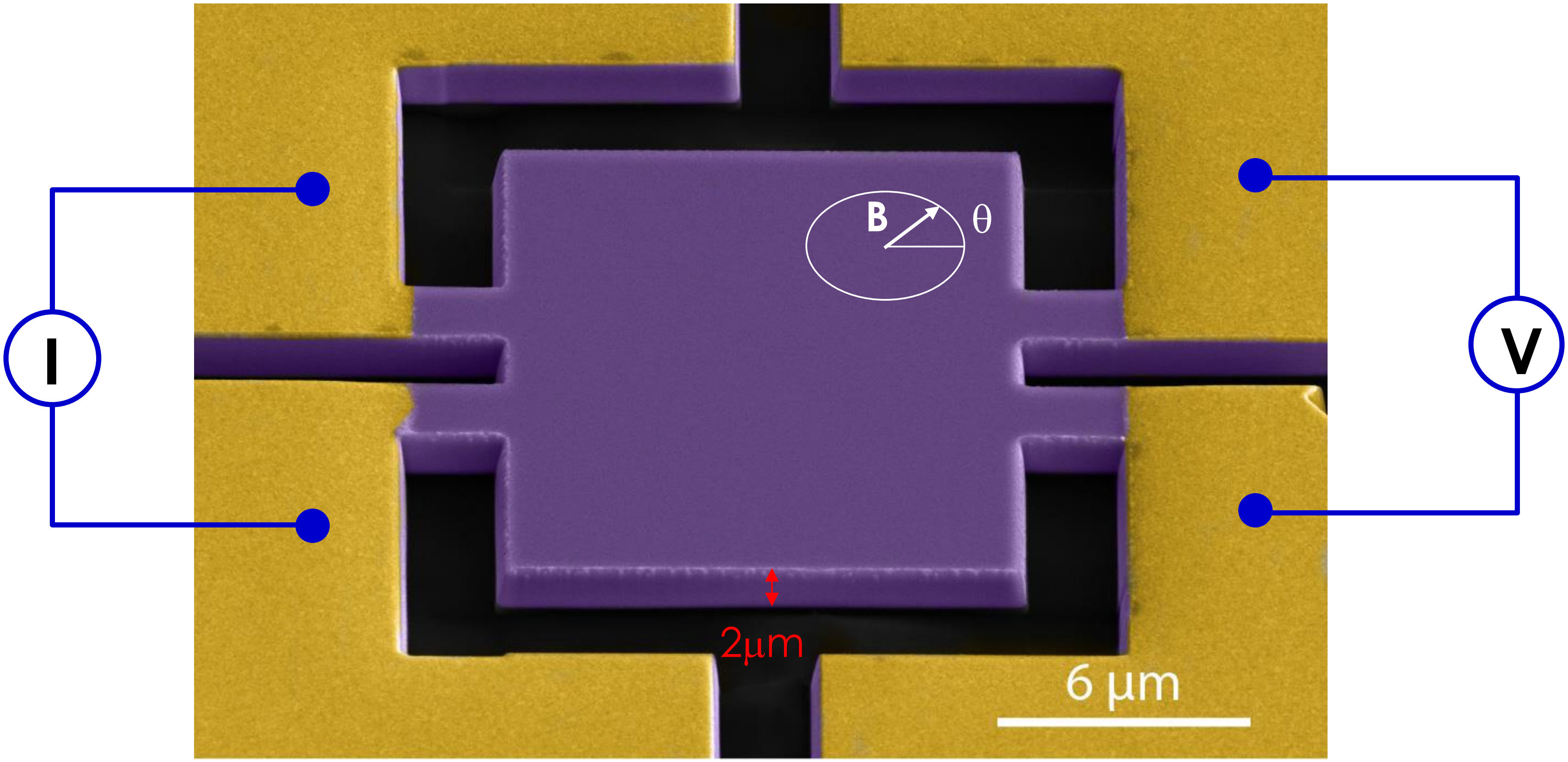

Non-local transport in Cd_3As_2

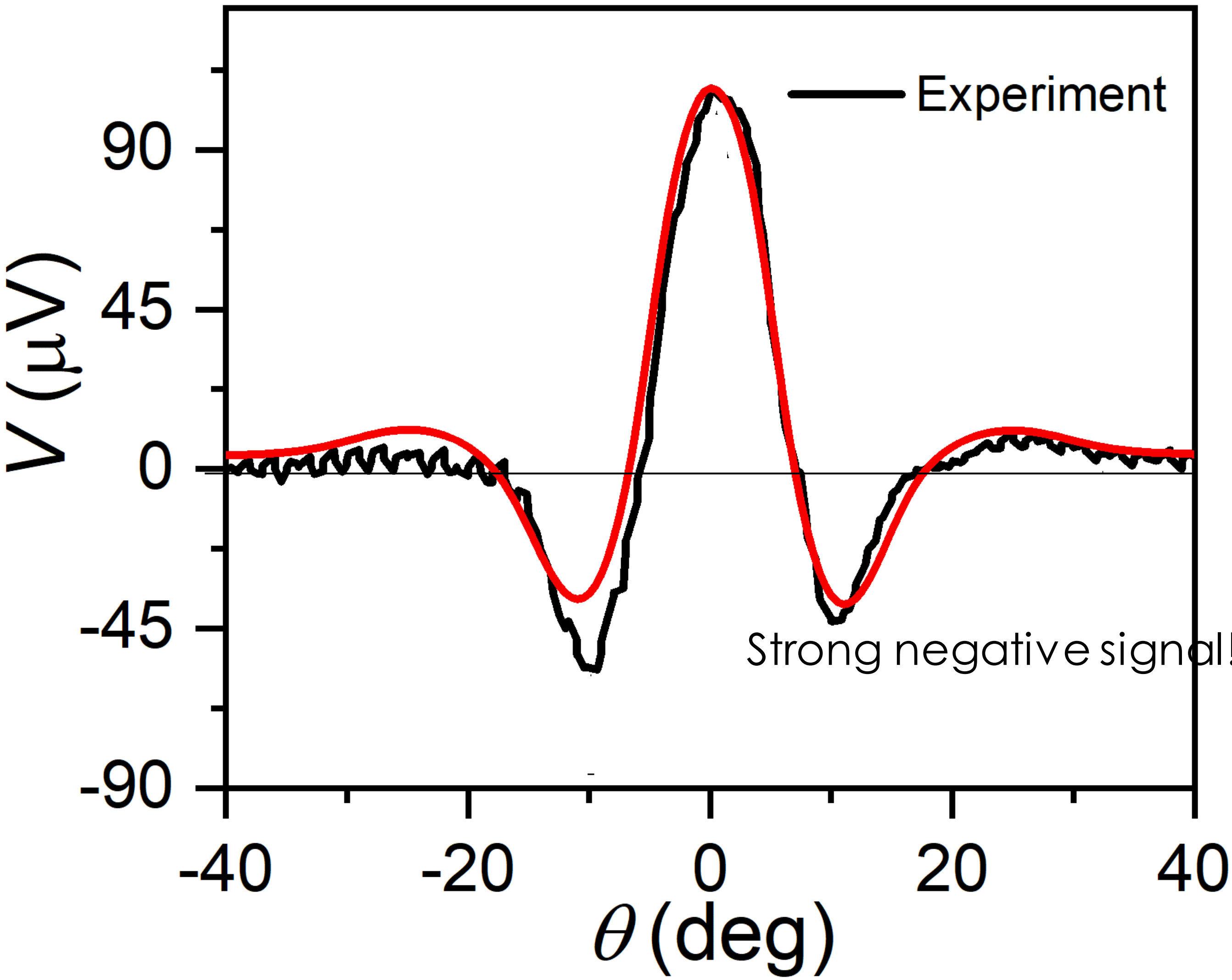

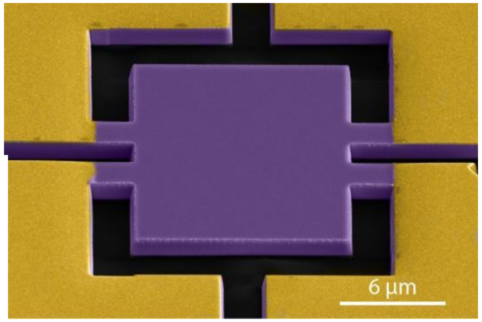

Strong negative signal!

Beware of semiclassics!

Huge field-induced anisotropy + large Hall effect

Zero field: isotropic metal
14T: conducts >700 times better along field than perpendicular

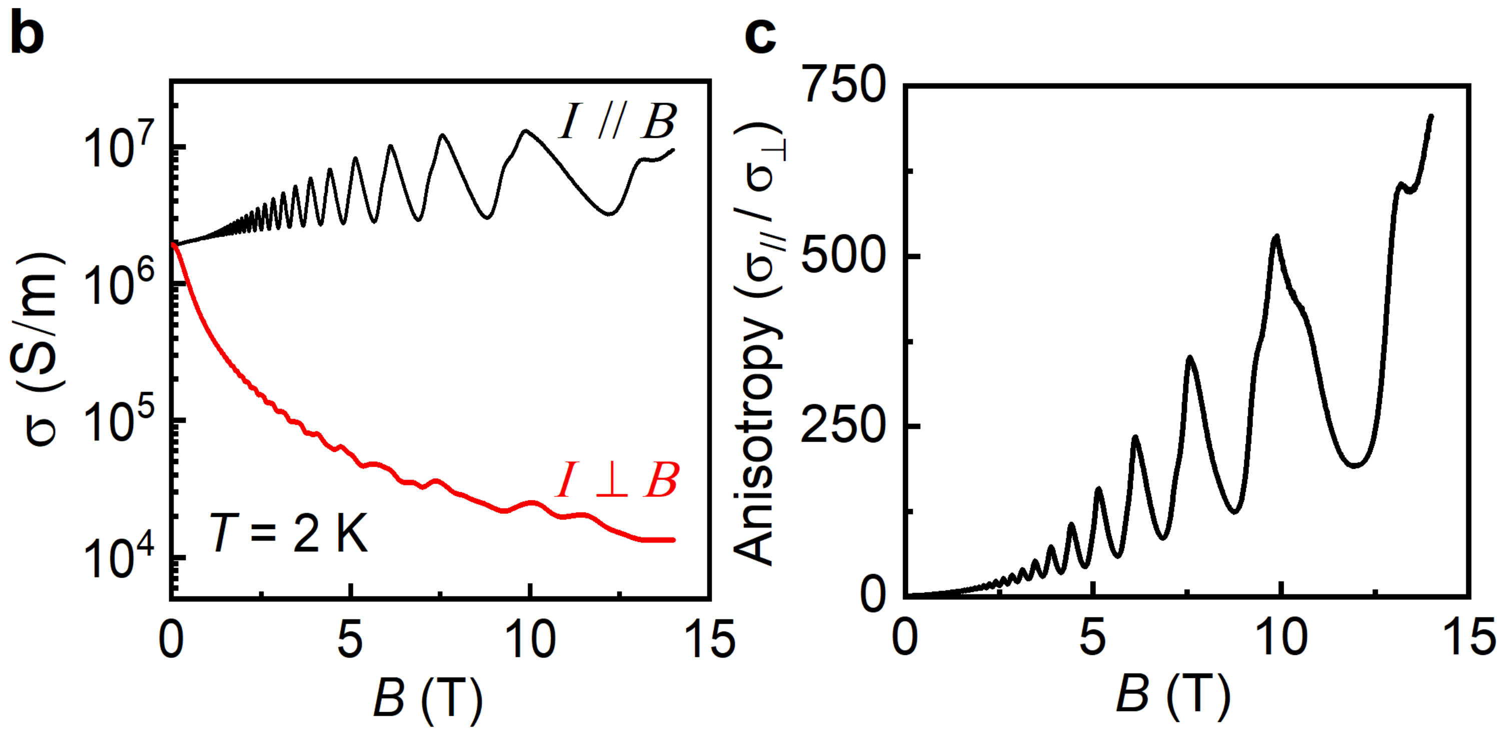

Current jets in high fields

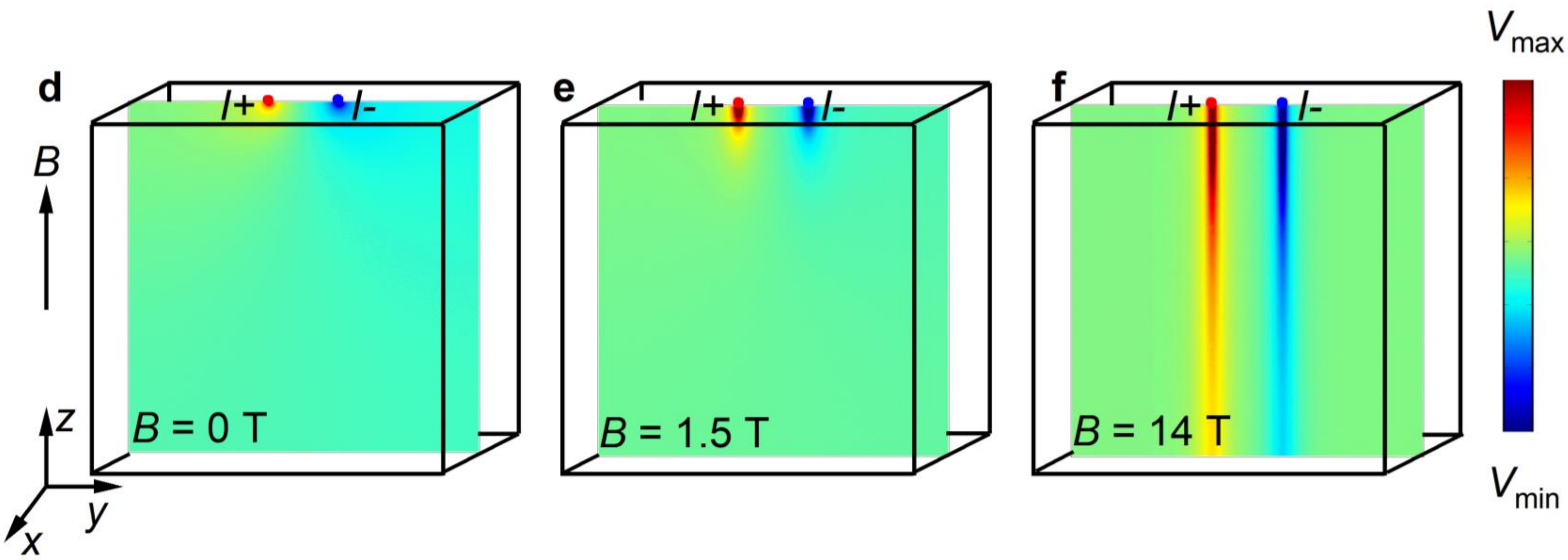

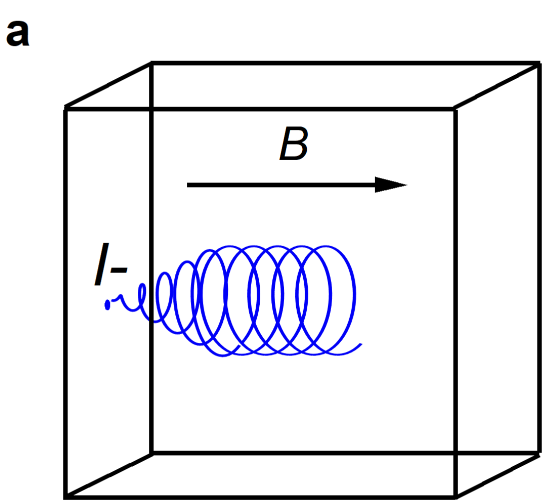

- Current beams form along the magnetic field
- Range well beyond mean-free-path

Current jetting

Current jetting has plagued high-mobility, low carrier density semi-metals for dec

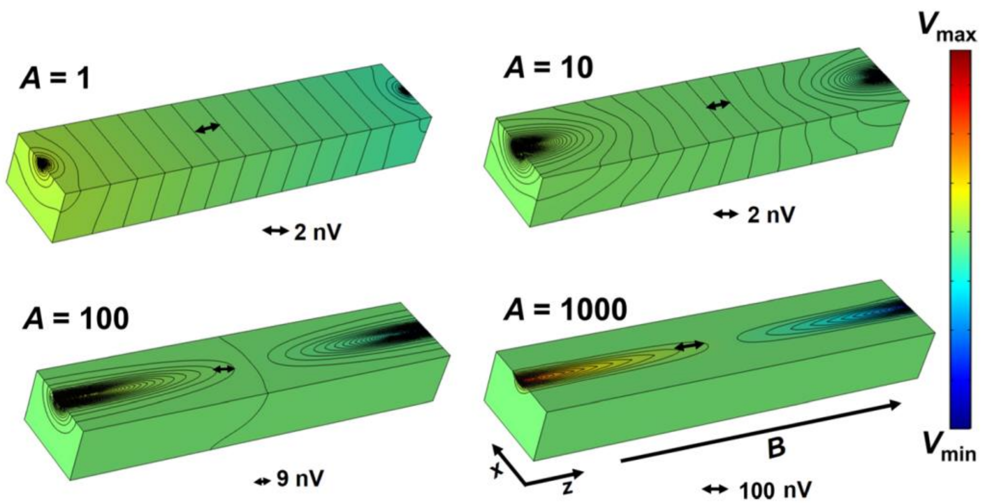

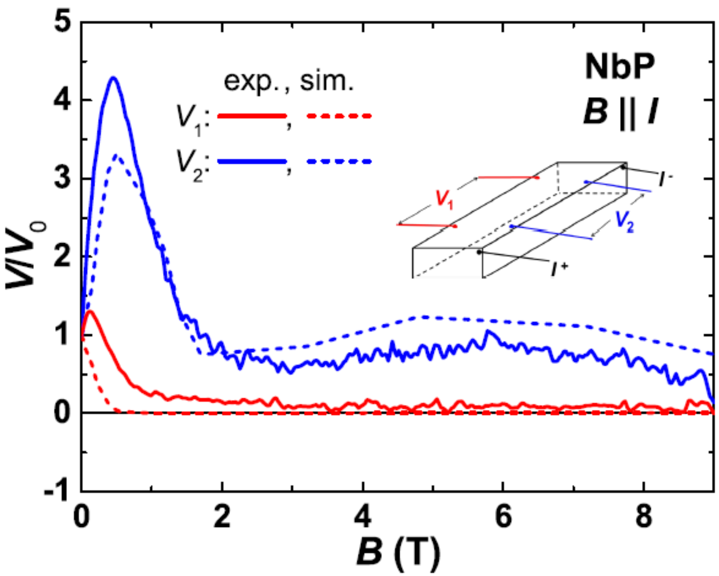

New focus due to negative magnetoresistance expectations due to chiral anom

R. Reis et al., NJP 18:085006 (2016)
Nielsen & Ninomiya, Phys. Lett. B 130, 389-396 (1983)

Usually imperfect contacts

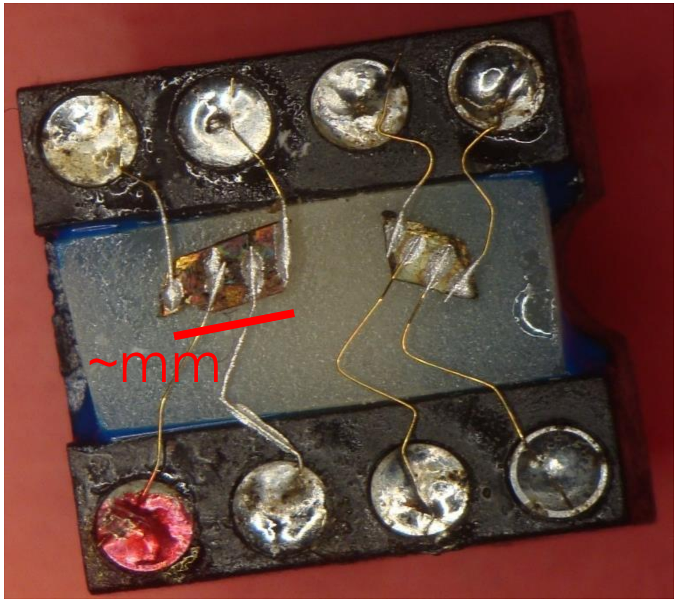

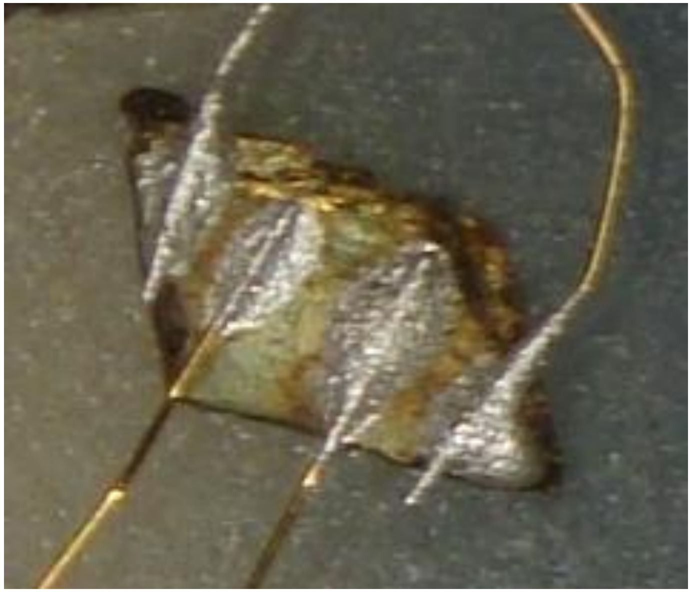

FIB machining allows microscopic control over current jet

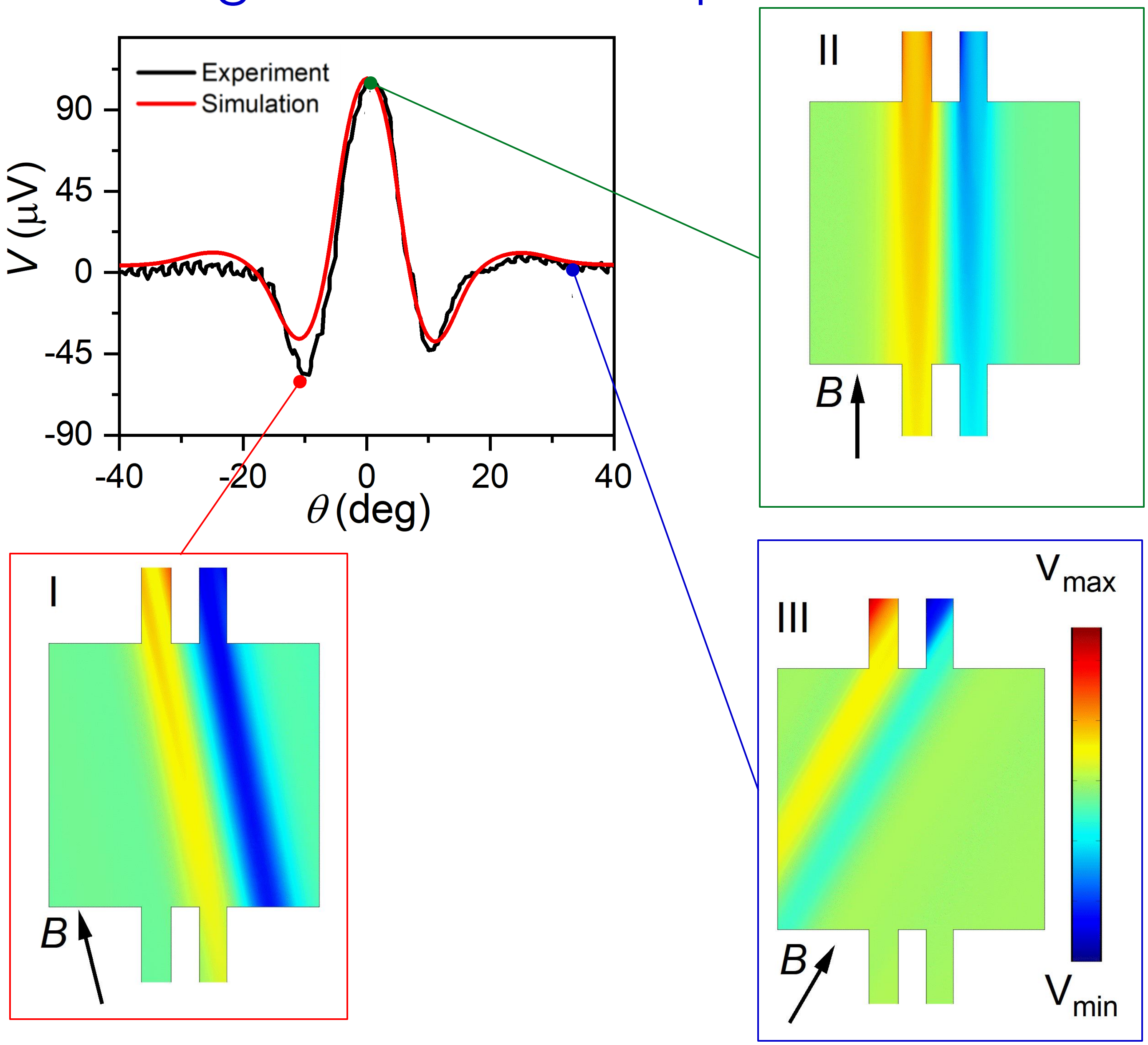

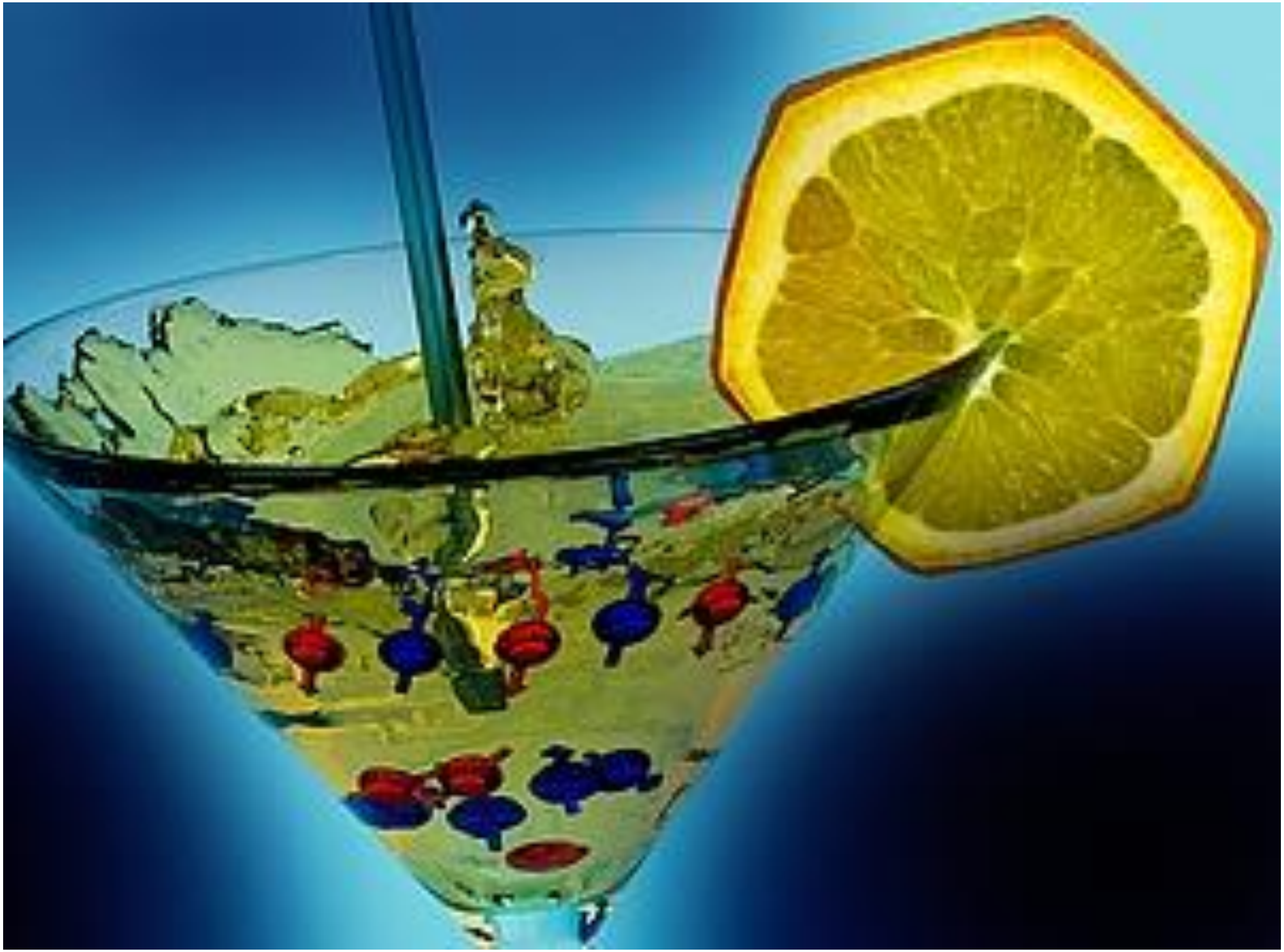

Current jetting devices

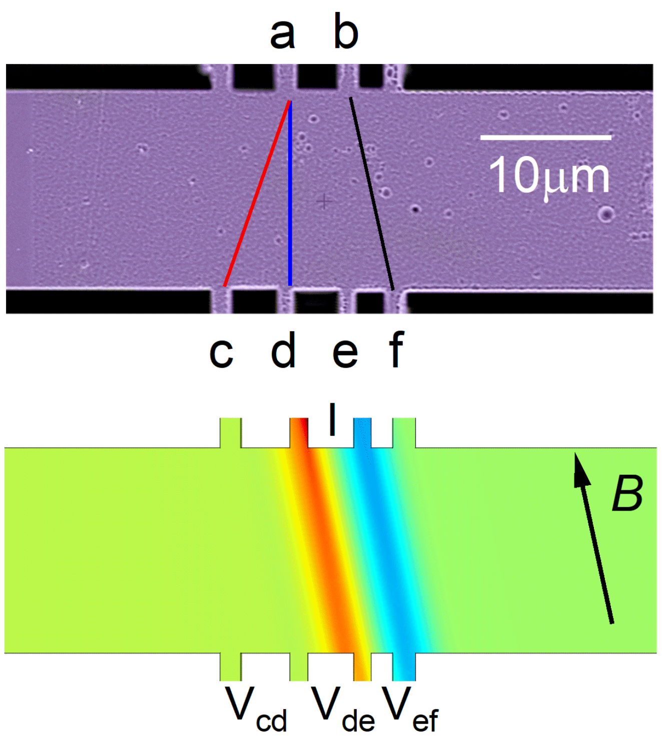

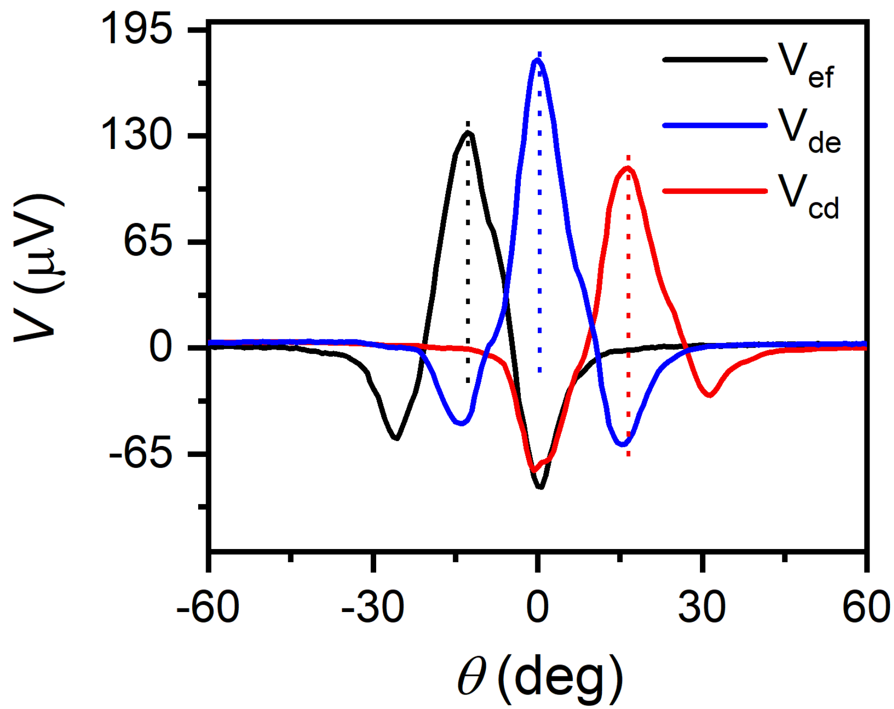

Controlled generation of electron beams in a solid

- Beams steered by magnetic field
- Long ranged non-local signal propagation (neuromorphic applications)
- Solid-state multiplexing

X. Huang et al., on arXiv soo

Fun Intermezzo (time permitting)

Manipulating quantum states

Approach: Cantilever bending mode

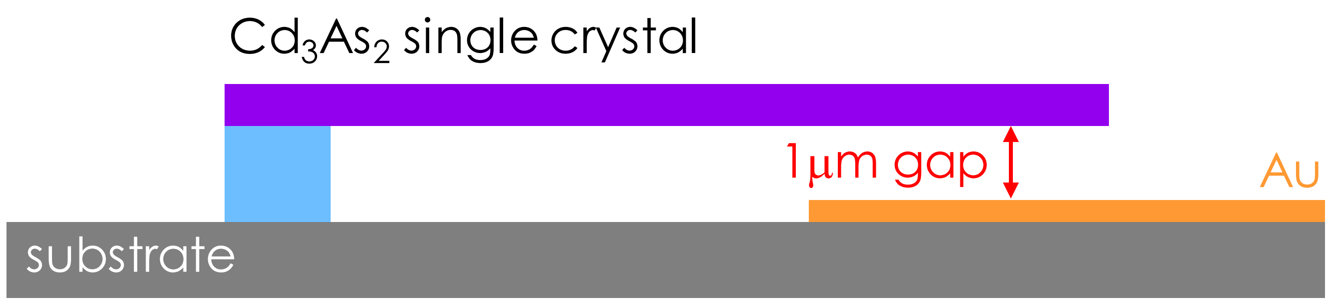

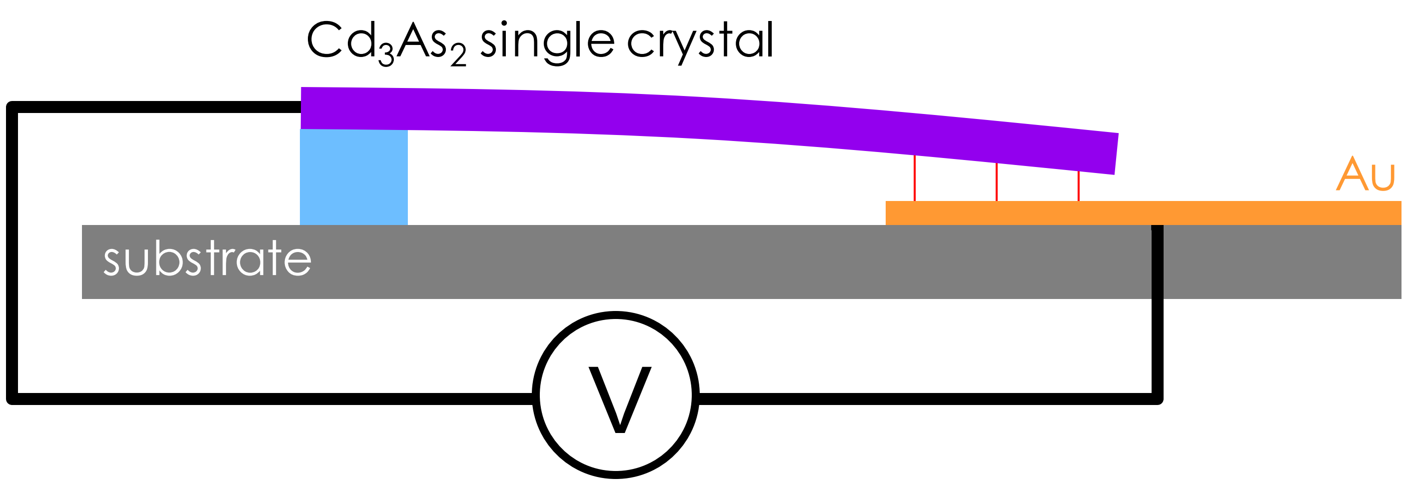

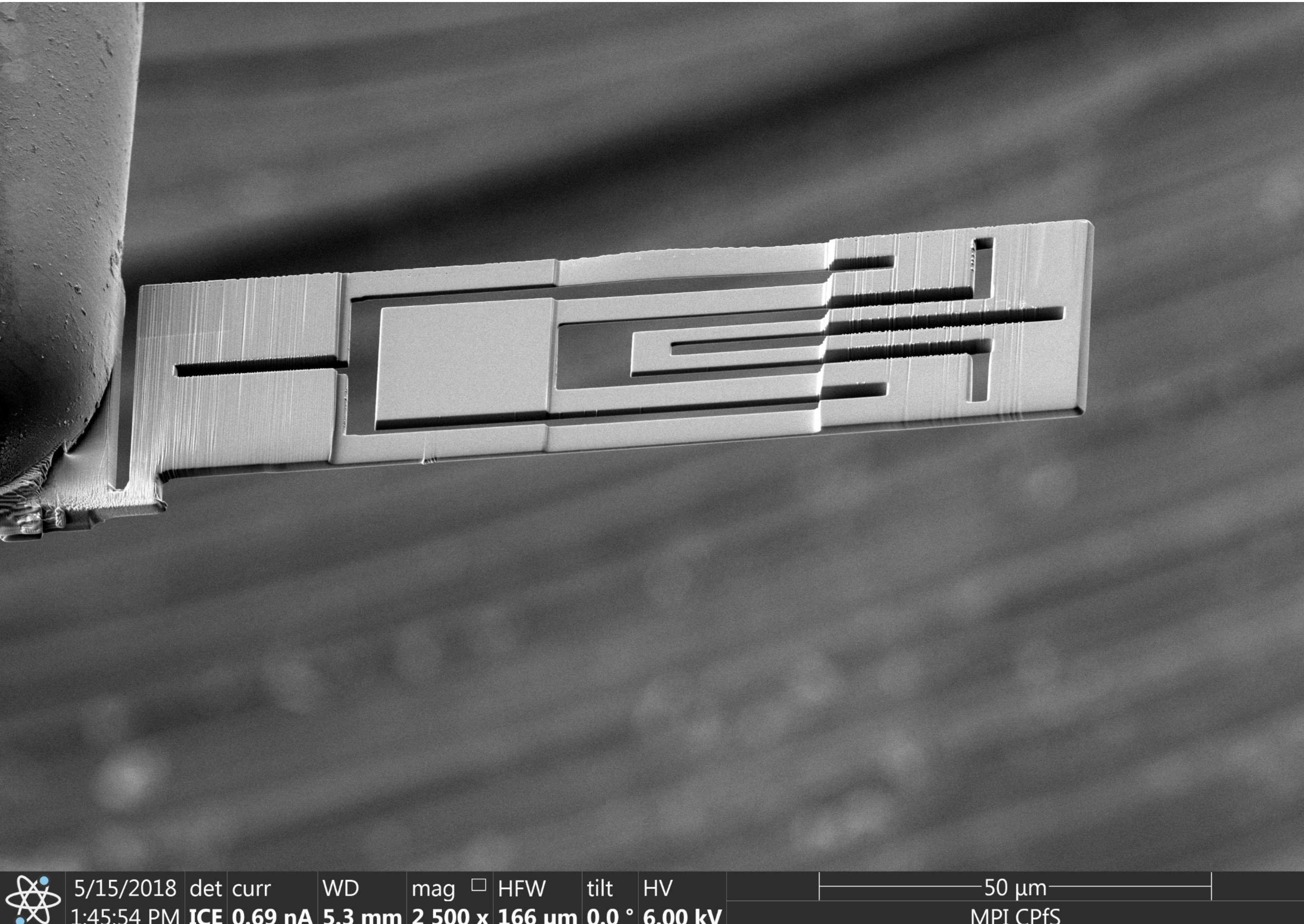
5/15/2018 1:45:54 PM
det ICE
curr 0.69 nA
WD 5.3 mm
mag 2 500 x
HFW 166 µm
tilt 0.0 °
HV 6.00 kV
50 µm
MPI CPfS


Micromanipulator
5/15/2018
5:23:06 PM
det
ICE
curr
0.69 nA
WD
3.9 mm
mag
1 200 x
HFW
345 µm
tilt
52.0 °
HV
6.00 kV
100 µm
MPI CPfS

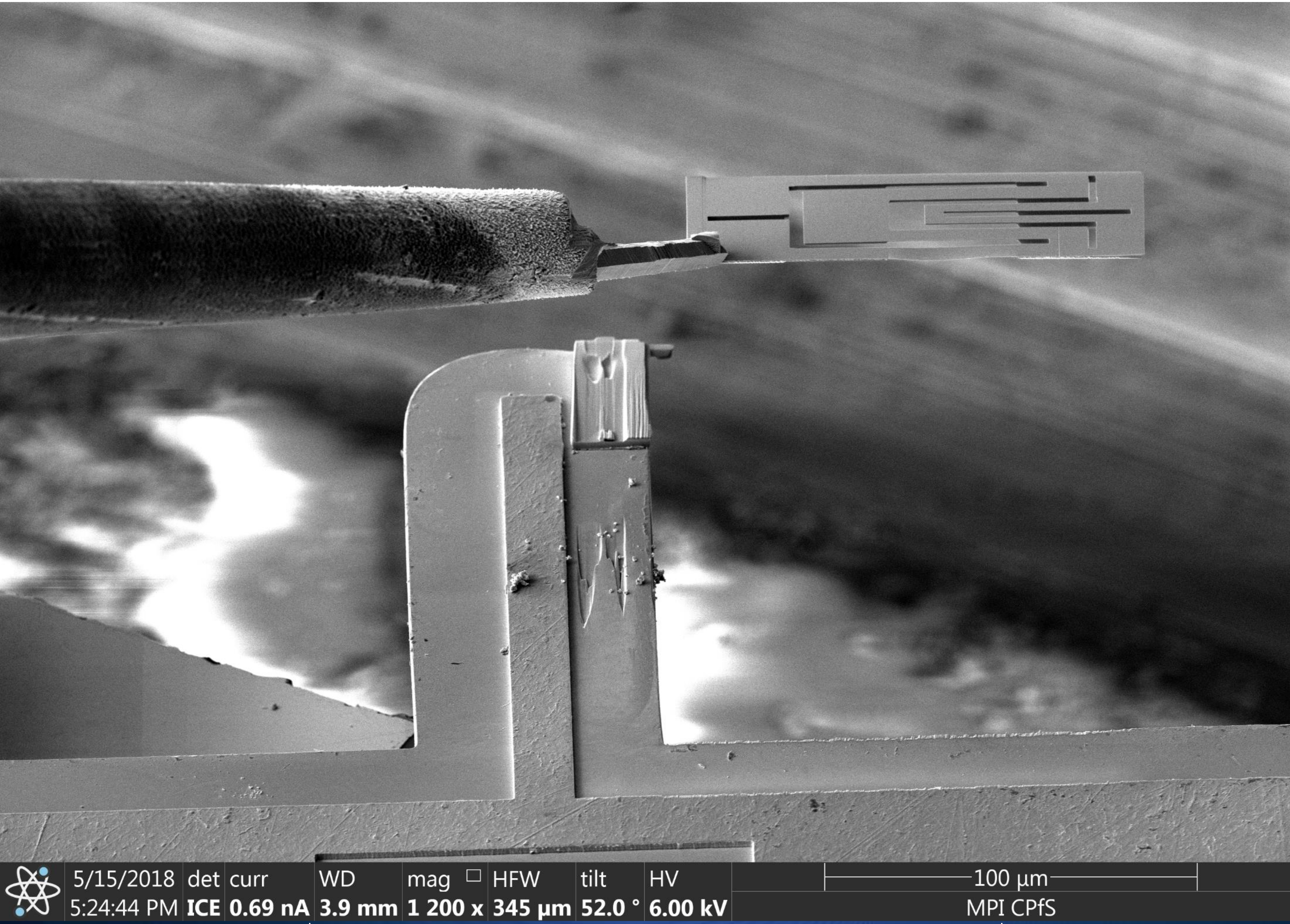
5/15/2018
5:24:44 PM
det
ICE
curr
0.69 nA
WD
3.9 mm
mag
1 200 x
HFW
345 µm
tilt
52.0 °
HV
6.00 kV
100 µm
MPI CPfS

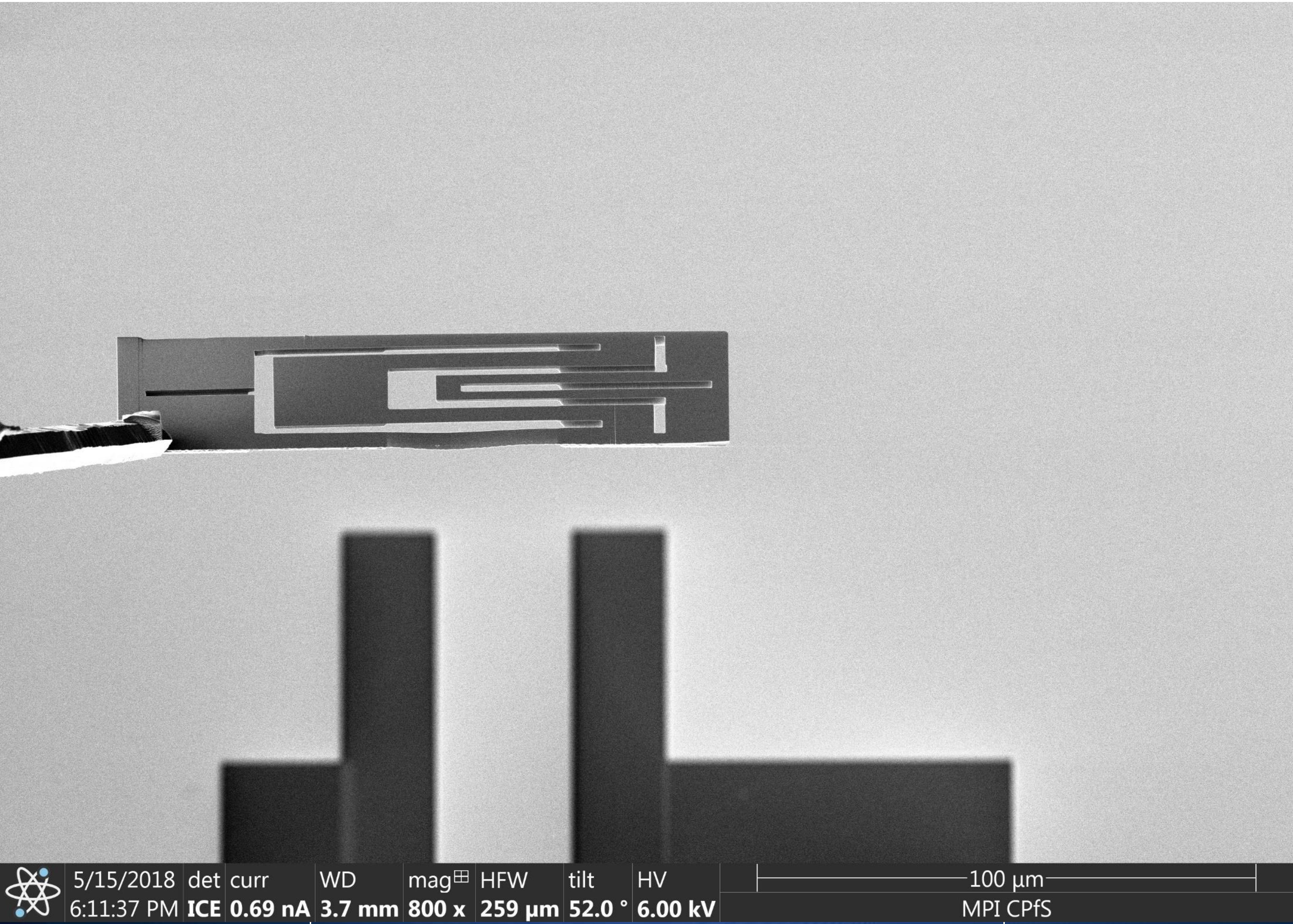
5/15/2018
6:11:37 PM
det
ICE
curr
0.69 nA
WD
3.7 mm
mag
800 x
HFW
259 µm
tilt
52.0 °
HV
6.00 kV
100 µm
MPI CPfS

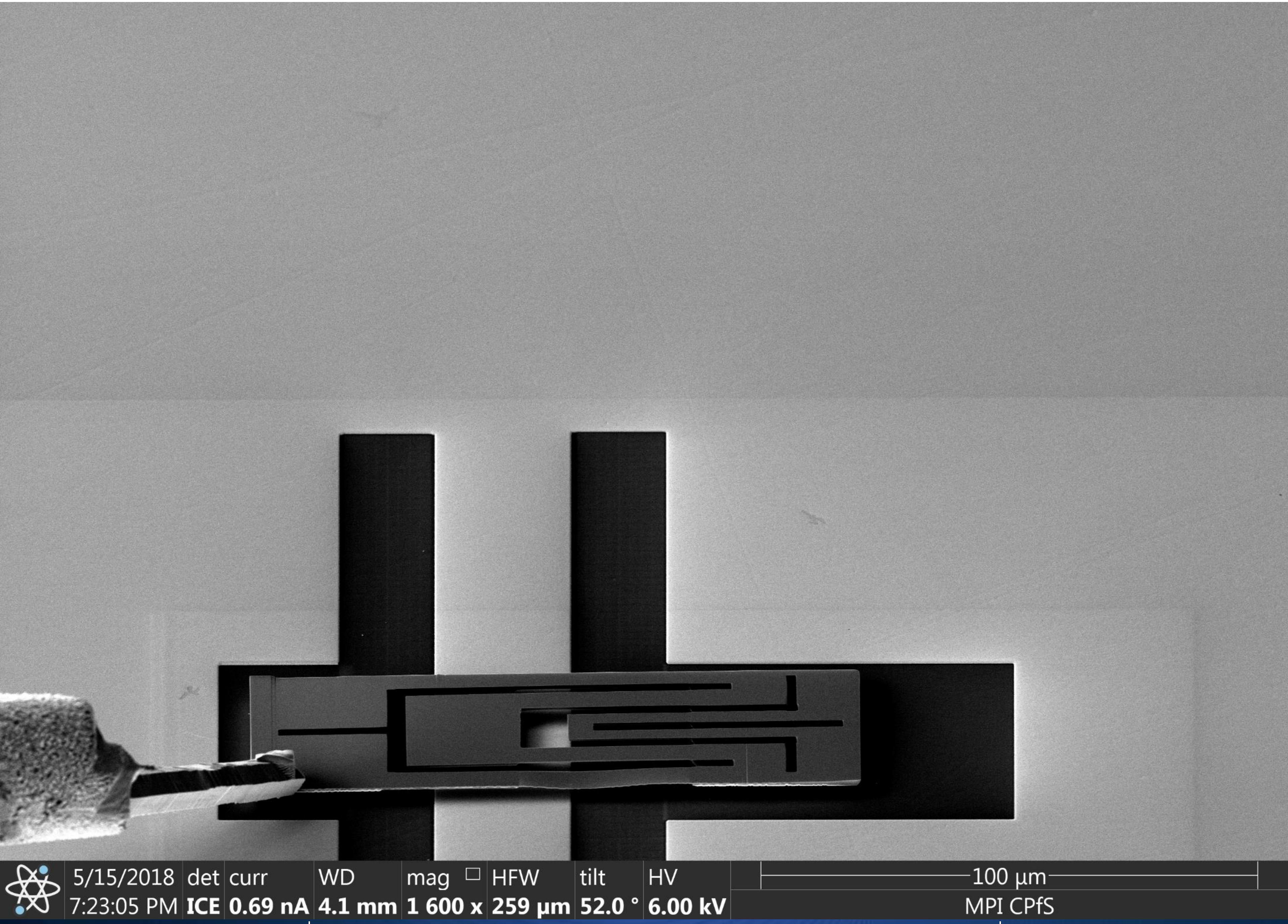
5/15/2018
7:23:05 PM
det
ICE
curr
0.69 nA
WD
4.1 mm
mag
1 600 x
HFW
259 µm
tilt
52.0 °
HV
6.00 kV
100 µm
MPI CPfS

Real Cd_3As_2 device in motion

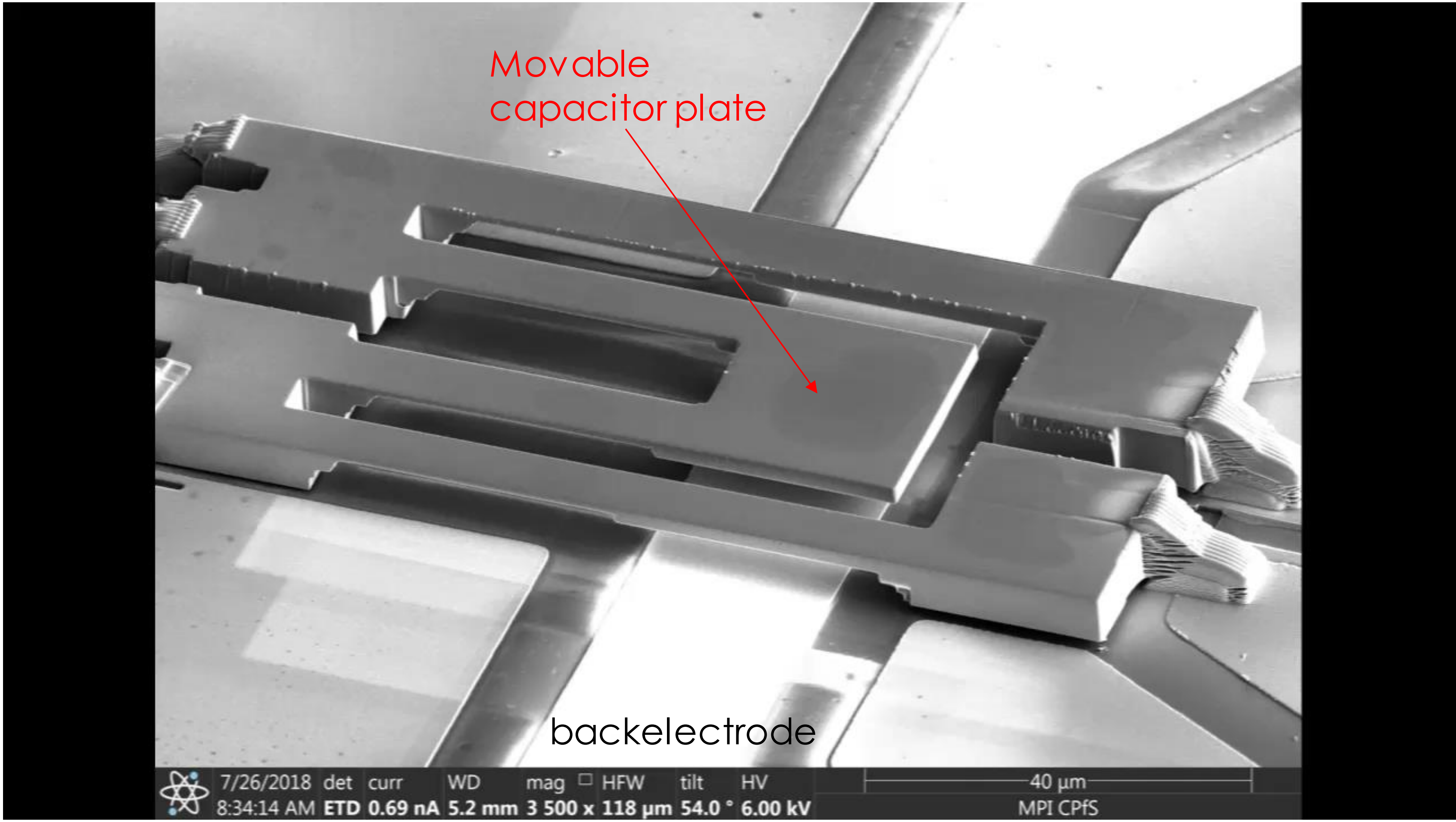

Macroscopic bending

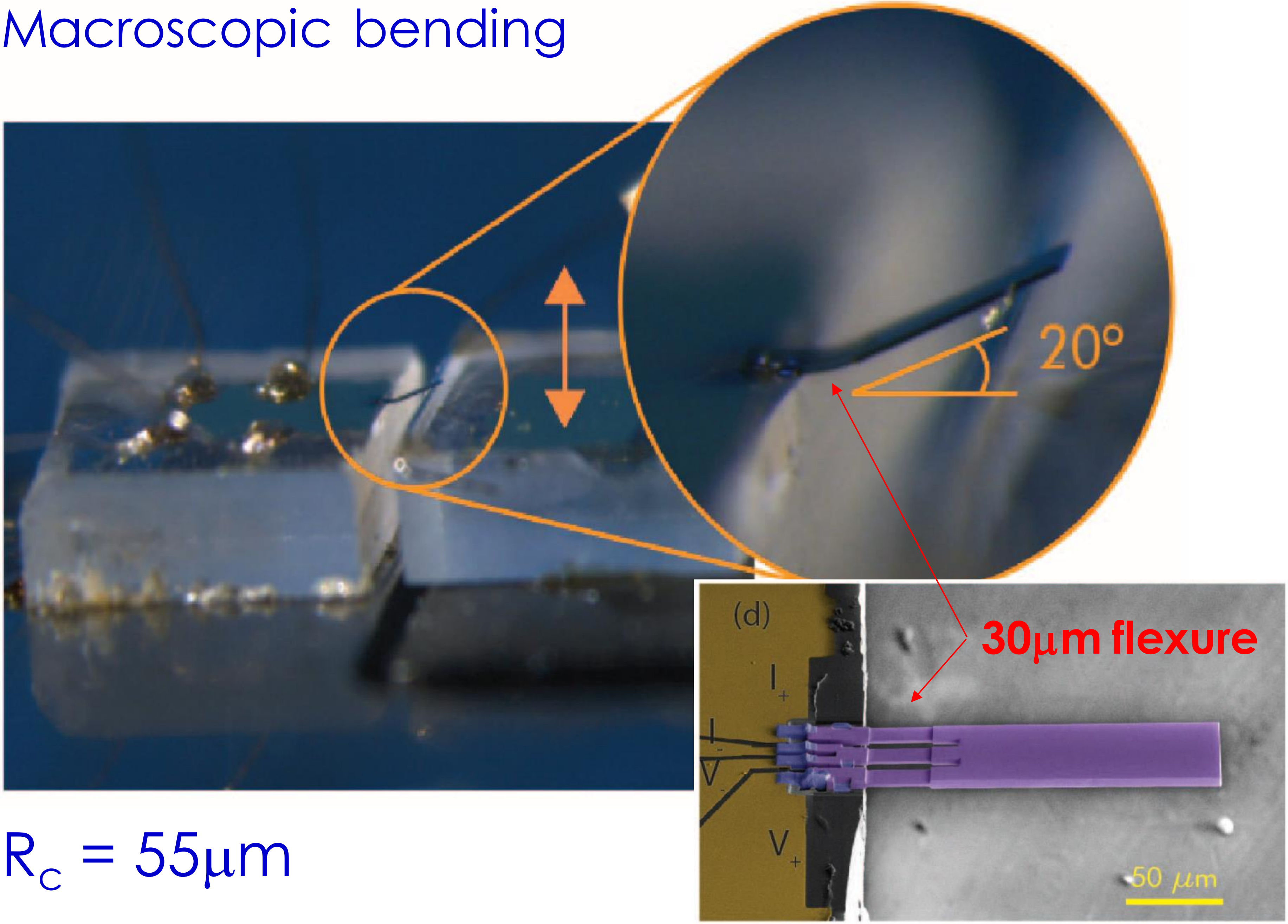

$R_c = 55\mu m$

Estimate extreme bending parameters

$R_c = 55\mu m$

$T = 1\,\mu m$

~1% strain on top

~2%/μm

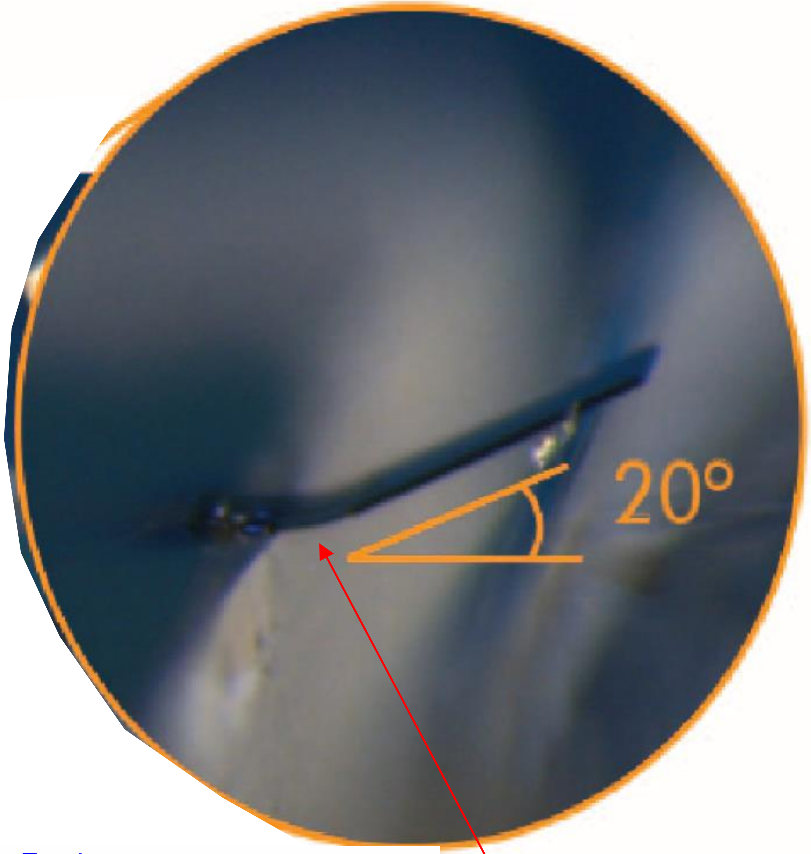

30µm flexure

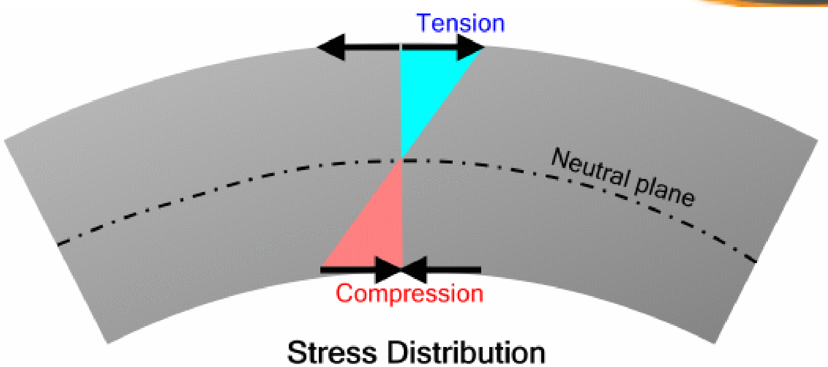

Preliminary results

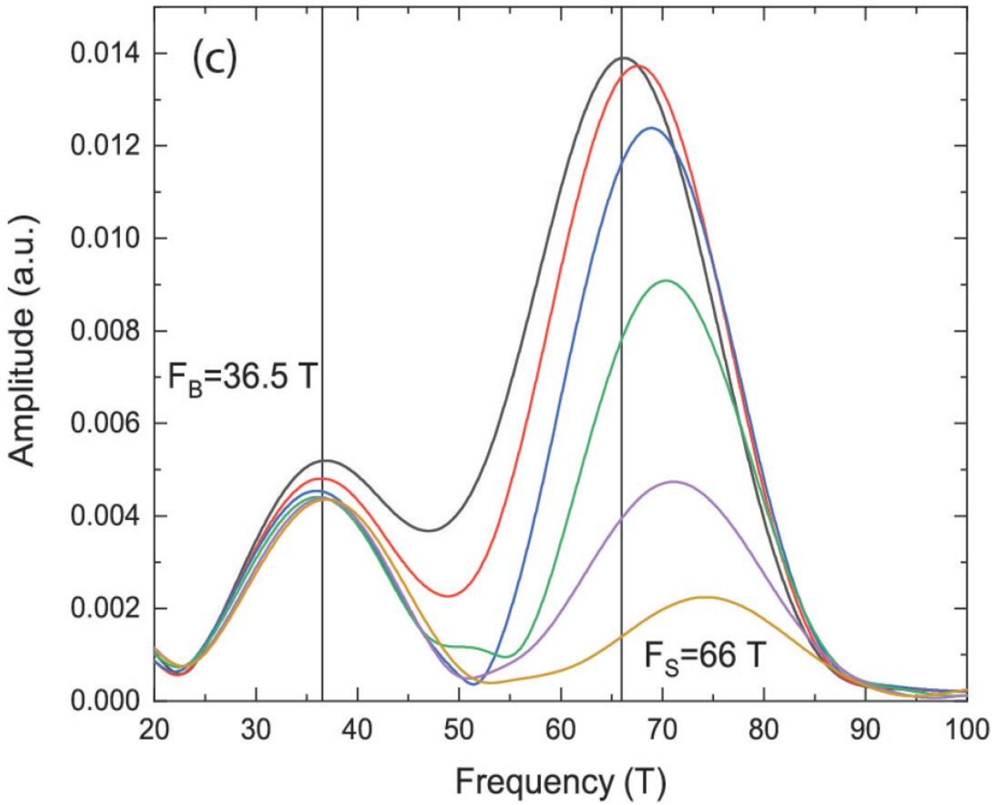

- Bulk peak does not shift
- Weyl orbit does not split
- Moves to higher frequencie

No signs of plastic deformatio

B_5 ~5T at maximal strain

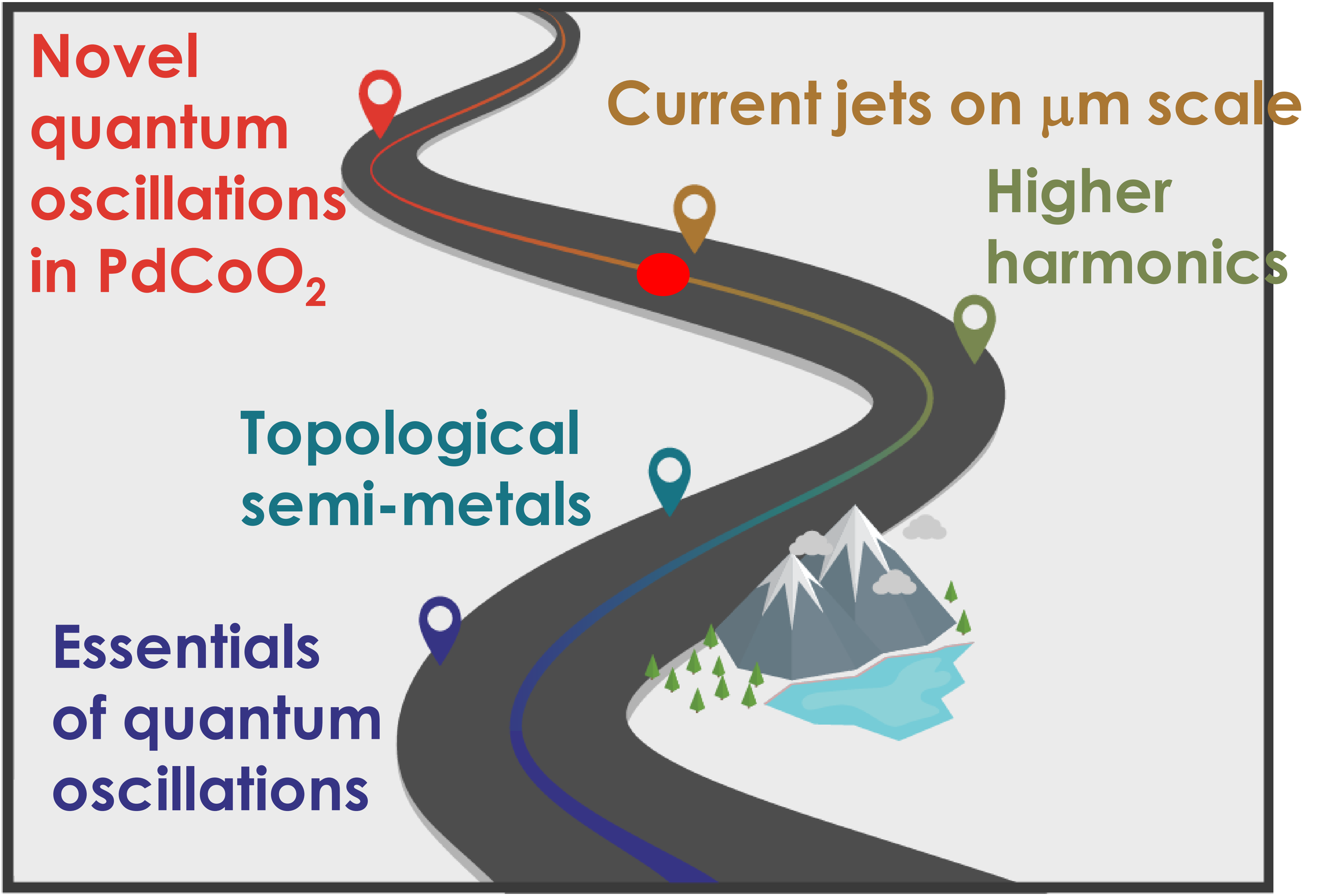
Novel quantum oscillations in $PdCoO_2$
Current jets on µm scale
Higher harmonics
Topological semi-metals
Essentials of quantum oscillations

Key points:

- Surprises can happen in seemingly trivial, single-particle systems
- Novel Field-linear magnetoresistance oscillations in layered metals
- Quantum coherence over macroscopic distances possible

$PdCoO_2$: ultra-clean metal

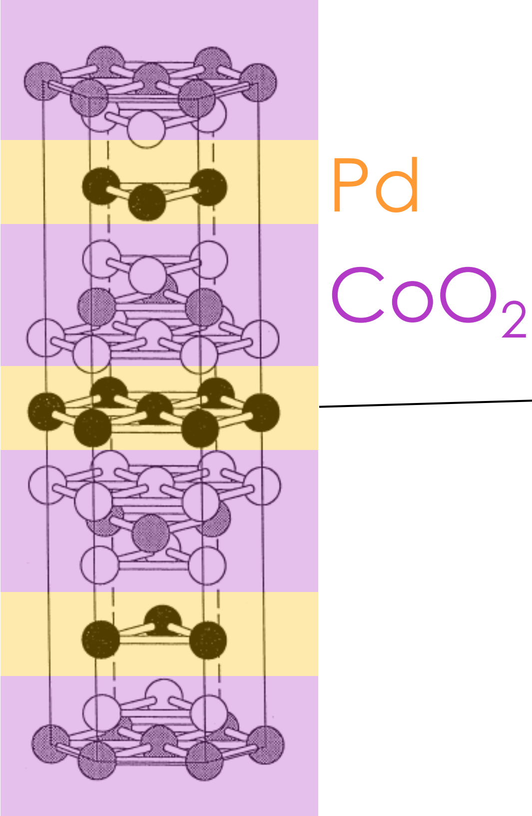

Quasi-hexagonal Fermi surface

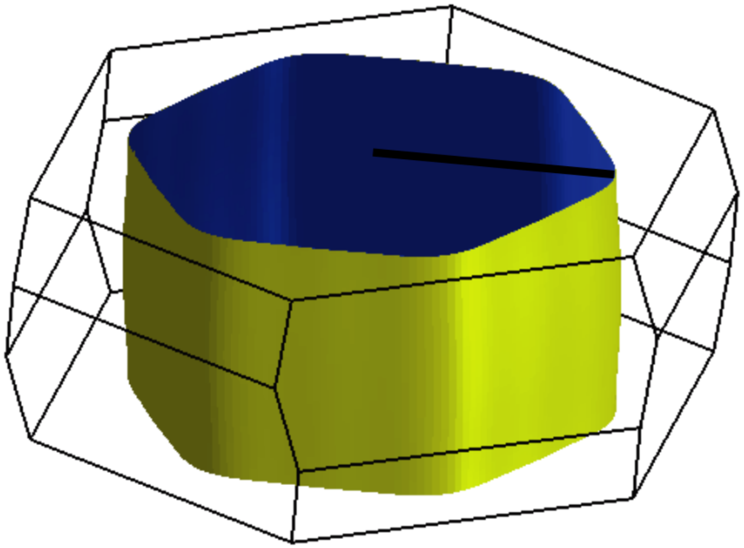

QO: C.W. Hicks et al., PRL **109**, 116401 (2012)
ARPES: H.J. Noh et al., PRL **102**, 256404 (2009)

$\rho = 2.6\mu\Omega\ cm$ vs. $1.7\mu\Omega\ cm$ in Cu (@ 300K)
… but Cu has 3 times more charge carriers!

ReO_3	$7\mu\Omega\ cm$
IrO_2	$24\mu\Omega\ cm$

Very long mean free path : $l\sim 20\mu m$ (@2K)

$PdCoO_2$: Very long mean free path

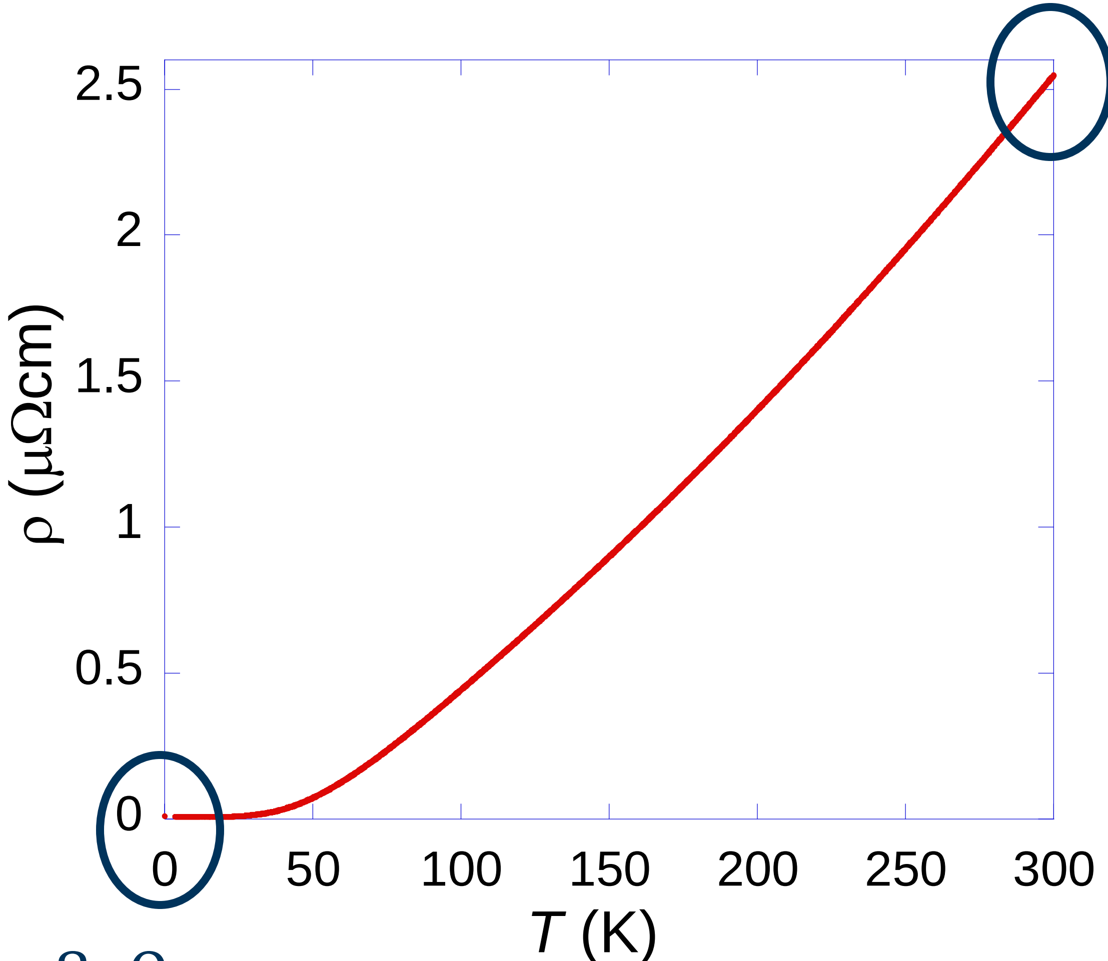

$2.6 \mu\Omega\ cm$

ReO_3 $7 \mu\Omega\ cm$

IrO_2 $24 \mu\Omega\ cm$

$8 n\Omega$ cm

$PdCoO_2$ is a coherent layered metal

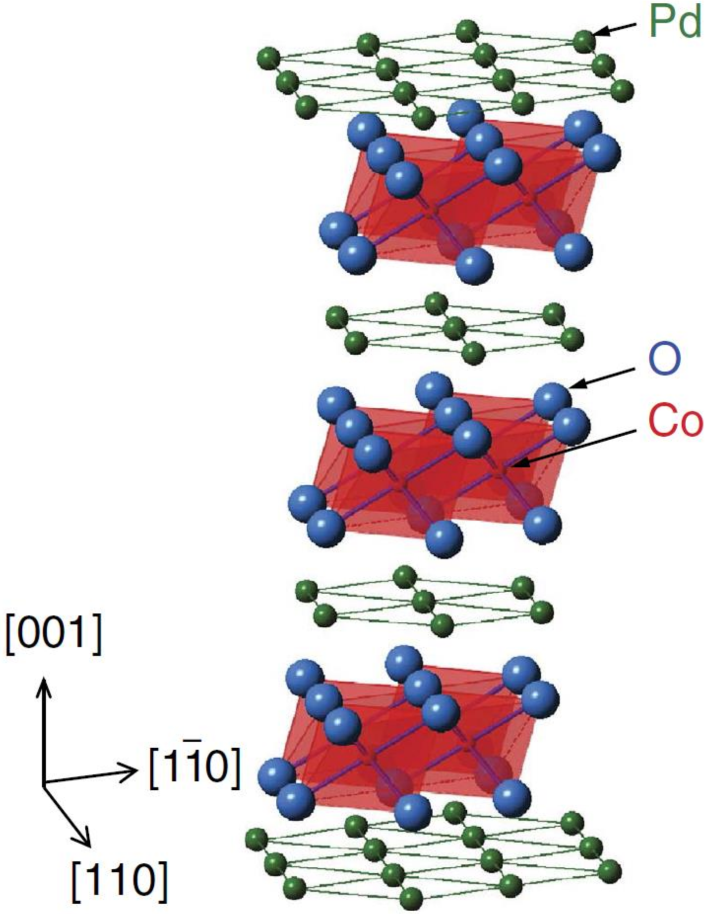

Quantum oscillations show warped cylinder

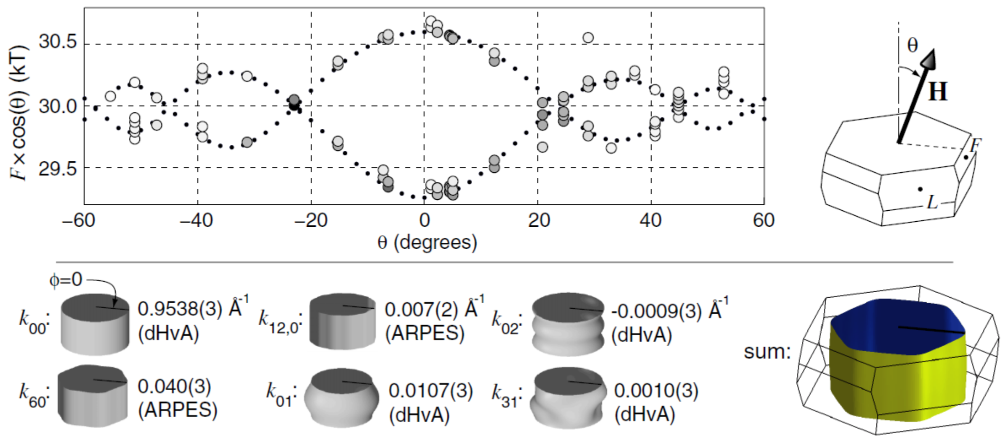

C.W. Hicks et al., PRL **109**, 116401 (2012)

Well supported by AMRO experiments

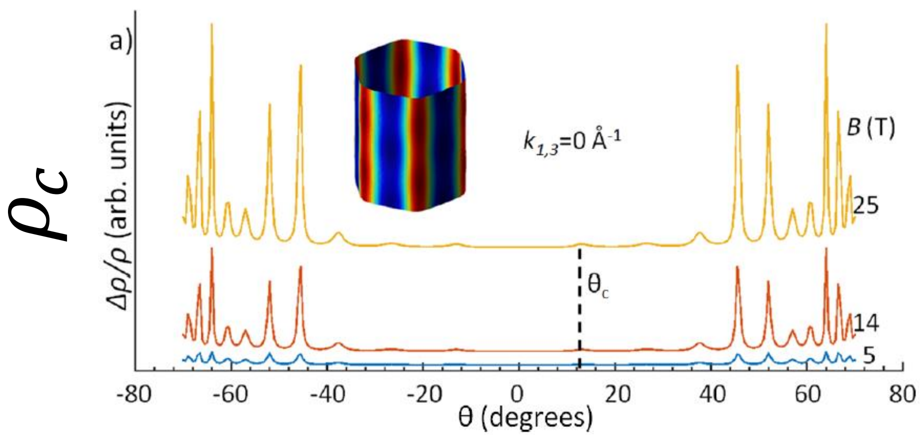

J.C.A. Prentice et al., Phys. Rev. B **93**, 245105 (2016)

Out-of-plane transport

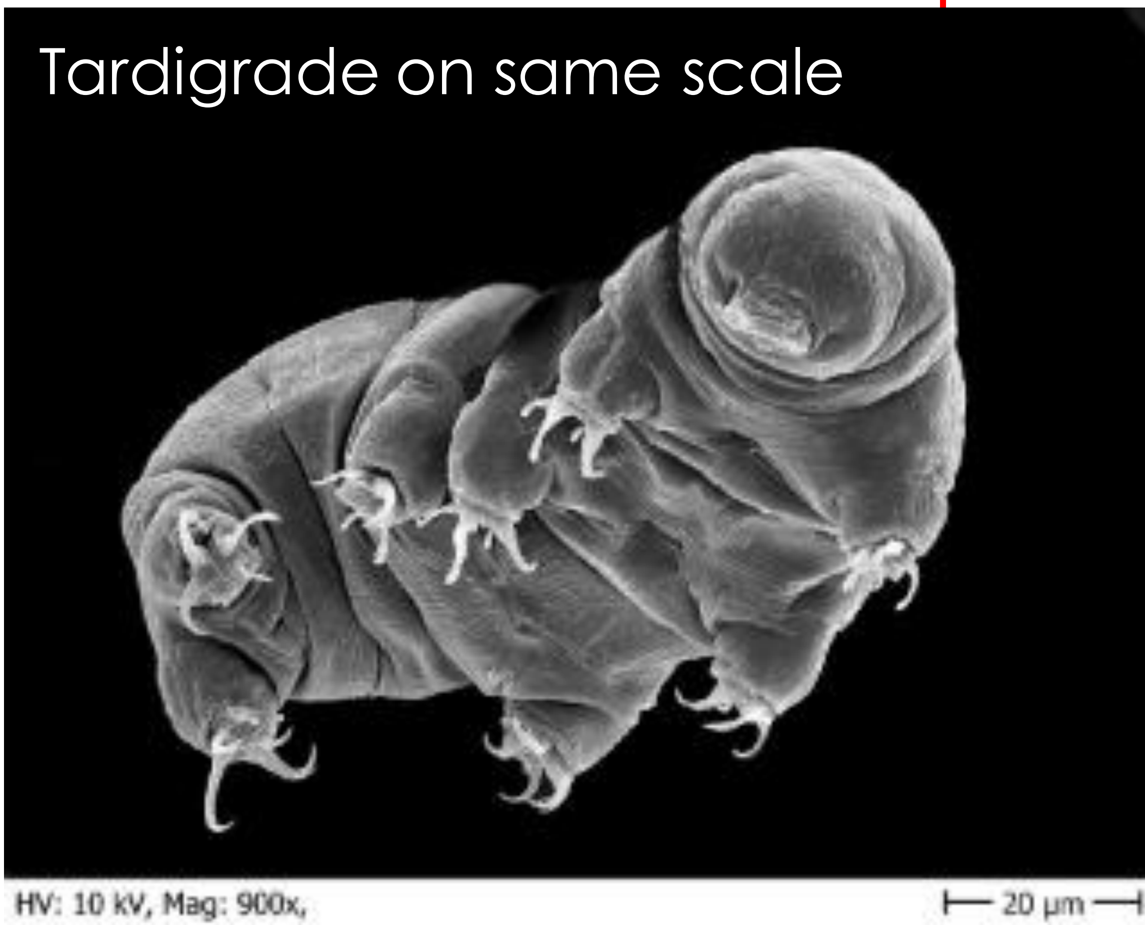

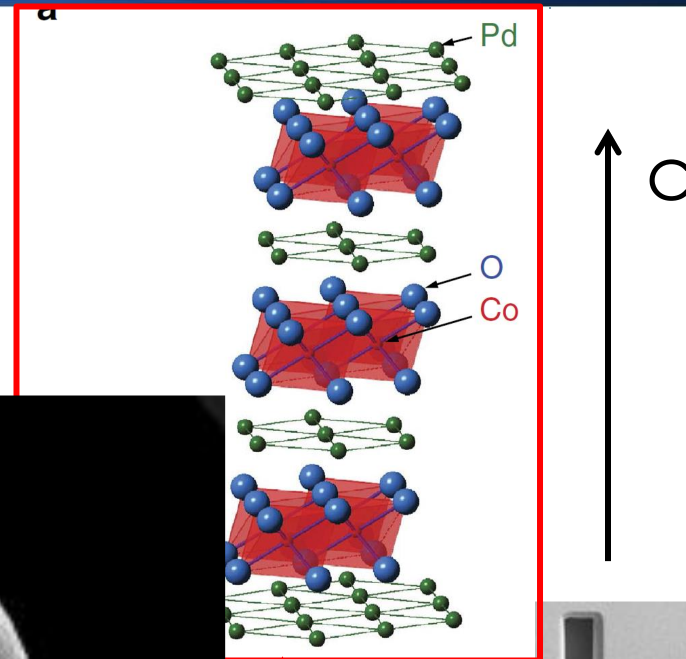

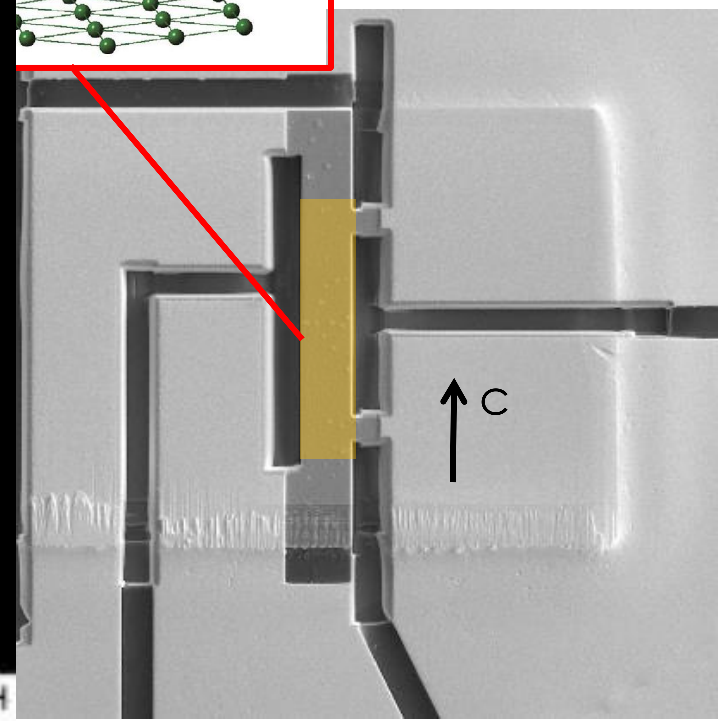

The experimental configuration

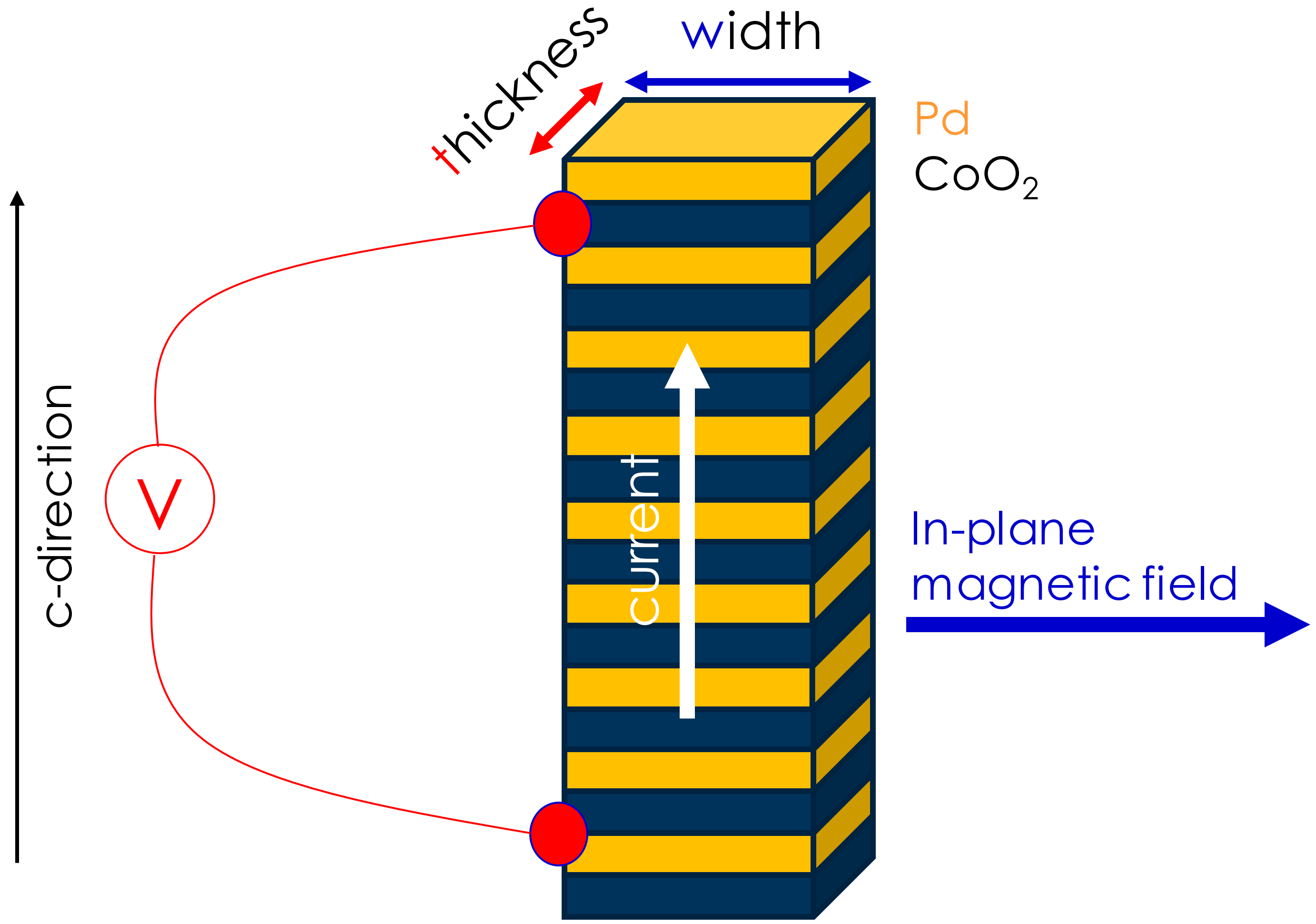

- Four-probe resistance of FIB-fabricated, c-aligned pillars
- In-plane magnetic field

Magnetoresistance oscillations

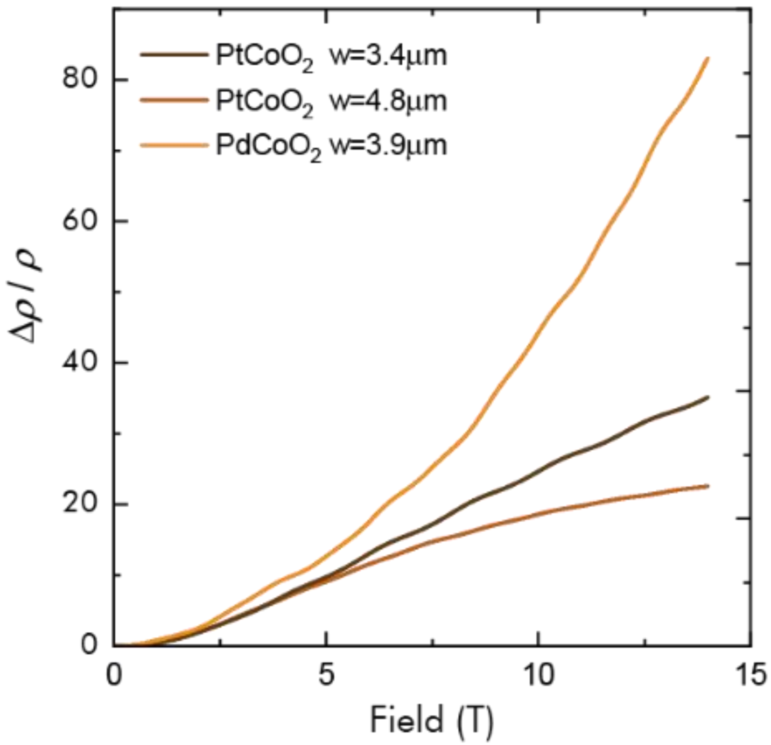

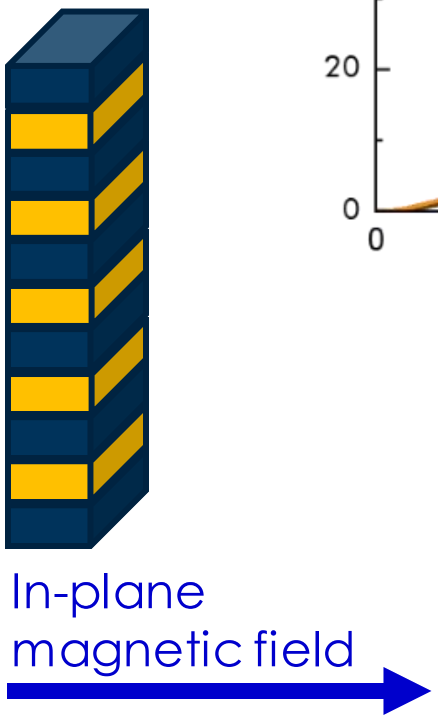
In-plane magnetic field

- Oscillations ontop of the c-direction magnetoresistance
- Periodic in B (not 1/B)
- Not material specific, but sample specific

NOT Shubnikov-de Haas

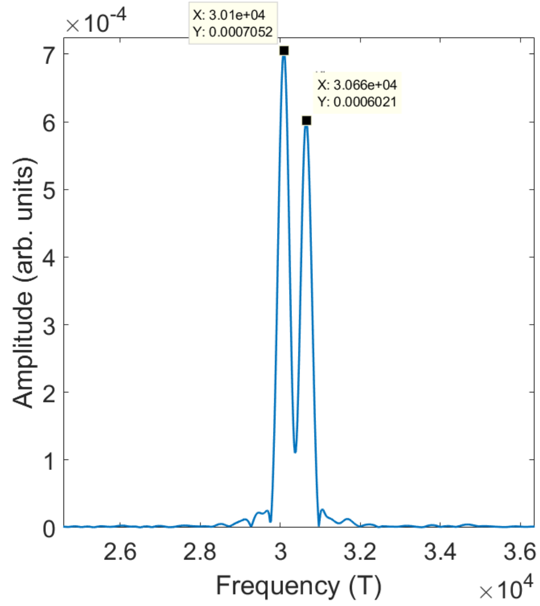

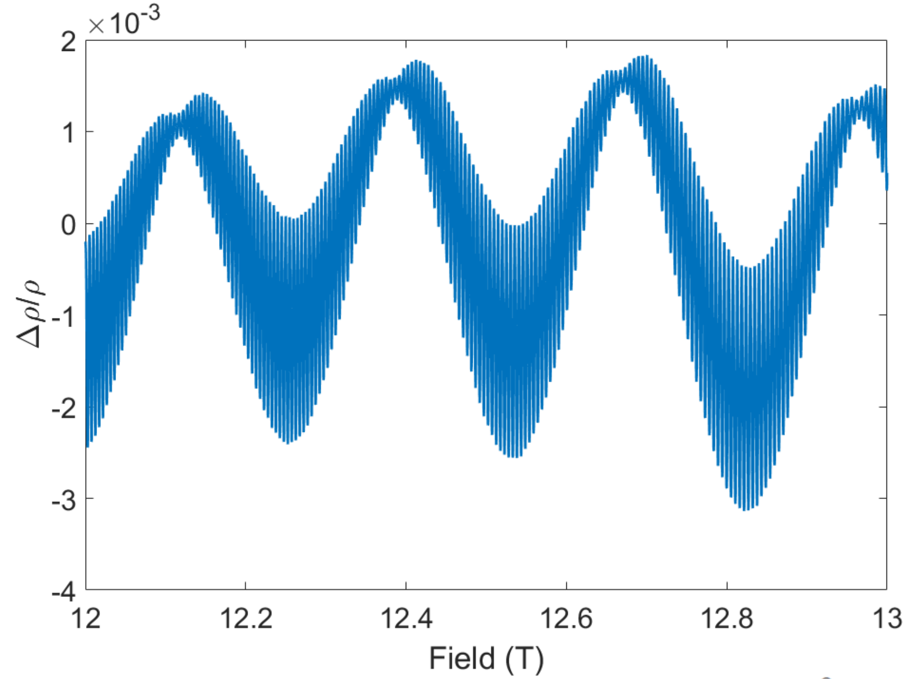

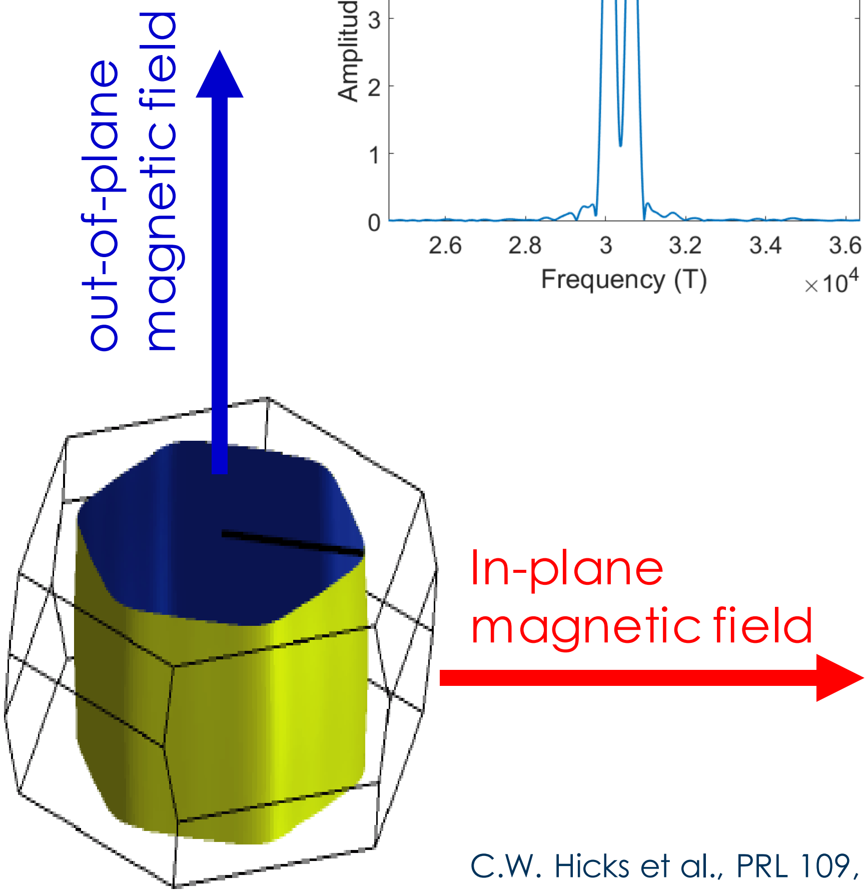

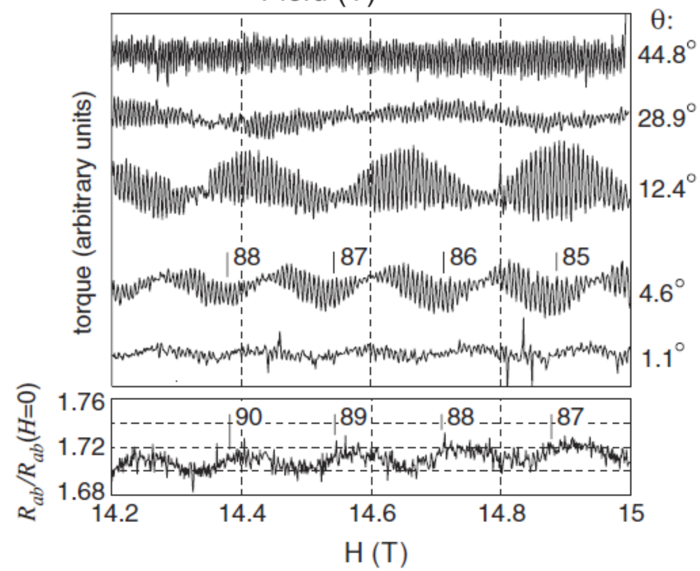

C.W. Hicks et al., PRL 109, 116401 (2012)

Flux physics in a single crystal

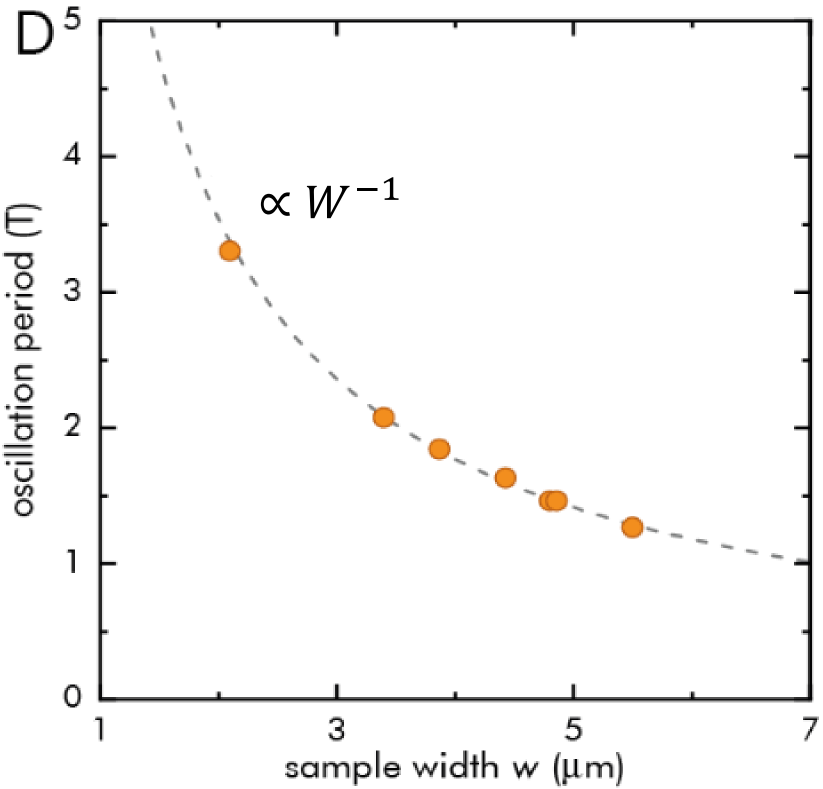

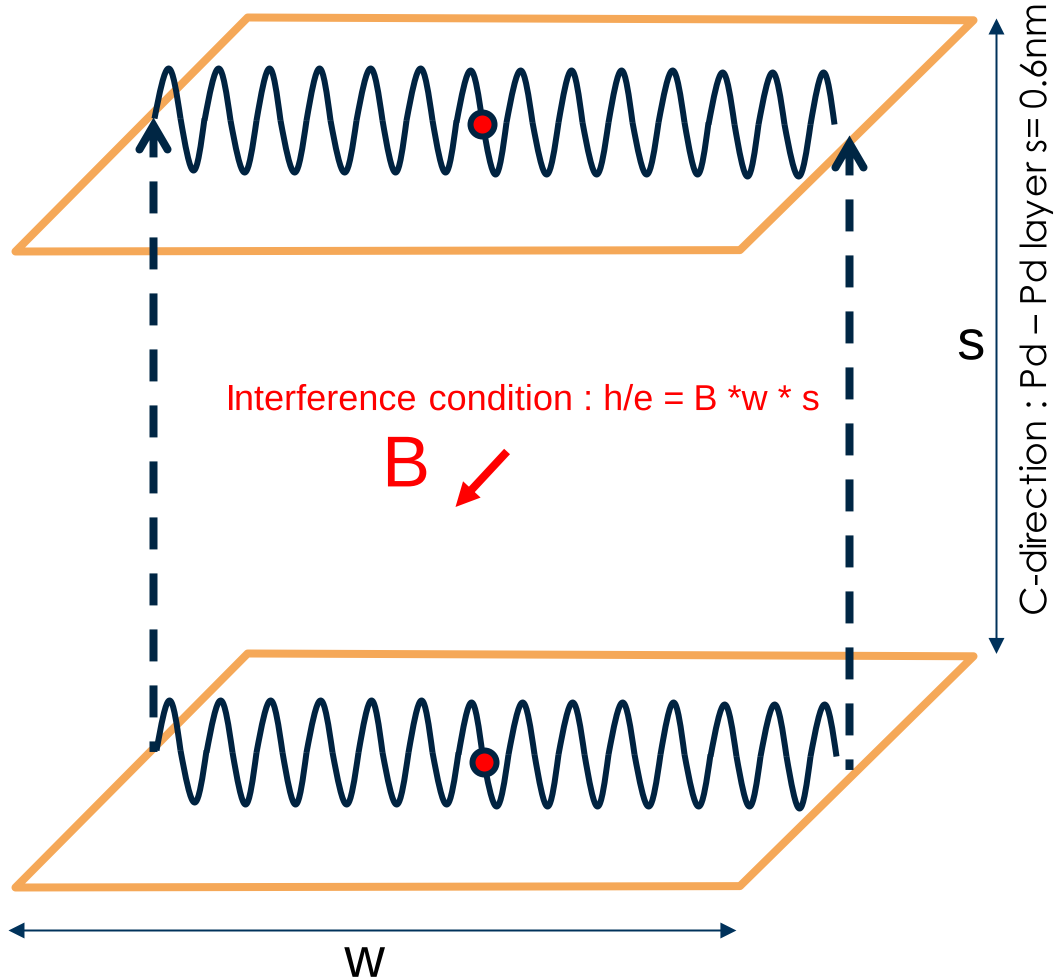

Period is given by one flux quantum $\Phi_0 = h/e$ in a box defined by the micron-sized width of the device, w, and the atomic Pd-Pd distance, s=0.6

This is the real aspect ratio of the box

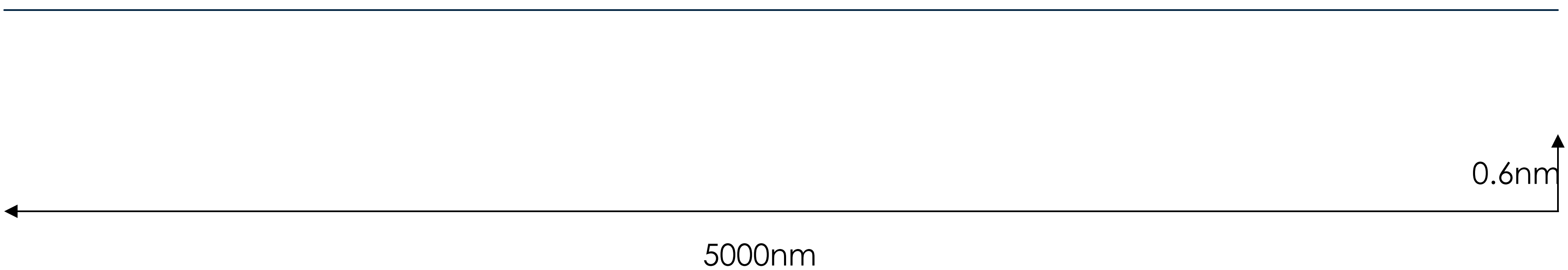

Two types of devices: single- and multi-frequency

Single frequency

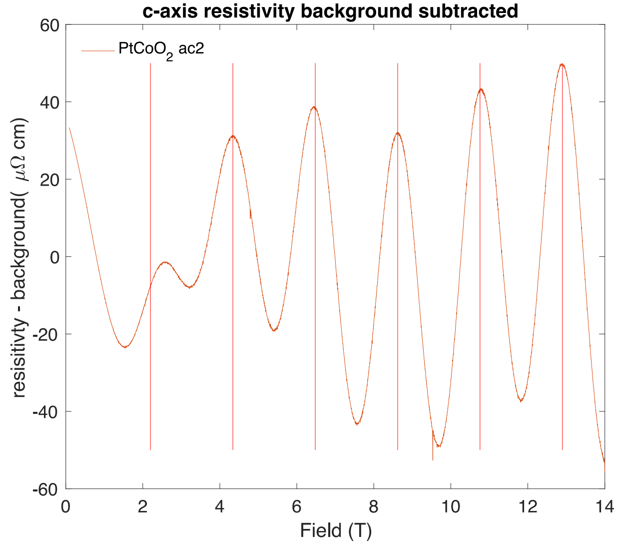

Multi-frequency

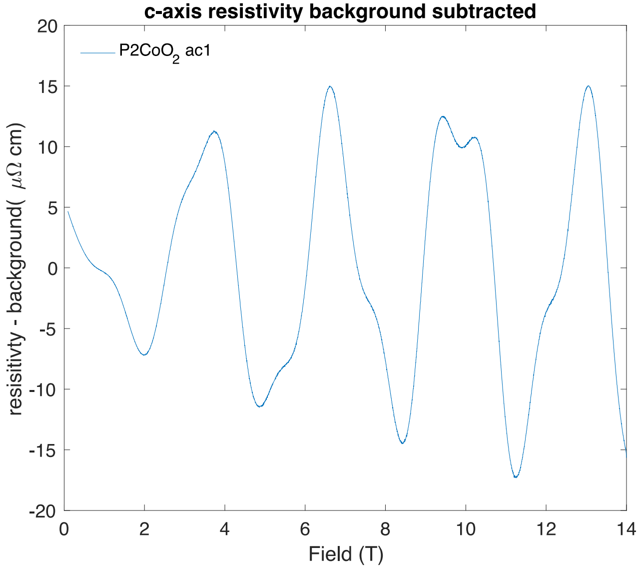

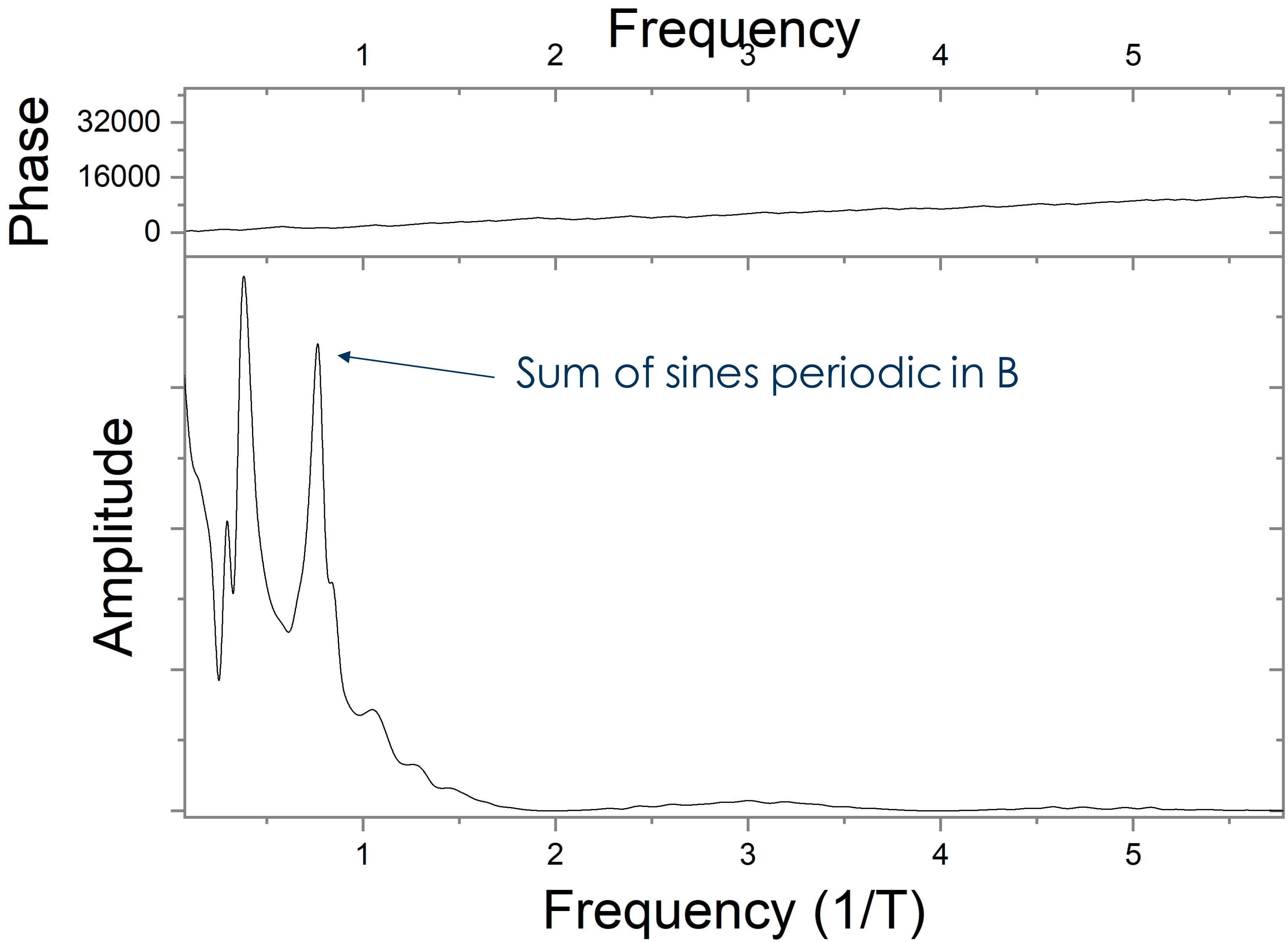

Frequency
1
2
3
4
5
Phase
32000
16000
0
Amplitude
Sum of sines periodic in B
Frequency (1/T)

Rotating the in-plane field

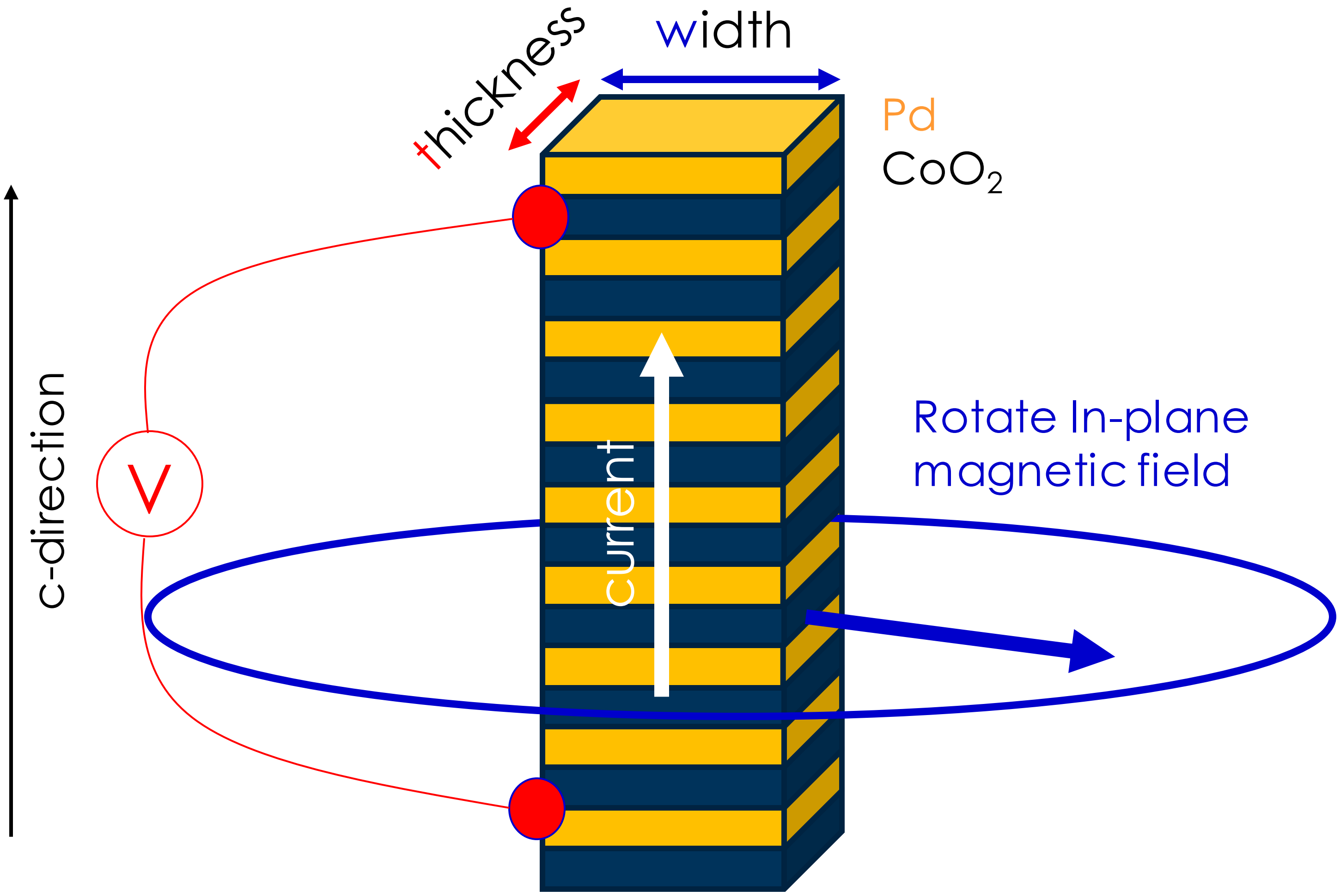

- Four-probe resistance of FIB-fabricated, c-aligned pillars
- In-plane magnetic field

Complex frequency evolution under rotation

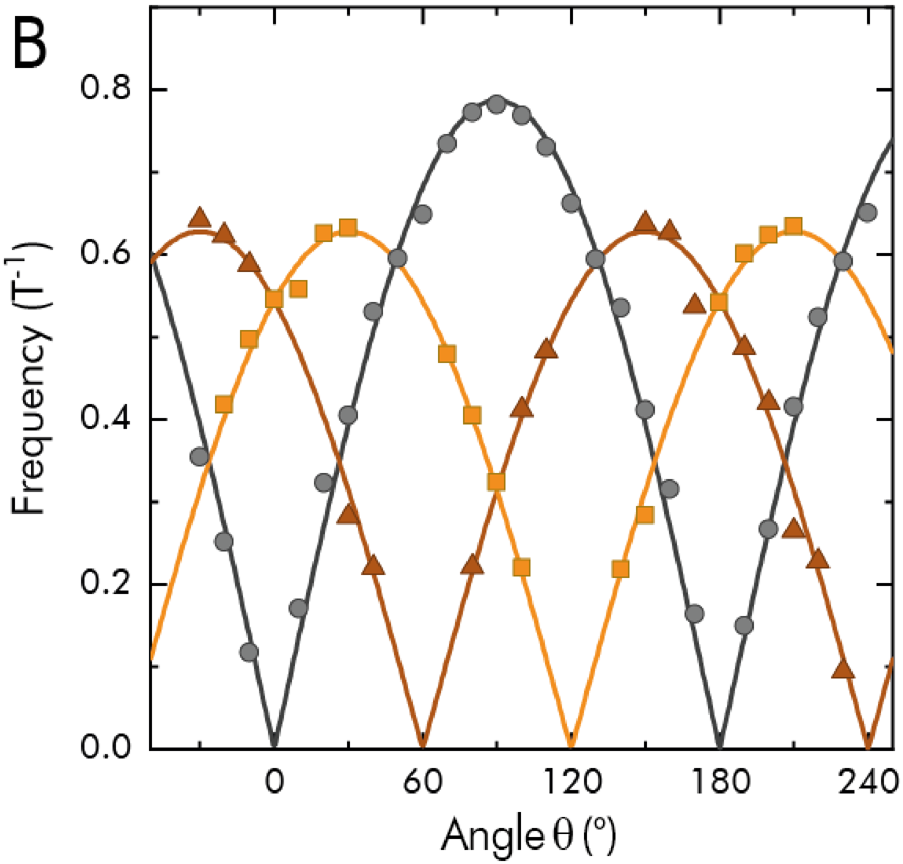

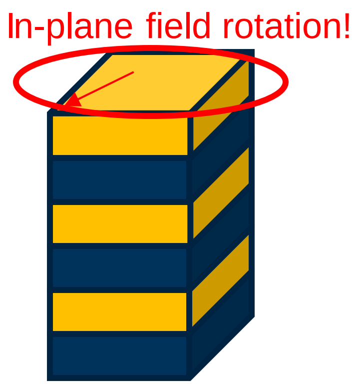

Ballistic motion on hexagonal Fermi surface

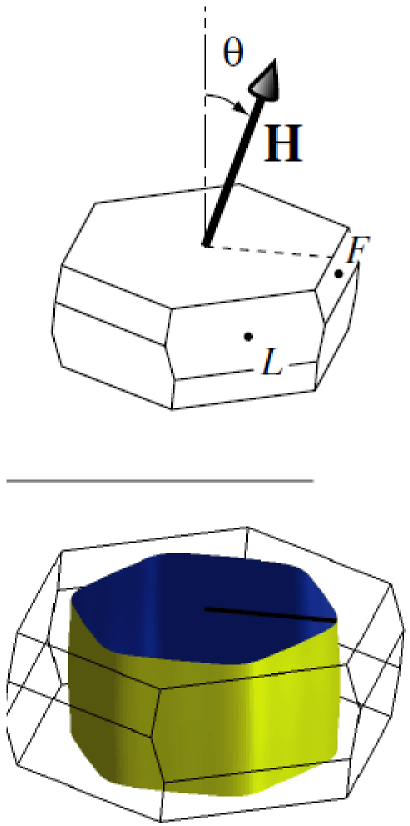

Circular Fermi surface

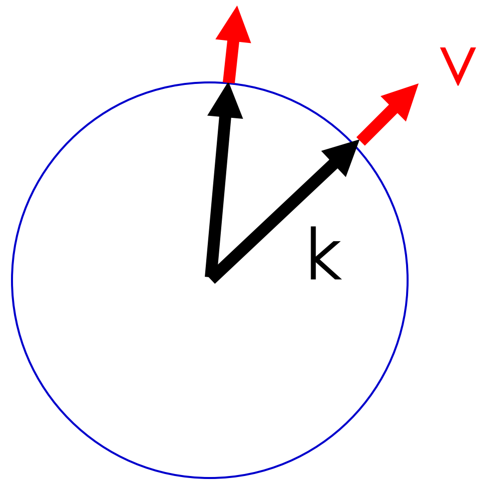

k || v

Hexagonal Fermi surface

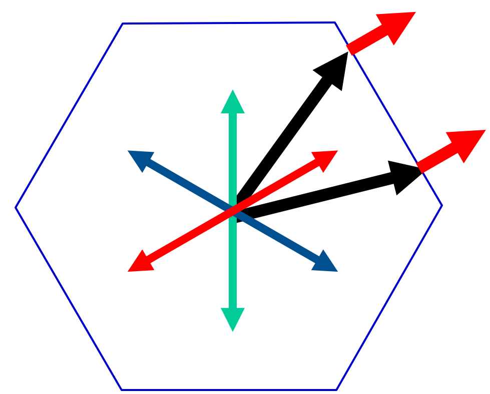

Three main propagation directions

Three quantum paths given by symmetry

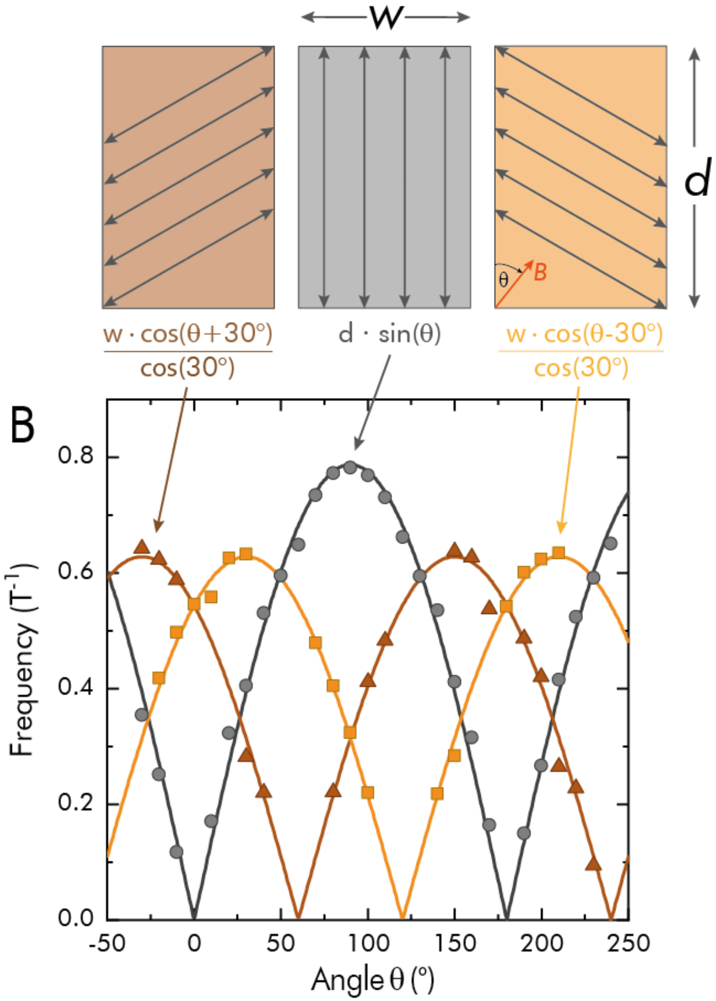

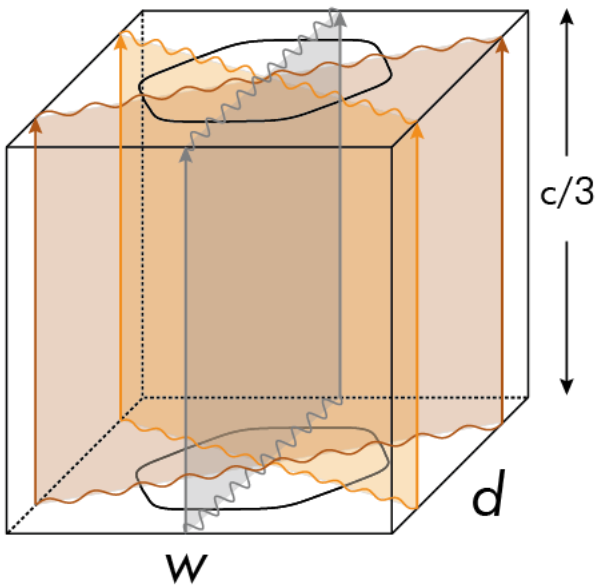

High temperature scale of 60K

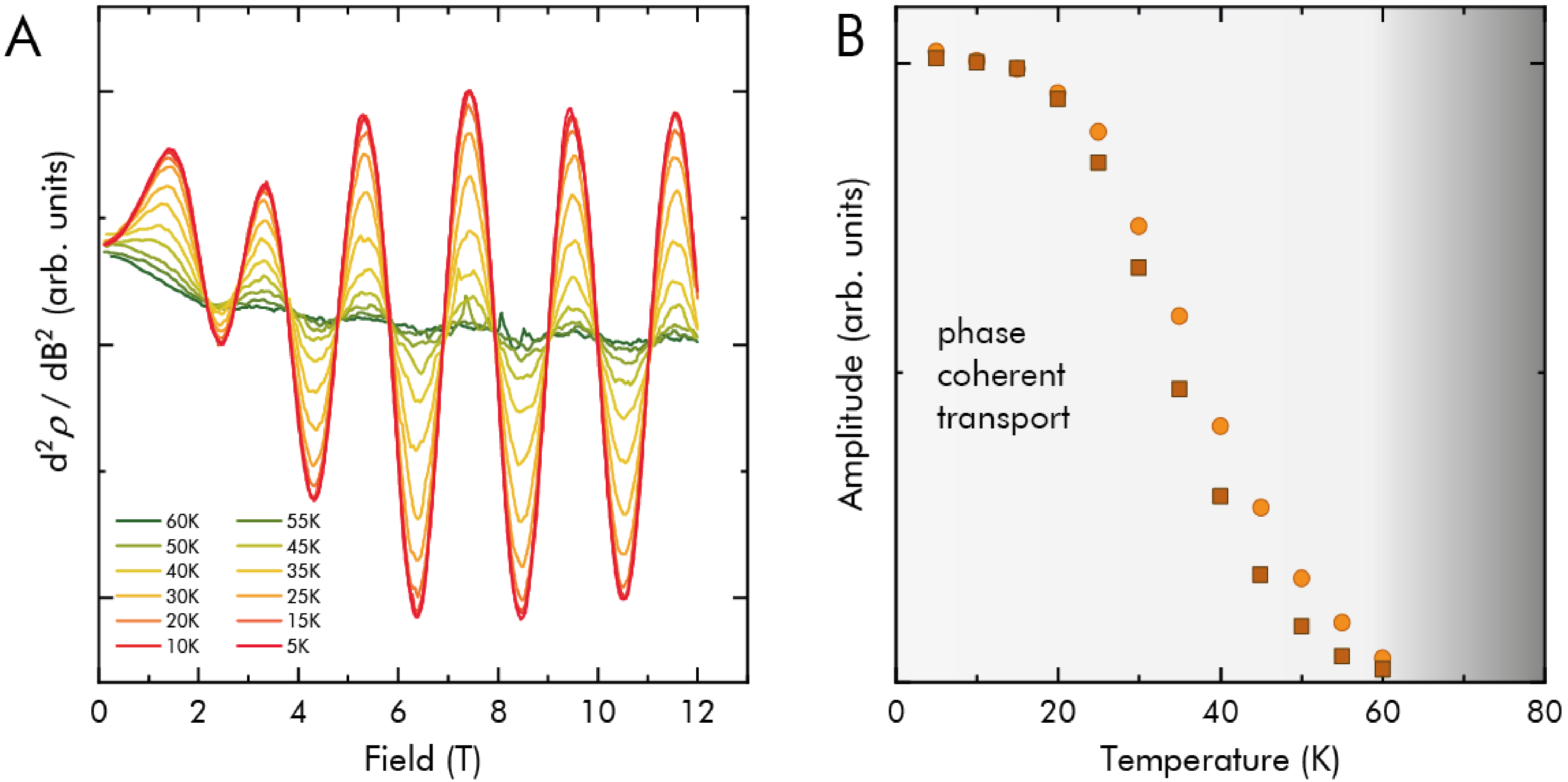

Three quantum paths given by symmetry

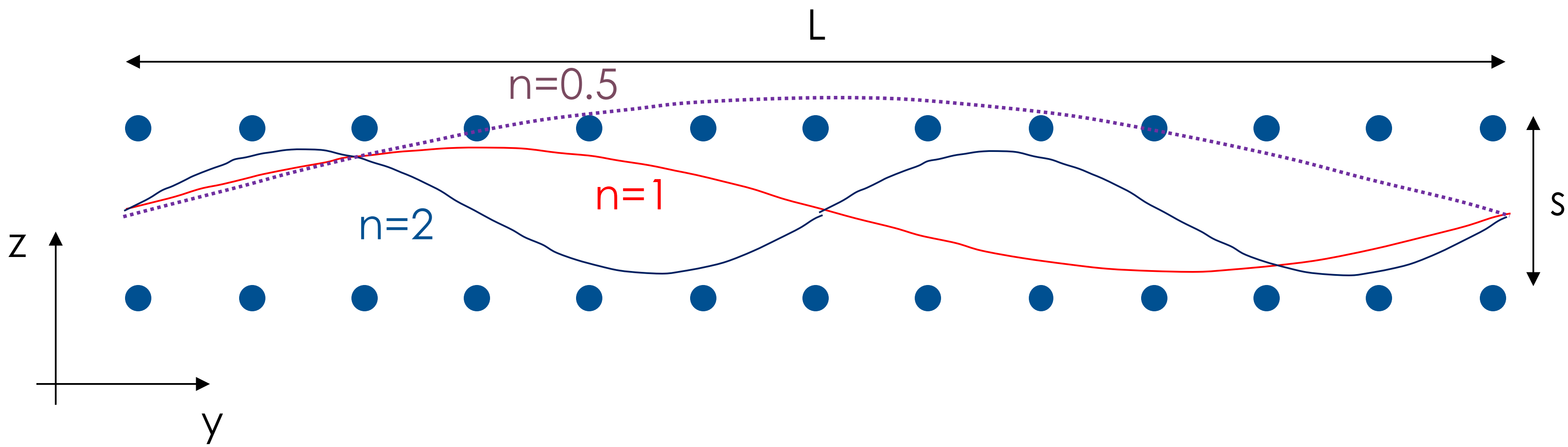

Apply flux to this double chain $\Phi = BLs \rightarrow \boldsymbol{A} = \begin{pmatrix} 0 \\ 0 \\ \frac{\Phi}{Ls}y \end{pmatrix}$

$$t_i \rightarrow t_i e^{-i\frac{e}{\hbar}\int_{r1}^{r2} \boldsymbol{A}(\boldsymbol{r}')d\boldsymbol{r}'} = t_i e^{-i\,\frac{e}{\hbar}\frac{\phi}{L}y_i} = t_i e^{-i\,2\pi\,\frac{\phi}{\Phi_0}\,\frac{y_i}{L}}$$

Three quantum paths given by symmetry

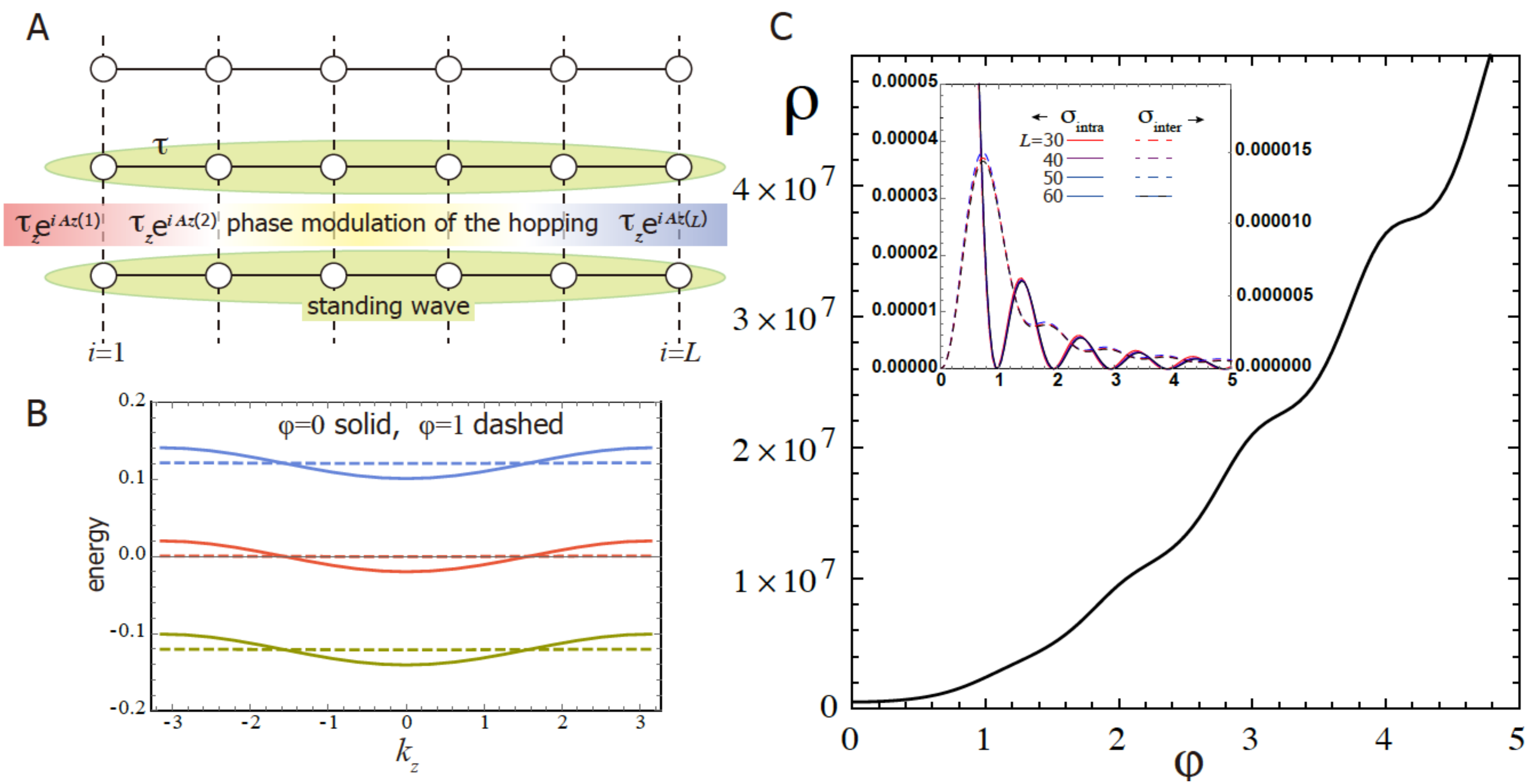

What are the “smoking guns” for topology in gapless 3D systems?

- New devices: mechanical motion on the microscale

Work in progress; Carsten Putzke, Jonas Dia

- Quantum oscillations are powerful probes of phases, they detect everything *not just Berry*. M. Guo et al, soon on arXiv

- Controlling current jetting on the micron-scale.

X. Huang et al., soon on arXiv